

Application of virtual anthropology methods to fossil human dental remains

Dissertation

der Mathematisch-Naturwissenschaftlichen Fakultät
der Eberhard Karls Universität Tübingen
zur Erlangung des Grades eines
Doktors der Naturwissenschaften
(Dr. rer. nat.)

vorgelegt von
Catherine Claudia Bauer
aus Hof/Saale

Tübingen, 2015

Tag der mündlichen Qualifikation:

23. Oktober 2015

Dekan:

Prof. Dr. Wolfgang Rosenstiel

1. Berichterstatter:

Prof. Dr. Katerina Harvati

2. Berichterstatter:

Prof. Nicholas Conard, PhD

TABLE OF CONTENTS:

| | | |
|--|---|-----|
| | Abstract | 5 |
| | Zusammenfassung | 7 |
| | List of publications included in this thesis | 9 |
| | Introduction | 11 |
| | 1. Background | 12 |
| | 2. Taxonomical methods and geometric morphometrics | 13 |
| | 3. Objectives | 17 |
| | 4. Materials and methods used in this study | 18 |
| | 5. Results | 22 |
| | 6. Conclusions | 25 |
| | 7. Future work | 26 |
| | 8. References | 26 |
| | Paper I: Early dispersal of modern humans in Europe and implication for Neanderthal behaviour | 33 |
| | Paper II: A human deciduous molar from the Middle StoneAge (Howiesons Poort) of Klipdrift Shelter, South Africa | 65 |
| | Paper III: Using elliptical best fits to characterize dental shapes | 85 |
| | Paper IV: Geometric morphometric analysis and internal structure measurements of the Neanderthal lower fourth premolars from Kalamakia, Greece | 97 |
| | Curriculum Vitae | 115 |
| | List of publications | 117 |
| | Acknowledgements | 119 |

ABSTRACT

Although being relatively small in size, teeth play an important role in the fossil record. With the enamel being the hardest material the human body can produce which is highly mineralised and consists of almost no organic material it forms a perfect protective cover for the softer dentine underneath. These material properties increase the likeliness for dental material being preserved at archaeological sites.

This cumulative thesis addresses the fact that teeth can be used for taxonomic distinction between Neanderthals and modern humans. Paper I of this thesis shows that the Uluzzian technocomplex in southern Europe, formerly attributed to be a Neanderthal transitional industry, which contains modern aspects, such as personal ornaments, is actually a product of anatomically modern humans. This could be proven by a reanalysis of a deciduous left upper first molar (dM¹, Cavallo-B) and a deciduous left upper second molar (dM², Cavallo-C) which were found in archaic and evolved Uluzzian layers of the Grotta del Cavallo, Apulia, southern Italy and were previously classified as Neanderthal (Cavallo-B) and modern human (Cavallo-C). In our analyses based on μ CT-scans and measurements both specimens clearly fell with recent and Upper Paleolithic modern humans and away from the Neanderthals. Measurements on enamel thickness strengthen the results with the two specimens again falling into the modern human range. New radiocarbon dates revealed an age of 47,530–43,000 years before present thus making these two specimens the earliest European anatomically modern human fossils known to date.

Paper II introduces a dental specimen (KDS PBE) from Klipdrift rockshelter, South Africa. It was found in Middle Stone Age (MSA) layers corresponding to the Howiesons Poort technocomplex also containing highly innovative artifacts, such as backed tools used for arrows and also material culture, for example engraved ostrich eggshells and the use of ochre. KDS PBE is the only complete human tooth crown so far from South African Pleistocene layers. In morphological description, measurements and analyses based on μ CT-scans KDS PBE fell into the range of archaic Pleistocene and recent human variation thus fitting into the mosaic of morphological variation typical for specimens associated with the MSA period.

Paper III introduces a new approach to analyse dental morphology. Using elliptical best fits on two tooth classes (dM² and M³) we show that this approach can be used for taxonomic distinction between Neanderthals and recent modern humans. A clear advantage of this

method is, that the specimens under consideration do not have to be oriented accurately for the ellipses to be the shape descriptor. A further advantage of the approach is, that it is way less time consuming than the approach in paper I, II and IV and might act as an additional useful tool when analysing the shape of internal and external features of dental remains.

Paper IV introduces the first study of internal structures of the Neanderthal Kalamakia 6 (KAL6) and Kalamakia 9 (KAL9) (both from Kalamakia, Greece) lower fourth premolars (P₄) as well as the investigation of an external feature, the crown outline shape. Both specimens exhibit clear Neanderthal features, such as transverse crests, crown asymmetry and mesially placed metaconids. In a comparative analysis with Neanderthal, early *Homo sapiens* and recent specimens KAL9 exhibited the most extreme Neanderthal shape whereas KAL6 was less extreme. The modern human sample shows a large spread in a principal-component analysis (PCA), only the Khoi San seem to represent a more homogenous population. The results of the measurements on internal dental structures, the crown height (CH), the contact surface area of the enamel-dentine junction (EDJ) and the lateral dentine and pulp chamber volume (LDPV) of the P₄ differed significantly between Neanderthals, early *Homo sapiens* and recent specimens regarding the EDJ and the LDPV measurements whereas the CH showed a large overlap. Although being considered highly diagnostic for taxonomic distinction our analysis of the P₄ shows a wide range of variation within the Neanderthals and the recent *Homo sapiens* sample, which highlights the need for more research to better capture human variability.

ZUSAMMENFASSUNG

Trotz ihrer relativ kleinen Größe spielen Zähne eine wichtige Rolle im Fossilbestand. Der Zahnschmelz stellt das härteste Material dar, welches der menschliche Körper bilden kann. Dieses besteht größtenteils aus mineralischen und nur wenig organischen Komponenten. Aufgrund dieses Umstandes stellt der Zahnschmelz eine perfekte Schutzhülle für das darunterliegende, weichere Dentin dar. Die Materialeigenschaften eines Zahnes erhöhen so die Möglichkeit, dass Zahnmaterial an archäologischen Fundstellen erhalten bleiben kann.

Diese kumulative Dissertation befasst sich mit der Tatsache, dass Zähne für taxonomische Unterscheidung zwischen Neanderthalern und modernen Menschen herangezogen werden können. Paper I dieser Dissertation beweist, dass der Uluzzien-Technokomplex in Südeuropa, welcher moderne Aspekte enthält wie beispielsweise persönliche Ornamentik, und vormals als Übergangsindustrie dem Neanderthaler zugeschrieben wurde, eigentlich durch moderne Menschen erzeugt wurde. Dies konnte anhand einer erneuten Analyse eines linken oberen ersten Milchmolaren (dM¹, Cavallo-B) sowie eines rechten oberen zweiten Milchmolaren (dM², Cavallo-C), welche in archaischen und weiterentwickelten Schichten des Uluzzien der Grotta del Cavallo, Apulien, Süditalien, gefunden wurden, bewiesen werden. Diese wurden vormals als Neanderthaler (Cavallo-B) sowie als moderner Mensch (Cavallo-C) bestimmt. In unseren Analysen, die auf μ CT-Scans und Vermessungen basieren, fielen beide Zähne in den Variationsbereich rezenter sowie mittelpaläolithischer modernen Menschen und außerhalb des Variationsbereiches der Neanderthaler. Messungen an der Schmelzdicke unterstützen diese Resultate, da auch hier beide Zähne im Bereich moderner Menschen lagen. Neue Radiocarbonatierungen ergaben ein Alter von 47 530 – 43 000 Jahren, was diese beiden Individuen bis dato zu den ersten, anatomisch modernen Menschen in Europa macht.

Paper II stellt einen weiteren Milchzahnfund (KDS PBE) aus der Felsnische von Klipdrift, Südafrika vor, ein unterer zweiter Milchmolar. Dieser wurde in Schichten des Middle Stone Age (MSA) gefunden. Diese Schichten korrespondieren mit dem Howiesons Poort-Technokomplex und enthalten ebenfalls hochinnovative Artefakte, beispielsweise rückengestumpfte Stücke, die für Pfeile verwendet wurden, aber auch Materialkultur, welche durch gravierte Straußeneierschalen und die Verwendung von Ocker vertreten ist. KDS PBE ist bisher die einzige komplette menschliche Zahnkrone aus pleistozänen Schichten

Südafrikas. Eine morphologische Untersuchung, Vermessungen und Analysen basierend auf μ CT-Scans stufen KDS PBE in den Varianzbreitenbereich archaischer pleistozäner sowie rezenter moderner Menschen, was das Mosaik der morphologischen Variation typisch für das MSA bestätigt.

Paper III stellt eine neue Herangehensweise zur Analyse der Zahnmorphologie vor. Anhand Elliptical Best Fits wurden zwei Zahntypen (dM^2 und M^3) untersucht und wir zeigen, dass diese Vorgehensweise für eine taxonomische Unterscheidung zwischen Neanderthalern und modernen Menschen herangezogen werden kann. Ein klarer Vorteil dieser Methode ist, dass eine akkurate Orientierung der einzelnen Proben nicht nötig ist, wenn die Ellipsen die Formbeschreibung darstellen. Ein weiterer Vorteil ist, dass die Datenaufbereitung wesentlich weniger zeitaufwendig ist als die Herangehensweise die in Paper I, II und IV angewendet wurde. Diese Methode stellt eine weitere Möglichkeit dar, wenn Formanalysen an internen und externen Aspekten von Zahnmaterial Grund der Untersuchungen sind.

Paper IV zeigt die erste Untersuchung interner Zahnstrukturen der unteren vierten Neanderthaler-Prämolaren (P_4), Kalamakia 6 (KAL6) und Kalamakia 9 (KAL9), beide aus der Höhlenfundstelle Kalamakia, Griechenland, sowie auch eine Untersuchung externer Eigenschaften, die Untersuchung des Kronenumrisses. Beide Proben zeigen klare Merkmale der Neanderthaler, beispielsweise transverse Grate, Kronenasymmetrie und eine mesiale Position des Metaconids. In einer Vergleichsstudie mit Proben von Neanderthalern, frühen modernen Menschen und rezenten Proben zeigte KAL9 die meist extreme Neanderthalerform wohingegen KAL6 diesbezüglich weniger auffällig war. Die Proben der modernen Menschen zeigten eine extreme Streuung in einer Hauptkomponentenanalyse, lediglich die Proben der Khoi San scheinen eine eher homogene Gruppe zu bilden. Die Ergebnisse der Messungen der Kronenhöhe (CH), der Oberflächengröße der Schmelz-Dentin-Grenze (EDJ) sowie dem Volumen des lateralen Dentins zusammen mit der Pulpahöhle (LDPV) der P_4 zeigten eine signifikante Unterscheidung zwischen Neanderthalern und den Proben rezenter Menschen für EDJ und LDPV, CH zeigte hierbei die deutlichste Überlappung. Obwohl P_4 als hochdiagnostisch zur Unterscheidung zwischen Neanderthalern und modernen Menschen eingestuft werden, zeigen unsere Analysen eine breite Streuung der Variation innerhalb der Neanderthaler und auch der Proben rezenter *Homo sapiens*, was die Wichtigkeit weiterer Forschung herausstellt um die menschliche Variationsbreite besser fassen zu können.

LIST OF PUBLICATIONS

Publications submitted or in preparation to fulfil the requirements for a cumulative dissertation. Percentages of the own contribution to the articles or manuscripts are listed in parentheses (original idea/data collection/data analysis/writing and publication).

Paper I (0/20/10/10)

Benazzi, S., Douka, K., Fornai, C., **Bauer, C. C.**, Kullmer, O., Svoboda, J., Pap, I., Mallegni, F., Bayle, P., Coquerelle, M., Condemi, S., Ronchitelli, A., Harvati, K., Weber, G. W. (2011): Early dispersal of modern humans in Europe and implications for Neanderthal behaviour. *Nature* 479, 525 – 528. doi:10.1038/nature10617.

Paper II (0/50/30/30)

Harvati, K., **Bauer, C. C.**, Grine, F. E., Benazzi, S., Ackerman, R. R., van Niekerk, K. L., Henshilwood, C. S. (2015): A human deciduous molar from the Middle Stone Age (Howiesons Poort) of Klipdrift Shelter, South Africa. *Journal of Human Evolution* 82, 190 – 196. doi:10.1016/j.jhevol.2015.03.001.

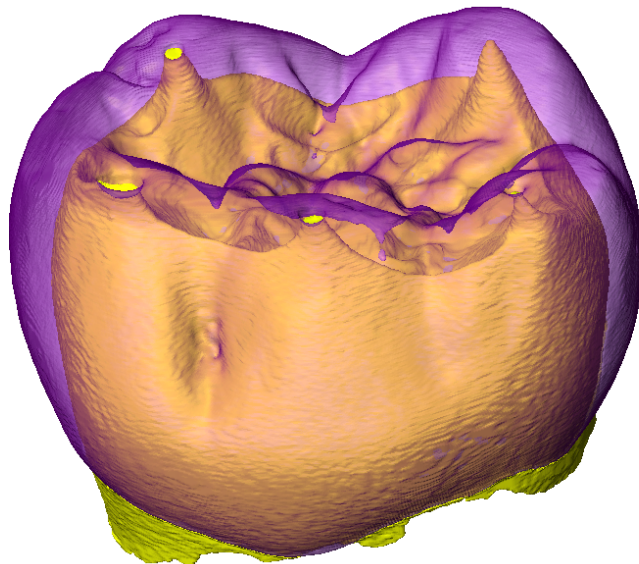
Paper III (60/100/70/60)

Bauer C. C., Bons, P. D., Benazzi, S., Harvati, K. (in revision): Technical Note: Using elliptical best fits to characterize dental shapes. Resubmitted to the *American Journal of Physical Anthropology* after revision.

Paper IV (50/100/90/60)

Bauer, C. C., Benazzi, S., Darlas, A., Harvati, K. (in prep): Geometric morphometric analysis and internal structure measurements of the Neanderthal lower fourth premolars from Kalamakia, Greece. Manuscript in preparation for the *American Journal of Physical Anthropology*, close to submission.

Introduction



“[...] much remains to be done, but the ‘state of dental darkness’ described by Keith over 60 years ago is slowly emerging into the light.”

Scott and Turner (2010).

1. Background

Ever since the publication of Darwin's "On the Origin of Species" (Darwin 1859), the question was, and still is, who our ancestors are and how our species, *Homo sapiens*, spread over and occupied the entire Earth. At about the same time, in 1856, a strangely shaped human calotte was found in the Feldhofer Grotte, in the Neanderthal (archaic spelling, Neander valley), Germany, associated with further skeletal fragments (Hrdlička 1927, Spencer & Smith 1981, Wahl 2005). In 1864, after a long debate over its taxonomic assignment, it was declared non-human by King (1864). Until then, partly for religious reasons, it was assumed impossible that any other hominid species ever existed (Gieseler 1936, Bolus 2004). However, already 1859, Fuhlrott (1859) published an article questioning this aspect, which was later confirmed by Schaafhausen (1888).

Since then, our genus *Homo* has gained a range of new members, such as *Homo heidelbergensis/steinheimensis*, *Homo antecessor* or the Denisovans (Berckhemer 1933, Weinert 1936, Bermúdez de Castro 1997, Reich et al. 2010). Fossil remains found in Olduvai Gorge, at Lake Turkana and Koobi Fora, Kenya, are assumed to represent the oldest member of the genus *Homo*. This 2.6 million year old specimen was declared *Homo habilis*, the skillful man, for its apparent serial production of stone tools (Isaac et al., 1971, Howell 1978). Followed by *Homo ergaster*, *H. erectus*, *H. heidelbergensis* and *H. antecessor*, our genus started to leave the African cradle and subsequently spread out into Europe, the Near East and Asia (Dubois 1937, Bermúdez de Castro et al. 1997, Schwartz & Tattersall 2002, 2003, Shen et al. 2009, Lordkipanidze et al. 2013).

Around 200 ka BP another member of the human clade became successful in Europe, the Neanderthals. Neanderthals may have developed out of *H. erectus* parallel to the evolution of our own species, *H. sapiens* in Africa, as fossils from Herto and Omo in East Africa and Klasies River Mouth in South Africa suggest (Bräuer 1989, Schwartz & Tattersall 2002, Forster 2004). In a second expansion out of Africa, the latter reached the near East at least around 120 ka BP (Schwarcz et al. 1988, Grün & Stringer 1991). How and when *H. sapiens* occupied the whole African continent remains poorly known, especially in southern Africa where the dental fossil record is very poor and analyses are limited to (broken) dental specimens and stone tools (Grine 2012, Harvati et al. 2015). This issue will be addressed in paper II.

While Neanderthals were widespread all over Europe and parts of Asia, as the fossil record indicates (Schwartz & Tattersall 2002, Harvati & Harrison 2007, Harvati et al. 2013, paper IV), they were increasingly challenged by anatomically modern humans until the last Neanderthals were pushed back as far as southern Portugal (Zilhão 2000). Several studies addressed the question of why the quite successful species *H. neanderthalensis* was basically run over by *H. sapiens* who, by 30 ka BP, completely replaced the Neanderthals (Stringer et al. 2004, Finlayson 2004, Stringer 2008). To address this question, it is of particular interest how and when anatomically modern humans entered Europe. So far, the oldest known anatomically modern human in Europe originates from southern Italy (see paper I).

With the demise of *H. neanderthalensis*, anatomically modern humans became the only representatives of the genus *Homo*, and quickly spread out over the entire world, even reaching Australia by latest around 50 ka ago (Thorne et al. 1999, Bowler et al. 2003, Reyes-Centeno et al. 2014) and the American continent around 25 - 15 ka ago (Forster 2004, Hubbe et al. 2010). This spread over different continents and climatic regions resulted in a large regional variety of several traits, such as body size, overall cranial and facial shape, but also dental shape and trait frequency (Turner 1990, Scott & Turner 1997, Kitagawa 2000, Noback et al. 2011). One of the main questions is therefore to assess and quantify these differences within our species but also between different, close members of our genus.

Summarising, although much is known about the general emergence and radiation of anatomically modern humans, questions remain. For example, on the timing and pathways of migration. One prerequisite to address these questions is correct taxonomical assignment of fossil remains. This is topic of this thesis, which in particular deals with the quantified description and analysis of dental remains.

2. Taxonomical methods and geometric morphometrics

The aforementioned discussion already indicates the need of quantification in shape differences. One major focus of Paleoanthropology is therefore the study of human (fossil) remains in order to clarify the difference between members of the genus *Homo* and its ancestors. Equally important in this discipline is the analysis of variation between the different modern human populations worldwide. The entire human skeleton, including the dentition,

can be used for comparative analyses. This thesis focuses solely on the analysis of dental remains. Below I first give a short introduction into dental morphology and tissues. This section is followed by a brief review of paleoanthropological methods, in particular those applied to dental remains and used in this thesis. The objectives and results of this study, published in, or in review/preparation for four journal papers, are presented in the final section of this introduction.

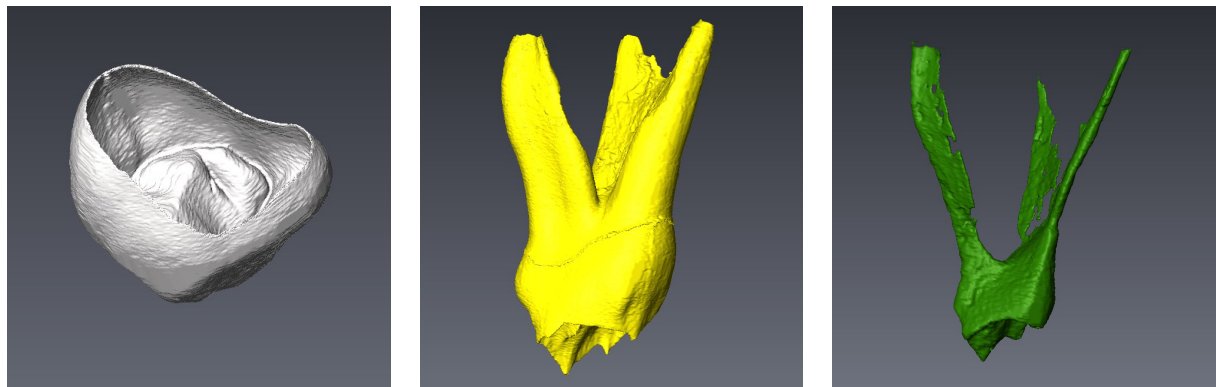


Fig. 1: Illustration of the three dental tissues by a virtually segmented μ CT-scan. From left to right: Internal view of the enamel cap, the dentine and the pulp chamber.

2.1 Dental tissues and morphology

A tooth consists of three main tissues/parts: (1) the enamel cap, (2) the dentine, and (3) the pulp chamber (Fig. 1). The enamel cap that covers each tooth forms the hardest, highly mineralised material in the human body. It only contains about 4% of organic matter, whereas e.g. dentine and bone consist 15 – 26%. These 4% of organic material are formed by 1% protein and approximately 3% of water. 96% of the anorganic, mineral part consists of hydroxyapatite crystals (Eastoe 1960, Cuy et al. 2002, Hillson 1996, Nanci 2012). Underneath the enamel lies the dentine, which partly contributes to the crown but also forms the root and contains the pulp chamber that hosts the nerve (Weber 2010). Dentine is built by 70% hydroxiapatite, 20% organic material (collagen) and 10% water, and is thus less mineralized than the enamel, making the tissue less brittle (Nanci 2012). As mentioned above, the dentine also forms the pulp chamber, which hosts the innervation of the tooth and blood vessels (ibid.). Coating the root, a thin cementum layer can be observed forming the attachment to the alveolar bone via periodontal fibers (Hillson 1996, Wittwer-Backofen et al. 2003).

2.2. Dental remains in the human fossil record

Despite their relatively small size, teeth can provide an extensive record of an individual's life history. The study of teeth is very common in Paleoanthropology. They can be used for a variety of purposes, such as age determination (stage of eruption, abrasion, enamel hypoplasia, tooth cementum annulation etc.), dietary reconstruction (microwear analysis) or taxonomic purposes (shape analysis, taurodontism, genetics) (Gustavson 1950, Ferembach et al. 1979, Charles et al. 1986, Condon et al. 1986, Zilberman & Smith 1992, Reid & Dean 2000, Bailey 2002, Wittwer-Backofen et al. 2003, Ungar et al. 2005, Grine et al. 2006, Green et al. 2010, Benazzi et al. 2011a, b, c, El-Zaatari et al. 2011, Benazzi et al. 2012, Benazzi et al. 2015, Harvati et al. 2015). Teeth also play an important role in the fossil record. Because of their robust material properties, it is highly likely that dental remains are preserved. Many studies have investigated dental remains using a variety of different approaches on different tooth classes (Bailey 2002, 2004, Bailey and Lynch 2005, Bailey and Liu 2010, Benazzi et al. 2011a, b, c, Benazzi et al. 2012, Harvati et al. 2015).

2.3. Geometric morphometrics

Basic measurements, such as the bucco-lingual or mesio-distal diameter, and the observation of morphological traits, were the first approaches undertaken already from the 19th century, focusing on differences between worldwide populations and fossils (von Carabelli 1842, Hrdlička 1911, 1920, 1921, 1924, Martin 1928, Bräuer 1998, Wood & Abbot 1983, Wood et al. 1983, Wood & Uytterschaut 1987, Scott & Turner 2000). In the 1960s, studies started to also take inner dental morphology into account, especially the enamel dentine junction using either incompletely formed teeth (Korenhof 1982) or applying invasive techniques, thus damaging the sample (e.g. Nager, 1960, Macho 1994). Avoiding damage of fossil samples is evidently of particular interest.

With the increase of computer power in the early 90s of the 20th century, new methods for shape analysis were developed: the geometric morphometrics methods (GM) (Rohlf 1990, Rohlf & Marcus 1993). GM allows datasets consisting of either 2D- or 3D-landmark coordinates of the shape of an object to be analyzed. Not only are comparisons between two points possible, but between all the landmarks used. The main focus when applying GM lies

on examining differences in shape, irrespective of their individual size (Corti 1993, O'Higgins 2000, Slice 2001). Shape is the only difference that remains when position, size and orientation have been removed. Therefore, a key feature in GM is the so-called Procrustes superimposition, by which these aforementioned factors are removed before subsequent analyses (O'Higgins 2000, Larsen 2005, McLeod 2009). Examining differences in shape only offered a completely new approach and made way for numerous re-assessments of data analyses, for taxonomy when working with human fossils, amongst other purposes (Benazzi et al. 2011a, b, c, 2012, 2013, 2014, Harvati et al. 2015).

Not only external, but also internal structures of teeth could be investigated in more detail with the introduction of μ CT imaging in dental anthropology in the 1990s (Spoor et al. 1993, Nielsen et al. 1995, Weber et al. 1998). One major advantage of using μ CT scans in palaeoanthropology is that it is a completely non-destructive approach, which is particularly important when dealing with human fossils. In μ CT images, the three parts can easily be determined since the enamel appears bright white because of its higher density and the dentine has several shades of grey. The pulp chamber remains dark. Using powerful software, such as AVIZO® versions 7.0 and 7.1 (© FEI), these parts can be distinguished and virtually segmented from each other. Parameters, such as the volume and the surface area of different tissues, can be measured after segmentation. For the outline shape analysis, the use of a CAD-software can be a helpful tool. For this study, RHINOCEROS® 5.0 (© Robert McNeel & Associates) was used.

A disadvantage of this approach is the fact that it can be very time-consuming. Depending on the resolution and damage (such as fractures) of the specimen, this process can take up to a week per tooth. Thus, the creation of a large comparative sample is a cumbersome task. Given these facts, it is not surprising that until now, only limited data were available. In addition, these methods have not been applied to all tooth types.

3. Objectives

The objectives of this thesis are as follows:

- (1) The establishment of a μ CT-scan database of Neanderthals, early and recent anatomically modern humans for different tooth types to provide a comparative sample for this thesis and future research.
- (2) The creation of landmark data as well as surface and volumetric measurements for different tooth types for the understanding of Neanderthal and modern human variation and for future comparative analyses.
- (3) The development of new techniques to facilitate the partially time-consuming process of data collection and preparation for the approach mainly used in this thesis.

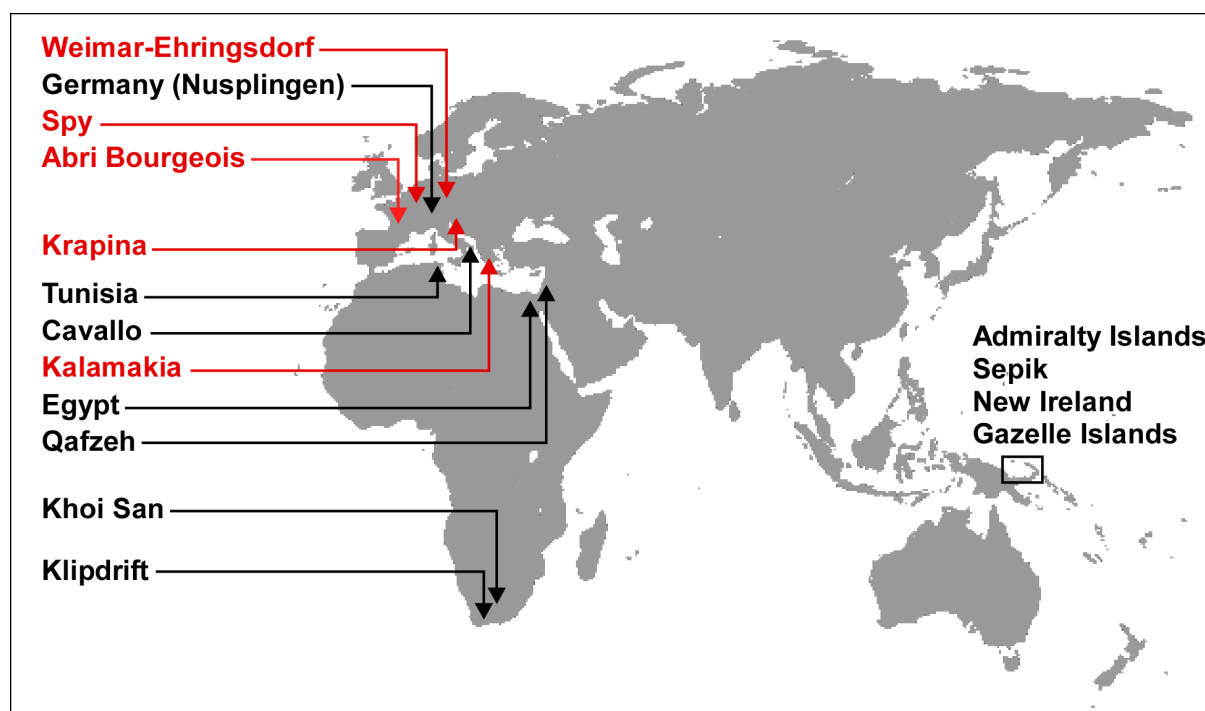


Fig. 2: Map illustrating the origin of the specimens that were processed and/or analysed by the author. Red: Neanderthals, Black: *Homo sapiens*.

4. Materials and methods used in this study

4.1. Materials

Most of the material for the studies in this thesis consists of individuals from the osteological collection of Tübingen University. This collection contains more than 10 000 individuals from all over the world and forms an excellent base for dental shape analyses. Data of additional specimens was kindly provided by Dr. Stefano Benazzi, Senior Lecturer at Bologna University, Italy. Most of the Neanderthal data was obtained via the online NESPOS database¹ (Fig. 2).

In our studies, we focused on tooth classes of the permanent but also the deciduous dentition, the upper first (dM¹) and second deciduous molar (dM²), the lower second deciduous molar (dM₂), the lower second premolar (P₄) and the upper third molar respectively (M³). dM¹s are usually characterised by three cusps in anatomically modern humans whereas Neanderthal specimens tend to form four cusps (Bailey & Hublin 2006, Benazzi et al. 2011c). dM²s, however are usually five-cusped as are dM₂s (Hillson 1996). In occlusal view, members of these tooth classes appear 'cloud-shaped', thus exhibiting a relatively complex shape. P₄s usually form two cusps, the larger on the buccal side and a smaller one on the lingual side. Their outline shape in occlusal view is roughly oval to circular in anatomically modern humans and tends to have a more distally shifted bulge in Neanderthals (Martínón-Torres et al. 2006). Despite their relatively simple shape, a large within-species variation can be observed (Fig. 3). This issue will be discussed in paper IV. For upper M³s a general description is unfortunately difficult. This tooth class is highly variable regarding cusp number and shape, which can range from peg-shape with only one cusp to a four-cusped, more triangular full molar (Hillson 1996). Therefore, M³s have generally been neglected in scientific analyses (Fig. 4).

¹ <https://www.nespos.org/display/openspace/Home>

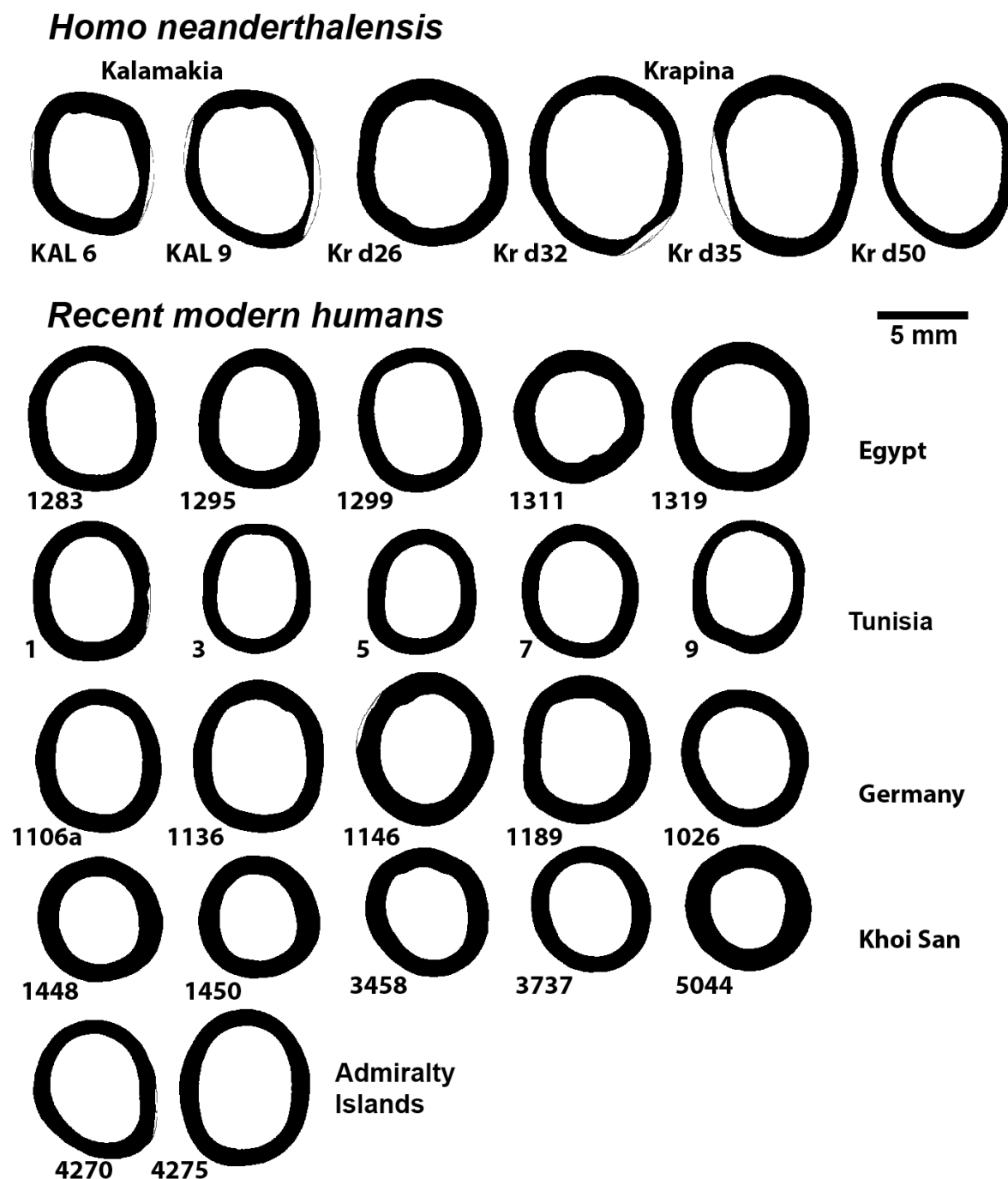


Fig. 3: Selection of the P₄-sample, cross-sections in occlusal view at the EDJ-plane to illustrate inter- and intra-species variation. Buccal to the top, mesial to the left.

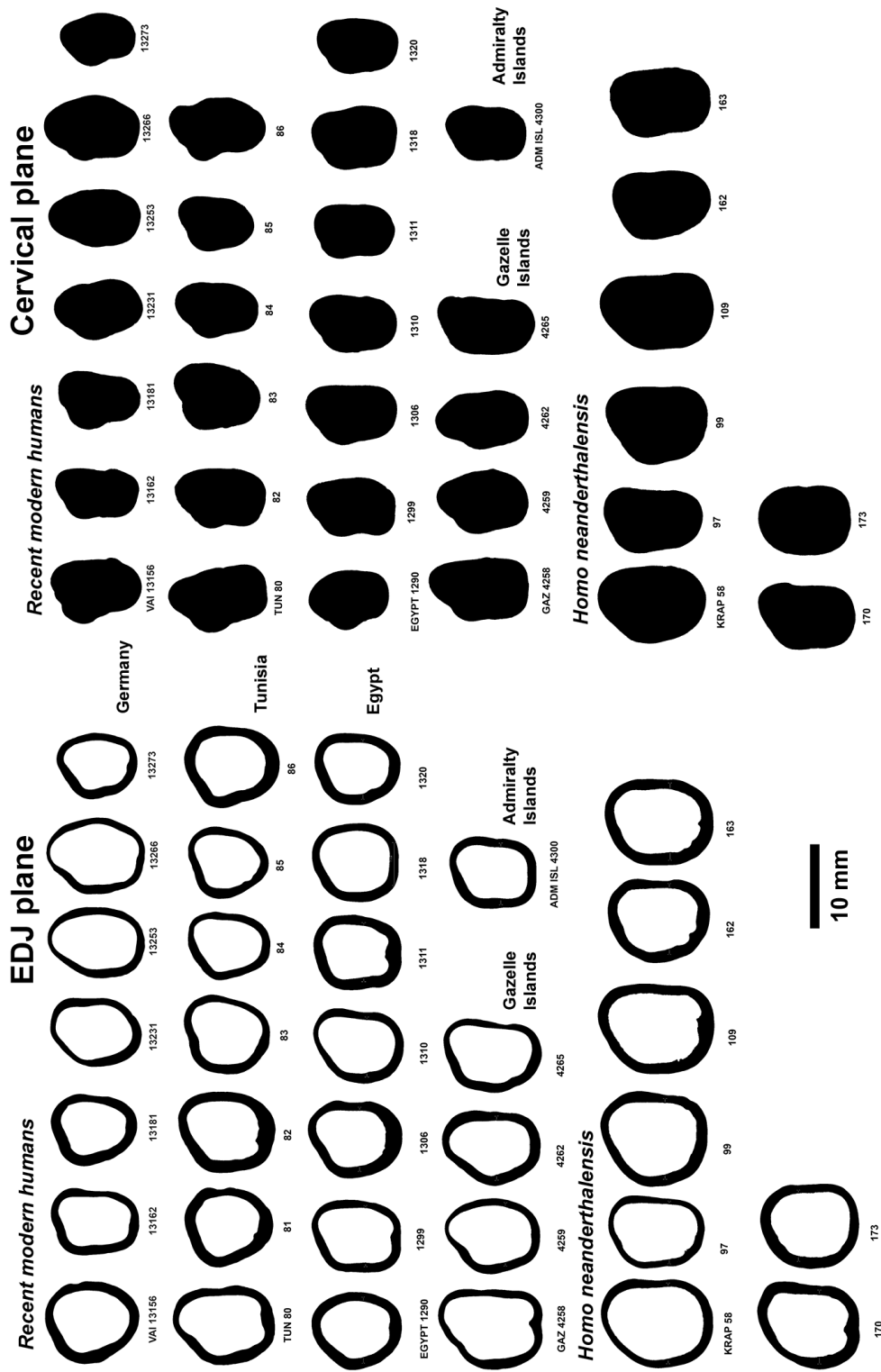


Fig. 4: Selection of M³ sample, cross sections in occlusal view at the EDJ-plane. Left: Illustration of enamel and dentine, right: Illustration of dentine at the cervical line, showing the intra- and inter-species variation.

4.2. Methods

The specimens from the osteological collection of Tübingen University were scanned with a GE Phoenix v|tome|x S scanner in the high-resolution μ CT-Laboratory of the Paleoanthropology group. Voxel size varied between 0.01 and 0.065 mm depending on size of the specimen (isolated teeth or hemi-/mandibles). After scanning, we followed the methods described in Benazzi et al. (2011a,b,c, 2012, 2013, 2014, 2015). Using the AVIZO® software (© FEI, versions 7.0 and 7.1), the best-fit plane of the cervical line for each tooth was determined. In a second step, each image stack was realigned to be entirely parallel to this best-fit plane previously mentioned. This was undertaken to have the z-axis of each scan parallel to a defined and comparable reference plane. This plane also formed the reference plane where the root of each specimen was virtually cut off. In RHINOCEROS® 5.0 (© Robert McNeel & Associates), each specimen was then rotated around the z-axis following pre-defined dental structures depending on the individual tooth class to ensure that all specimens were analysed in the same occlusal view position. Subsequently, the outline of the specimen was computed and as a following step, the centroid of each outline was shifted to the position 10,10,0 of the Cartesian coordinate system for superimposition. Landmark position along the crown outline shape was then defined by 16 equiangularly spaced radial vectors out of the centroid with the first vector being parallel to the y-axis of the Cartesian coordinate system cutting the outline (Fig. 5).

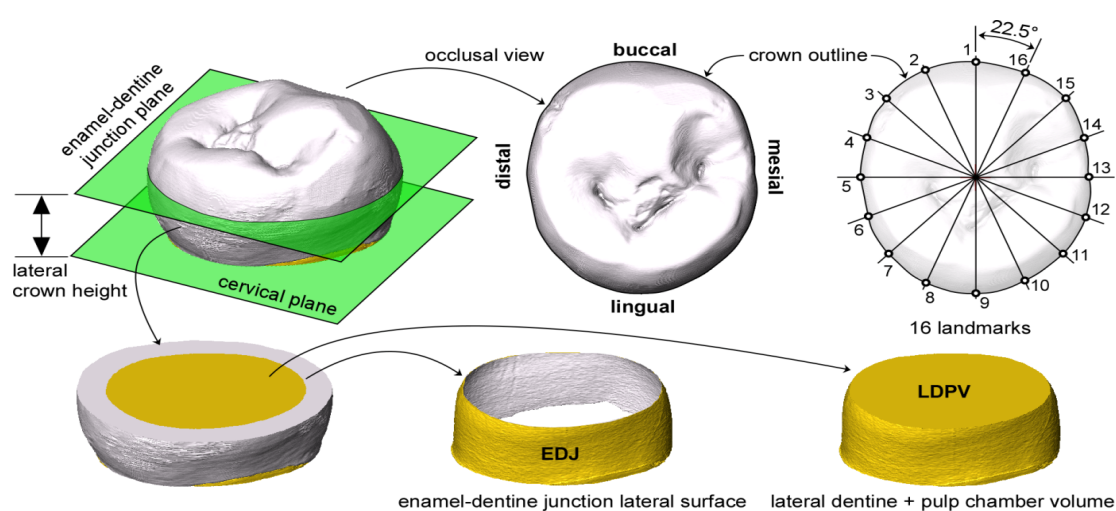


Fig. 5: Parameters measured in paper I, II and IV.

Landmark data analysis was performed with Morphologika 2.5 (O'Higgins & Jones 2006) and PAST 3.01 (Hammer et al., 2001). In addition to the outline shape, we also collected data on internal structures of the specimens. Since many of the specimens exhibited cuspal abrasion, we focused only on a certain, defined part of the crown. Parallel to the aforementioned best-fit plane of the cervical line, a second plane was created and positioned directly at the enamel-dentine junction of the occlusal basin. This second plane thus defined the reference plane where the dental cusps were cut off. On this remaining part of the tooth, the following parameters were measured: lateral crown height (LCH), the contact surface of the enamel-dentine junction (EDJ) and the lateral dentine and pulp chamber volume (LDPV) (Fig. 5). For details and illustration of the parameters measured, see figures in articles included in this thesis (see paper I, II and IV).

As no software is yet available for the elliptical best-fit method that is proposed in paper III, a C-language code was written in-house for this purpose. Screenshots of segmented teeth in the planes defined above (cervical and EDJ plane), converted to binary files were used for the analyses. Further details of the new method can be found in paper III.

5. Results

This thesis consists of four papers:

Paper I: Early dispersal of modern humans in Europe and implications for Neanderthal behaviour.

Nature 479, 525 – 528, 2011, by Benazzi, S., Douka, K., Fornai, C., Bauer, C. C., Kullmer, O., Svoboda, J., Pap, I., Mallegni, F., Bayle, P., Coquerelle, M., Condemi, S., Ronchitelli, A., Harvati, K., Weber, G. W.

In this paper we focused on two deciduous teeth from Grotta del Cavallo (Apulia, southern Italy). The two specimens, Cavallo B and C, were attributed to *Homo neanderthalensis* and therefore it was assumed that Neanderthals were responsible for the local Uluzzian technocomplex (Palma di Cesnola & Messeri 1967, Palma di Cesnola 1989, Churchill & Smith 2000). Using μ CT data of the two specimens and a comparative sample of 25 specimens (upper first deciduous molar, dM¹) ranging from the Upper Paleolithic to recent

time periods and 27 specimens for the upper second deciduous molar (dM²) respectively. Our analyses, however, did not confirm the association with *Homo neanderthalensis* but it showed that the two deciduous teeth were indeed anatomically modern humans. This is of particular interest when considering the dating of the layers they were found in, ca. 45 000 – 43 000 calendar years before present, thus making them the oldest known anatomically modern humans in Europe.

Paper II: A human deciduous molar from the Middle Stone Age (Howiesons Poort) of Klipdrift Shelter, South Africa.

Journal of Human Evolution 82, 190 – 196, 2015, doi:10.1016/j.jhevol.2015.03.001, by Harvati, K., Bauer, C. C., Grine, F. E., Benazzi, S., Ackerman, R. R., van Niekerk, K. L., Henshilwood, C. S.

In this article we analysed a human deciduous molar from Klipdrift Rockshelter, South Africa, KDS PBE. It was found covered with ochre in layers dating to 66 000 – 52 000 years before present. It is so far the only complete crown specimen from later Pleistocene South Africa. The tooth was scanned at the Tübingen Paleoanthropology μ CT Laboratory. This paper contains a detailed description of the specimen as well as comparative analyses, such as bucco-lingual (BL) and mesio-distal (MD) measurements but also geometric morphometrics approaches analysing the crown outline shape, lateral dentine and pulp chamber volume and lateral crown height. Sample sizes per group included varied from 3 – 68, depending on the availability of fossil specimens. The analyses confirmed KDS PBE being a deciduous upper second molar from a *Homo sapiens* child.

Paper III: Technical Note: Using elliptical best fits to characterize dental shapes.

Resubmitted after review to the *American Journal of Physical Anthropology* after revision, by Bauer C. C., Bons, P. D., Benazzi, S., Harvati, K.

This article introduces a new approach for shape analysis of modern human and Neanderthal teeth. Unlike other approaches, with pitfalls such as abrasion, damage or the inability to

consistently orient the specimens, this approach provides a useful tool to describe size and outline shape orientation-free. We focused on upper second deciduous molars (dm^2) and upper third molars (M^3), the latter being extremely variable in shape, making shape analyses very difficult. For the dm^2 we included 25 specimens and 33 for the M^3 , representing Neanderthals (NEA) and recent modern humans (RMH). In a principal components analysis (PCA) the dm^2 s showed a clear separation between the two species. For the M^3 s a partial separation was possible. This method can provide a useful additional tool in future tooth analyses.

Paper IV: Geometric morphometric analysis and internal structure measurements of the Neanderthal lower fourth premolars from Kalamakia, Greece.

Manuscript in preparation for the *American Journal of Physical Anthropology*, close to submission; by Bauer, C. C., Benazzi, S., Darlas, A., Harvati, K..

This paper introduces the shape analysis and internal tissue measurements of two Neanderthal specimens (KAL 6 and KAL 9) from Kalamakia, Greece. They were found in association with a Middle Paleolithic stone tool industry of Mousterian character. In total, 14 fragments of human remains could be recovered including ten dental remains, among these the two lower second premolars discussed in this paper.

With this study we contributed to a better understanding of the morphological features of the KAL specimens within a comparative sample of Neanderthals and early and recent anatomically modern humans. In addition, we thus investigated the geographical variation of modern humans as well. Our comparative sample consisted of Neanderthal specimens, early *Homo sapiens* and a sample of recent modern humans.

As before, we took landmarks along the outline shape in occlusal view and measured crown height, enamel-dentine junction surface area and the lateral dentine and pulp chamber volume. This study revealed that some specimens showed the typical traits according to their species, while other specimens acted as complete outliers in their assigned group. This suggests a larger variation within Neanderthal and modern human species than expected. More research with larger sample sizes is needed to better understand the results presented in this article.

6. Conclusions

- This dissertation presents some of the first applications of radial pseudolandmarks on the tooth classes dM^1 , dM^2 , dM_2 , and P_4 . The method proved to be highly effective in case of dM^1 , dM^2 and dM_2 (Paper I and II), but less so in case of P_4 (paper IV).
- P_4 crown outlines show large variation both within the species of *H. sapiens* and Neanderthals making a classification based purely on crown outline difficult. Other metric measurements need to be considered.
- Additionally, a new method based on elliptical best fits was developed and applied to dM^2 and M^3 . Again, the method proved very effective for dM^2 and to a lesser extent to M^3 for the separation between Neanderthals and *H. sapiens*.
- In the course of the study an extensive database was created which promises to be an excellent reference for future studies.
- Using the above techniques it could be shown:
 - The specimen Cavallo C formerly thought to be Neanderthal proved to be an anatomically modern human. This was first determined using equiangularly spaced pseudolandmarks (paper I) and confirmed with the best-fit ellipse technique (paper III). This reassignment has significant impact on our understanding of the first settlement of Europe of anatomically modern humans and the interpretation of the Uluzzian technocomplex.
 - The specimen KDS PBE, so far the only complete tooth crown from MSA archaeological contexts in South Africa, could be identified as anatomically modern human. The specimen also exhibits the morphological pattern discussed for MSA human remains, being chronologically between early *H. sapiens* and recent modern humans.
 - An additional method for dental shape analysis, the elliptical best-fit, was developed which is of particular interest when highly abraded specimens are included in the analysis.

7. Future work

- The analyzed tooth classes show a large variation with distinct patterns, in particular in case of P₄ and the Khoi San. For further investigations it is desirable to:
 - increase sample size,
 - include more groups,
 - and add more tooth classes to the database.
- Paper III on the application of best-fit ellipses to dental outlines is a pilot study. More work is needed to determine the applicability of the proposed method to other tooth classes and to establish its efficacy in comparison with other approaches (for example pseudolandmarks and elliptical Fourier analysis)
- Where possible, geometric morphometrics on dental remains may be combined with (palaeo-) genetics.
- To increase sample size and to improve data quality, new techniques should be developed to
 - enable faster segmentation;
 - achieve higher segmentation accuracy, especially in heavily mineralized specimens or poor-quality scans.

8. References

- Bailey S. 2002. A closer look at Neanderthal postcanine dental morphology: the mandibular dentition. *Anat Rec (New Anat)* 269, 148 – 156.
- Bailey S. 2004. A morphometric analysis of maxillary molar crowns of middle-late Pleistocene hominins. *J Hum Evol* 47, 183 – 198.
- Bailey S., Lynch J.M. 2005. Diagnostic Differences in Mandibular P4 Shape Between Neanderthals and Anatomically Modern Humans. *Am J Phys Anthropol* 126, 268 – 277.
- Bailey, S., Hublin, J. J. 2006. Dental remains from the Grotte du Renne at Arcy-sur-Cure (Yonne). *J Hum Evol* 50, 485 – 508.
- Bailey S., Liu W. 2010. A comparative dental metrical and morphological analysis of a Middle Pleistocene hominin maxilla from Chaoxian (Chaohu), China. *Quatern Int* 211, 14 – 23.
- Benazzi S., Coquerelle M., Fiorenza L., Bookstein F., Katina S., Kullmer O. 2011a. Comparison of Dental Measurement Systems for Taxonomic Assignment of First Molars. *Am J Phys Anthropol* 144, 342 – 354.

- Benazzi S., Fornai C., Bayle P., Coquerelle M., Kullmer O., Mallegni F., Weber G.W. 2011b. Comparison of dental measurement systems for taxonomic assignment of Neanderthal and modern human lower second deciduous molars. *J Hum Evol* 61, 320 – 326.
- Benazzi S., Douka K., Fornai C., Bauer C.C., Kullmer O., Svoboda J., Pap I., Mallegni F., Bayle P., Coquerelle M., Condemi S., Ronchitelli A., Harvati K., Weber G.W. 2011c. Early dispersal of modern humans in Europe and implications for Neanderthal behaviour. *Nature* 479, 525 – 528.
- Benazzi S., Fornai C., Buti L., Toussaint M., Mallegni F., Ricci S., Gruppioni G., Weber G.W., Condemi S., Ronchitelli A. 2012. Cervical and Crown Outline Analysis of Worn Neanderthal and Modern Human Lower Second Deciduous Molars. *Am J Phys Anthropol* 149, 537 – 546.
- Benazzi, S., Bailey, S. E., Mallegni, F., 2013. A morphometric analysis of the Neandertal upper second molar Leuca I. *Am J Phys Anthropol* 152, 300 – 305.
- Benazzi, S., Peresani, M., Talamo, S., Fu, Q., Mannino, M. A., Richards, M. P., Hublin, J.-J., 2014. A reassessment of the presumed Neandertal human remains from San Bernardino Cave, Italy. *J Hum Evol* 66, 89 – 94.
- Benazzi, S., Nguyen, H. N., Kullmer, O., Hublin, J. J. 2015. Exploring the biomechanics of taurodontism. *J Anat* 266 (2), 180 – 188.
- Berckhemer, F., 1933. Ein Menschen-Schädel aus den diluvialen Schottern von Steinheim a. d. Murr. *Anthropol Anz* 10, 318 – 321.
- Bermúdez de Castro, J M., Arsuaga, J. L., Carbonell, E., Rosas, A., Martínez, I., Mosquera, M. 1997. A Hominid from the Lower Pleistocene of Atapuerca, Spain: Possible Ancestor to Neandertals and Modern Humans. *Science* 276, 1392 – 1395.
- Bolus, M., 2004. Wer war der Neandertaler? In: Conard, N. J. (Ed.): *Woher kommt der Mensch?* Attempto Verlag, Tübingen.
- Bowler, J. M., Johnston, H., Olley, J. M., Prescott, J. R., Roberts, R. G., Shawcross, W., Spooner, N. A., 2003. New ages for human occupation and climatic change at Lake Mungo, Australia. *Nature* 421, 837 – 840.
- Bräuer, G., 1998. Osteometrie. In: Martin, R., Knußmann, R. (eds.): *Anthropologie. Handbuch der vergleichenden Biologie des Menschen.* Gustav Fischer Verlag, Stuttgart – New York, 160 – 230.
- Bräuer, G., 1989. The evolution of modern humans: a comparison of the African and non-African evidence. In: Mellars, P. & Stringer, C. (Eds.): *The human revolution: behavioural and biological perspectives in the origins of modern humans.* Edinburgh University Press.
- Charles, D. K., Condon, K., Cheverud, J. M., Buikstra, J. E. 1986. Cementum annulation and age determination in *Homo sapiens*. I. Tooth variability and observer error. *Am J Phys Anthropol* 71 (3), 311 – 320.
- Churchill S.E, Smith F.H. 2000. Makers of the early Aurignacian of Europe. *Am J Phys Anthropol* 113, Suppl. 31, 61 – 115.
- Condon, K., Charles, D. K., Cheverud, J. M., Buikstra, J. E., 1986. Cementum annulation and age determination in *Homo sapiens*. II. Estimates and accuracy. *Am J Phys Anthropol* 71 (3), 321 – 330.

- Corti, M., 1993. Geometric Morphometrics: An Extension of the Revolution. *Trends Ecol Evol* 8 (8), 302 – 303.
- Cuy, J. L., Mann, A. B., Livi, K. J., Teaford, M. F., Weihs, T. P. 2002. Nanoidentation mapping of the mechanical properties of human molar tooth enamel. *Arch Oral Biol* 47, 281 – 291.
- Darwin, C., 1859. *On the Origin of Species by Means of Natural Selection or the Preservation of Favoured Races in the Struggle for Life*. London: John Murray, Albemarle Street.
- Dubois, E., 1937. On the Fossil Human Skulls Recently Discovered in Java and *Pithecanthropus Erectus*. *Man* 37, 1 – 7.
- Eastoe, J. E. 1960. Organic Matrix of Tooth Enamel. *Nature* 187, 411 – 412.
- El-Zaatari, S., Grine, F. E., Ungar, P. S., Hublin, J. J. 2011. Ecogeographic variation in Neandertal dietary habits: Evidence from occlusal molar microwear texture analysis. *J Hum Evol* 61 (4), 411 – 424.
- Ferembach, D., Schwidetzky, I., Stloukal, M. 1979. Empfehlungen für die Alters- und Geschlechtsdiagnose am Skelett. *Homo* 30, 1 – 32.
- Finlayson, C., 2004. *Neanderthals and Modern Humans*. Cambridge University Press, Cambridge.
- Forster, P., 2004. Ice Ages and the mitochondrial DNA chronology of human dispersals: a review. *Phil Trans R Soc Lond B* 359, 255 – 264.
- Fuhlrott, C. J. (1859). Menschliche Überreste aus einer Felsengrotte des Düsselthals. Ein Beitrag zur Frage über die Existenz fossiler Menschen. *Verhandlungen des Naturhistorischen Vereins Preussen und Rheinland Westphalen* 16, 131-153.
- Gieseler, W., 1936. *Abstammungs- und Rassenkunde des Menschen I*. Hohenlohische Buchhandlung Ferdinand Rau, Oehringen.
- Green, R. E., Krause, J., Briggs, A. W., Maricic, T., Stenzel, U., Kircher, M., Patterson, N., Li, H., Zhai, W., Fritz, M. H.-Y., Hansen, N., Durand, E. Y., Malaspina, A.-S., Jensen, J. D., Marques-Bonet, T., Alkan, C., Prüfer, K., Meyer, M., Burbano, H. A., Good, J. M., Schultz, R., Aximu-Petri, A., Butthof, A., Höber, B., Höffner, B., Siegemund, M., Weihmann, A., Nusbaum, C., Lander, E. S., Russ, C., Novod, N., Affourtit, J., Egholm, M., Verna, C., Rudan, P., Brajkovic, D., Kucan, Ž., Gušić, I., Doronichev, V. B., Golovanova, L. V., Lalueza-Fox, C., de la Rasilla, M., Fortea, J., Rosas, A., Schmitz, R. W., Johnson, P. L. F., Eichler, E. E., Falush, D., Birney, E., Mullikin, J. C., Slatkin, M., Nielsen, R., Kelso, J., Lachmann, M., Reich, D., Pääbo, S., 2010. A Draft Sequence of the Neandertal Genome. *Science* 7, 710 – 722.
- Grine, F., 2012. Observations on Middle Stone Age human teeth from Klasies River Main Site, South Africa. *J Hum Evol* 63, 750 – 758.
- Grine, F., Ungar, P. S., Teaford, M. F., El-Zaatari, S. 2006. Molar microwear in *Praeanthropus afarensis*: Evidence for dietary stasis through time and under diverse paleoecological conditions. *J Hum Evol* 51, 297 – 319.
- Grün, R., Stringer, C., 1991. Electron spin resonance dating and the evolution of modern humans. *Archaeometry* 33, 153 – 199.
- Gustavson, G. 1950. Age determination on teeth. *J Am Dent Assoc* 41 (1), 45 – 54.

- Hammer, Ø., Harper, D.A.T., Ryan, P.D., 2001. PAST: Paleontological Statistics software package for education and data analysis. *Palaeontologia Electronica* 4(1), 1-9.
- Harvati, K., Bauer, C.C., Grine, F.E., Benazzi, S., Ackerman, R.R., van Niekerk, K.L., Henshilwood, C.S. 2015. A human deciduous molar from the Middle Stone Age (Howiesons Poort) of Klipdrift Shelter, South Africa, *J Hum Evol*, <http://dx.doi.org/10.1016/j.jhevol.2015.03.001>
- Harvati, K., Darlas, A., Bailey, S., Rein, T. R., El Zaatari, S., Fiorenza, L., Kullmer, O., Psathi, E., 2013. New Neanderthal remains from Mani peninsula, Southern Greece: The Kalamakia Middle Paleolithic cave site. *J Hum Evol* 64, 486 – 499.
- Harvati, K. & Harrison, T., 2007 (Eds.). *Neanderthals Revisited. New Approaches and Perspectives.* Springer Science + Business Media B. V., Dordrecht, The Netherlands.
- Hillson, S., 1996. *Dental Anthropology.* Cambridge University Press, Cambridge, New York, Port Melbourne, Madrid, Cape Town.
- Howell, F., 1978. Hominidae. In: Maglio, V., Cooke, H. B. S. (Eds): *Evolution of African Mammals.* Harvard University Press, Cambridge.
- Hrdlička, A., 1927. The Neanderthal Phase of Man. *J R Anthropol Inst G* 57, 249 – 274.
- Hubbe, M., Neves, W. A., Harvati, K., 2010. Testing Evolutionary and Dispersion Scenarios for the Settlement of the New World. *PLOS One* 5 (6), 1 – 9.
- Isaac, G. L., Leakey, R. E. F., Behrensmeyer A. K.: *Archaeological Traces of Early Hominid Activities, East of Lake Rudolf, Kenya.* *Science* 17 (173), nol 4002, 1129 – 1134.
- King, W., 1864. The reputed Fossil Man of the Neanderthal. *Q J Sci* 1, 88 – 97.
- Kitagawa, Y., 2000. Nonmetric Morphological Characters of Deciduous Teeth in Japan: Diachronic Evidence of the Past 4000 Years. *Int J Osteoarcheol* 10, 242 – 253.
- Larsen, R., 2005. Functional 2D Procrustes Shape Analysis. *Lect Notes Comput Sc* 3540, 205 – 213.
- Lordkipanidze, D., Ponce de Leon, M. S., Margvelashvili, A., Rak, Y., Rightmire, P., Vekua, A., Zollikofer, C. P. E., 2013. A Complete Skull from Dmanisi, Georgia, and the Evolutionary Biology of Early Homo. *Science* 342, no. 6156, 326 – 331.
- Macho, G., 1994. Variation in enamel thickness and cusp area within human maxillary molars and its bearing on scaling techniques used for studies of enamel thickness between Species. *Arch Oral Biol* 39 (9), 783 – 792.
- Martin, R., 1928. *Lehrbuch der Anthropologie.* 2nd edition, Gustav Fischer Verlag, Stuttgart.
- Martinón-Torres, M., Bastir, M., Bermúdez de Castro, J. M., Gómez, A., Sarmiento, S., Muela, A., Arsuaga, J. L., 2006. Hominin lower second premolar morphology: evolutionary inferences through geometric morphometrics. *J Hum Evol* 50, 523 – 533.
- Nager, G. 1960. Der Vergleich zwischen dem räumlichen Verhalten des Dentin-Kronenreliefs und dem Schmelzrelief der Zahnkrone. *Acta Anat* 42, 225 – 250.
- Nanci, A. 2012. *Ten Cate's Oral Histology, 8th Edition. Development, Structure and Function.* Elsevier, Mosby, St. Louis, Missouri.
- Nielsen, R. B., Alyassin, A. M., Peters, D. D., Carnes, D. L., Lancaster, J. 1995. Microcomputed tomography: an advanced system for detailed endodontic research. *J Endodont* 21 (11), 561 – 568.

- Noback, M. L., Harvati, K., Spoor, F., 2011. Climate-Related Variation of the Human Nasal Cavity. *Am J Phys Anthropol* 145 (4), 599 – 614.
- O’Higgins, P., 2000. The study of morphological variation in the hominid fossil record: biology, landmarks and geometry. *J Anat* 197, 103 – 120.
- O’Higgins, P., Jones, N. 2006. Tools for statistical shape analysis. Hull York Medical School. <https://sites.google.com/site/hymsfme/resources>.
- Palma di Cesnola, A., Messeri, M.P. 1967. Quatre dents humaines paléolithiques trouvées dans des cavernes de l’Italie Méridionale. *L’Anthropologie* 71, 249 – 262.
- Palma di Cesnola, A. 1989. L’Uluzzien: faciès italien du leptolithique archaïque. *L’Anthropologie* 93, 783 – 812.
- Reich, D., Green, R. E., Kircher, M., Krause, J., Patterson, N., Durand, E. Y., Viola, B., Briggs, A. W., Stenzel, U., Johnson, P. L. F., Maricic, T., Good, J. M., Marques-Bonet, T., Alkan, C., Fu, Q., Mallick, S., Li, H., Meyer, M., Eichler, E. E., Stoneking, M., Richards, M., Talamo, S., Shunkov, M. V., Derevianko, A. P., Hublin, J. J., Kelso, J., Slatkin, M., Pääbo, S., 2010. Genetic history of an archaic hominin group from Denisova Cave in Siberia. *Nature* 468, 1053 – 1060.
- Reid, D. J., Dean, M. C. 2000. The Timing of Linear Hypoplasias on the Human Anterior Teeth. *Am J Phys Anthropol* 113 (1), 135 – 139.
- Reyes-Centeno, H., Ghirotto, S., Déroit, F., Grimaud-Hervé, D., Barbujani, G., Harvati, K., 2014. Genomic and cranial phenotype data support multiple modern human dispersals from Africa and a southern route into Asia. *PNAS* 111 (20), 7248 – 7253.
- Rohlf, F. J., 1990. Morphometrics. *Annu Rev Ecol Syst* 21, 299 – 316.
- Rohlf, F. J., Marcus, L. F., 1993. A revolution in morphometrics. *Trends Ecol Evol* 8 (4), 129 – 132.
- Schaaffhausen, H., 1888. Der Neanderthaler Fund. *Archiv für Anthropologie*. Adolph Marcus, Bonn.
- Schwarcz, H., Grün, R., Vandermeersch, B., Bar-Yosef, O., Valladas, H., Tchernov, E., 1988. ESR dates for the hominid burial site of Qafzeh in Israel. *J Hum Evol* 17 (8), 733 – 737.
- Schwartz, J. H., Tattersall, I., 2002. *The Human Fossil Record, Volume One, Terminology and Craniodental Morphology of Genus Homo (Europe)*. John Wiley & Sons, New York.
- Schwartz, J. H., Tattersall, I., 2003. *The Human Fossil Record, Volume Two, Craniodental Morphology of Genus Homo (Africa and Asia)*. John Wiley & Sons, New York.
- Scott, G. R., Turner II, C. G., 1997. *The anthropology of modern human teeth, Dental morphology and its variation in recent human populations*. Cambridge University Press, Cambridge.
- Shen, G., Gao, X., Gao, B., Granger, D. E., 2009. Age of Zhoukoudian *Homo erectus* determined with ²⁶Al/¹⁰Be burial dating. *Nature* 458, 198 – 200.
- Slice, D. E., 2001. Landmark Coordinates Aligned by Procrustes Analysis Do Not Lie in Kendall’s Shape Space. *Syst Biol* 50 (1), 141 – 149.
- Spencer F. & Smith, F. H., 1981. The Significance of Aleš Hrdlička’s „Neanderthal Phase of Man“: A Historical and Current Assessment. *Am J Phys Anthropol* 56, 435 – 459.

- Spoor, C. F., Zonneveld, F. W., Macho, G. A., 1993. Linear measurements of cortical bone and dental enamel by computed tomography: applications and problems. *Am J Phys Anthropol* 91 (4), 469 – 484.
- Stringer, C. B., 2008. The Neanderthal-H. sapiens interface in Eurasia. In: Harvati, K., Harrison, T. (Eds.): *Neanderthals Revisited: New Approaches and Perspectives*. Springer Science+Business Media B. V., Dordrecht, The Netherlands.
- Stringer, C. B., Pálfi, H., van Andel, T., Huntley, B., Valdes, P., Allen, J., 2003. Climatic stress and the extinction of the Neanderthals. In: van Andel, T., Davies, W. (Eds.): *Neanderthals and Modern Humans in the European Landscape during the Last Glaciation*. McDonald Institute Monographs, Cambridge.
- Thorne, A., Grün, R., Mortimer, G., Spooner, N. A., Simpson, J. J., McCulloch, M., Taylor, L., Curnoe, D., 1999. Australia's oldest human remains: age of the Lake Mungo 3 skeleton. *J Hum Evol* 36 (6), 591 – 612.
- Turner, C. G., 1990. Major Features of Sundadonty and Sinodonty, Including Suggestions About East Asian Microevolution, Population History, and Late Pleistocene Relationships With Australian Aborigines. *Am J Phys Anthropol* 82, 295 – 317.
- Ungar, P. S., Grine, F. E., Teaford, M. F., El-Zaatari, S. 2005. Dental microwear and diets of African early Homo. *J Hum Evol* 50, 78 – 95.
- Wahl, J., 2005. Vom Stirn runzelnden Eskimo zum U-Bahnfahrer in Nadelstreifen – Das Erscheinungsbild des Neandertalers im Wandel der Zeiten. In: Conard, N. J., Kölbl, S., Schürle, W. (Eds.): *Vom Neandertaler zum modernen Menschen*. Jan Thorbecke Verlag der Schwabenverlag AG, Ostfildern.
- Weber, G. W., Recheis, W., Scholze, T., Seidler, H., 1998. Virtual Anthropology (VA): methodological aspects of linear and volume measurements – first results. *Coll Antropol* 22, 575 – 584.
- Weber T. 2010. Zahnmedizin. 3rd Issue, Georg Thieme Verlag, Stuttgart, New York.
- Weinert, H., 1936. Der Urmenschenschädel von Steinheim. *Z Morph Anthropol* 35, 463 – 518.
- Wittwer-Backofen, U., Gampe, J., Vaupel, J. W. 2003. Tooth cementum annulation for age estimation: Results from a large known-age validation study. *Am J Phys Anthropol* 123 (2), 119 – 129.
- Zilberman, U., Smith, P. 1992. A comparison of tooth structure in Neanderthals and early Homo sapiens sapiens: a radiographic study. *J Anat* 180 (3), 387 – 393.
- Zilhão, J., 2000. The Ebro frontier: A Model for the Late Extinction of Iberian Neanderthals. In: Stringer, C. B., Barton, R. N. E., Finlayson, J. C. (Eds.): *Neanderthals on the Edge*. Oxbow Books, The Short Run Press, Exeter.

Online resources

- MacLeod, N., 2009. Who is Procrustes and What Has He Done With My Data? http://www.palass.org/modules.php?name=palaeo_math&page=23, last opened 16.06.2015.



Letter

Early dispersal of modern humans in Europe and implications for Neanderthal behaviour

Stefano Benazzi¹, Katerina Douka², Cinzia Fornai¹, Catherine C. Bauer³, Ottmar Kullmer⁴, Jiří Svoboda^{5,6}, Ildikó Pap⁷, Francesco Mallegni⁸, Priscilla Bayle⁹, Michael Coquerelle¹⁰, Silvana Condemi¹¹, Annamaria Ronchitelli¹², Katerina Harvati¹³ & Gerhard W. Weber¹

¹Department of Anthropology, University of Vienna, Althanstrasse 14, 1090 Vienna, Austria;

²Oxford Radiocarbon Accelerator Unit, Research Laboratory for Archaeology and the History of Art, University of Oxford, Dyson Perrins Building, South Parks Road, Oxford OX1 3QY, United Kingdom;

³Paleoanthropology, Department of Early Prehistory and Quaternary Ecology, Eberhard Karls Universität Tübingen, Rümelnstrasse 23, Tübingen 72070, Germany;

⁴Department of Paleoanthropology and Messel Research, Senckenberg Research Institute Frankfurt a. M., Senckenberganlage 25, D-60325 Frankfurt am Main, Germany;

⁵Institute of Archaeology, Academy of Sciences of the Czech Republic, Královopolská 147, 612 00 Brno;

⁶Department of Anthropology, Faculty of Science, Masaryk University, Viničská 5, 603 00 Brno, Czech Republic;

⁷Department of Anthropology, Hungarian Natural History Museum, Ludovika tér 2-6, 1083 Budapest, Hungary;

⁸Department of Biology, University of Pisa, Via S. Maria 53, 56126 Pisa, Italy;

⁹UMR 5199 PACEA, Université Bordeaux 1, avenue des Facultés, 33405 Talence, France ;

¹⁰Paleoanthropology group, Department of Paleobiology Museo Nacional de Ciencias Naturales (MNCM-CSIC), C/ José Gutiérrez Abascal 2, 28006 Madrid – Spain;

¹¹UMR 6578 - Unité d'Anthropologie Bioculturelle, Faculté de Médecine / Secteur Nord, CS80011 Bd Pierre Dramard 13344, Marseille Cedex 15, France;

¹²Department of Environmental Sciences "G. Sarfatti", U.R. Prehistoric Ecology, University of Siena, via T. Pendola 62, 53100 Siena, Italy;

¹³Senckenberg Center for Human Evolution and Paleocology, Eberhard Karls Universität Tübingen, Rümelnstrasse 23, Tübingen 72070, Germany.



The appearance of modern humans in Europe and the nature of the transition from the Middle to Upper Paleolithic are matters of intense debate. Most researchers accept that prior to the arrival of modern humans, Neanderthals had adopted several so-called ‘transitional’ technocomplexes. Two of these, the Uluzzian of southern Europe and the Châtelperronian of western Europe, play a key role in current interpretations regarding the timing of arrival of modern humans in the region and their potential interaction with Neanderthal populations. They are also central to current debates regarding the cognitive abilities of Neanderthals and the reasons behind their extinction¹⁻⁶. The actual fossil evidence associated with these assemblages however is scant and fragmentary⁷⁻¹⁰ and recent work has questioned the attribution of the Châtelperronian to Neanderthals on the basis of taphonomic mixing and lithic analysis¹¹⁻¹². Here we reanalyze the deciduous molars from the Grotta del Cavallo (southern Italy), associated with the Uluzzian and originally classified as Neanderthal^{13,14}. Using two independent morphometric methods based on microtomographic (μ CT) data, we show that the Cavallo specimens are anatomically modern humans. The secure context of the teeth provides crucial evidence that the makers of the Uluzzian technocomplex were therefore not Neanderthals. In addition, new chronometric data for the Uluzzian levels of Grotta del Cavallo obtained from associated shell beads and included within a Bayesian age model show that the teeth must date to ~45,000-43,000 cal BP. The Cavallo human remains are therefore the oldest known European modern humans, confirming a rapid dispersal of moderns across the continent prior to the Aurignacian and the disappearance of Neanderthals.

Two deciduous molars (Cavallo-B and Cavallo-C) were excavated in 1964 from the site of Grotta del Cavallo (Apulia, southern Italy; Supplementary Information). Cavallo is important as the type-site of the Uluzzian technocomplex¹⁵, one of the main three transitional industries alongside the Châtelperronian and Szeletian, in Franco-Cantabria and Central Europe, respectively. These are strongly suspected of being produced by Neanderthals, although the actual fossil evidence in association is scant¹⁶.

Cavallo-B is a deciduous left upper first molar (dm^1), found in Layer EIII (archaic Uluzzian). Cavallo-C is a deciduous left upper second molar (dm^2) found 15-20 cm above Cavallo B, in Layer EII-I (evolved Uluzzian)¹³ (Fig. S1; Table S1). The specimens (Fig. 1) were described in 1967 by Palma di Cesnola and Messeri¹³ who classified Cavallo-B as modern human and



Cavallo-C as Neanderthal. On this basis, the authors suggested a persistence of Neanderthal populations in southern Italy after the appearance of modern humans¹⁷.

Although information about these specimens is scarce and contradictory, most scholars accept that the deciduous molars from Grotta del Cavallo are attributable to Neanderthals, and therefore that Neanderthals produced the Uluzzian. This attribution was proposed by Churchill and Smith¹⁴ for Cavallo-B on the basis of the specimen's crown diameters (Cavallo-C's dimensions were found to be compatible with both Neanderthals and modern humans). However, the Cavallo-B buccolingual and mesiodistal diameters used by Churchill and Smith¹⁴ appear to have been accidentally substituted for each other when compared to the crown diameters reported by Palma di Cesnola and Messeri¹³. The correct crown diameter values do not support Neanderthal affinities for Cavallo-B, neither does the crown morphology of the two specimens. Cavallo-B shows three dental cusps, typical of modern human dm^1 s¹⁰, with the lingual cusps mesially oriented and separated from the buccal cusps by a well-defined sagittal sulcus. Conversely, Neanderthal dm^1 s are more frequently four-cusped with cusp tips compressed internally¹⁰. Cavallo-C has a sub-square crown outline, similar to modern human dm^2 s and different from the typical rhomboid outline with distolingual hypocone expansion of Neanderthal dm^2 s¹⁰.

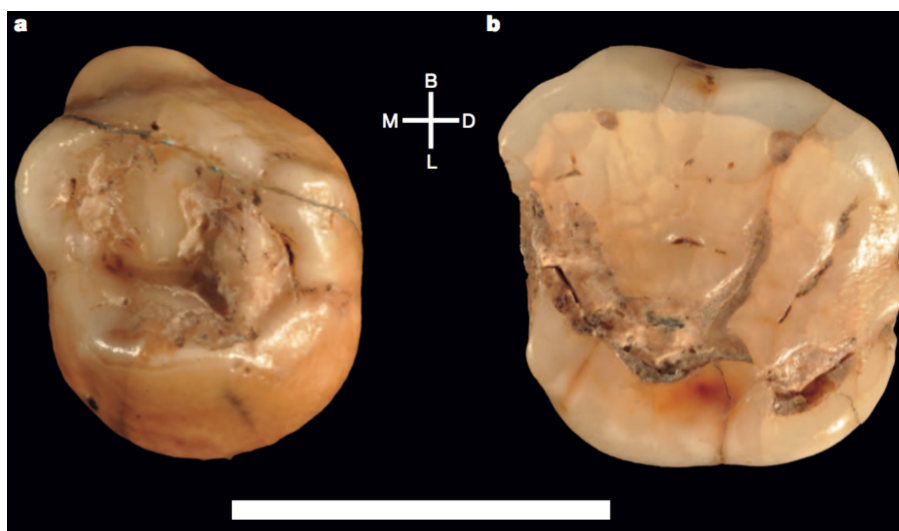


Fig. 1: Occlusal view of the deciduous molars from the Uluzzian levels of Grotta del Cavallo (Apulia, southern Italy). **a**, Cavallo-B (deciduous left upper first molar – dm^1). **b**, Cavallo-C (deciduous left upper second molar – dm^2). B: buccal; D: distal; L: lingual; M: mesial. The white bar in the figure is equivalent to 1 cm.

In order to firmly establish the taxonomic affinities of the Cavallo human remains, we re-analyzed Cavallo-B and Cavallo-C with two independent morphometric methods, using a comparative sample of Neanderthal (N), Upper Paleolithic modern human (UPMH) and recent modern human (RMH) dm^1 and dm^2 specimens (Tables S2-S4).

Our first approach is a geometric morphometric analysis of outlines obtained from the dental crown¹⁸ (see Methods), for which the group shape variation was evaluated through a shape-space Principal Component Analysis (PCA).

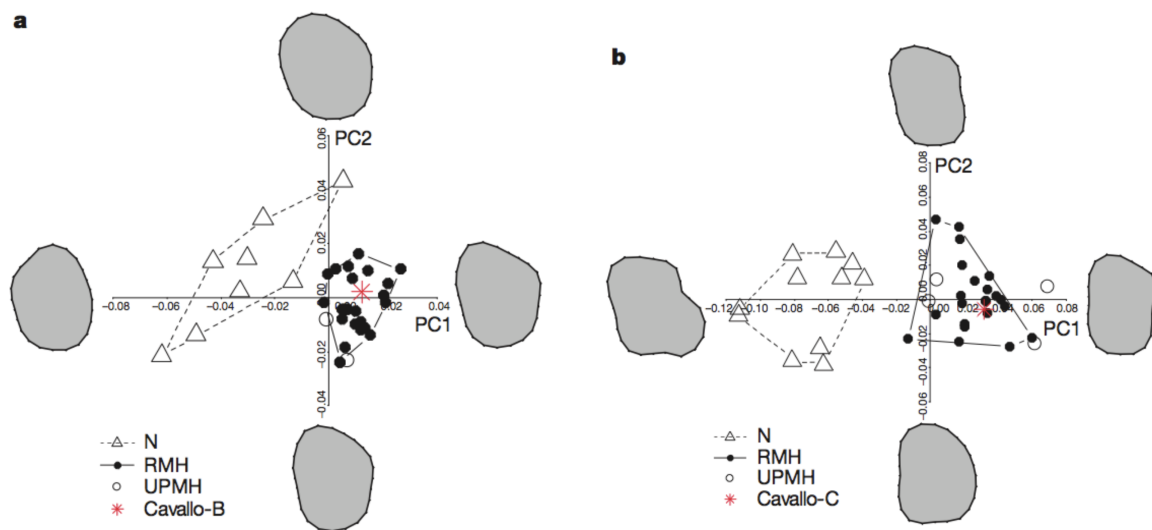


Fig. 2. Shape-space PCA plots of dm^1 crown outlines and dm^2 cervical outlines. **a**, dm^1 crown outline. **b**, dm^2 cervical outline. The deformed mean crown outline in the direction of the PC is drawn at the extremity of each axis. N: Neanderthal; RMH: recent modern human; UPMH: Upper Paleolithic modern human.

For the dm^1 crown outlines (Fig. 2a), the first two principal components (PCs) account for about 63% of the total variance. Neanderthals and modern humans separate along PC1 (42.7%), which characterizes size-independent shape variation ($r = -0.33$; $p = 0.06$). Neanderthal dm^1 s show an ovoid outline, while RMH and UPMH specimens are more irregularly shaped for the presence of well-expressed tuberculum molare (molar tubercle of Zuckerkandl) and metacone (buccodistal) cusp, and for a general distolingual constriction due to the reduction of the hypocone. Cavallo-B plots well within the range of variability of the

modern human sample. The cross-validation Quadratic Discriminant Analysis (QDA) of the PC1 scores classified Cavallo-B as modern human with a posterior probability ($P_{\text{post}} > 0.90$) (Table S4).

In the analysis of the dm^2 cervical outlines (Fig. 2b), the first two PCs account for about 84% of the total variance. Neanderthals and modern humans are even more clearly separated along PC1 (71.4%), which expresses size-dependent shape variation (static allometry, $r = 0.74$; $p < 0.001$). Neanderthal dm^2 s are characterized by a rhomboid cervical outline due to their large hypocone, while UPMH and RMH specimens have sub-square outlines. Cavallo-C plots unambiguously within the modern human range. The cross-validation QDA of the first two PC scores attributes Cavallo-C to modern human with a $P_{\text{post}} > 0.90$ (Table S4).

The second morphometric method considers the internal structures of the teeth and consists of the two-dimensional (2D) enamel thickness and dental tissue proportions analysis (Fig.3) (see Methods and Tables S3-S4). The average and relative enamel thickness (AET and RET, respectively) have been described as effective taxonomic discriminators between Neanderthals and modern humans since Neanderthal molars are characterized by significantly thinner enamel relative to dentine volume¹⁹.

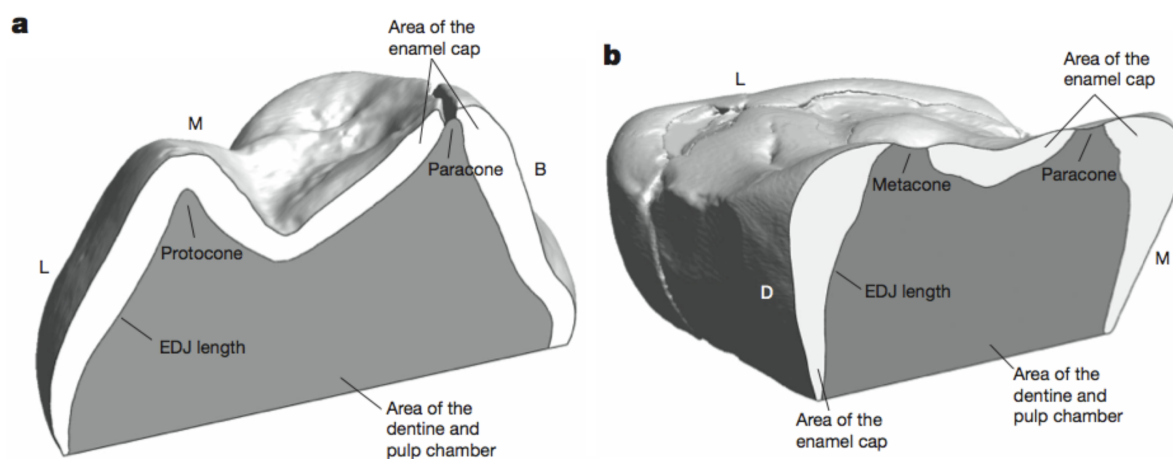


Fig. 3. Cross-sections of Cavallo-B and Cavallo-C for 2D enamel thickness analysis. **a**, Buccolingual cross-section of Cavallo-B through the dentine horns of the protocone and paracone. **b**, Mesiodistal cross-section of Cavallo-C through the dentine horns of the paracone and metacone. EDJ: enamel dentin junction; B: buccal; D: distal; L: lingual; M: mesial.

The dm^1 modern human samples (UPMH and RMH) shown in Table 1 have been divided into sub-groups on the basis of their degree of wear (unworn/wear stage 1 distinguished by wear stage 3; based on Smith²⁰) to ease the comparison with the Neanderthal dm^1 's sample, which is entirely affected by wear stage 3. The Neanderthal dm^1 RET indexes are significantly lower than those of RMH at similar wear stages ($p < 0.001$; permutation test, $n = 1000$) on group mean and variance differences. The AET and RET indexes of Cavallo-B lie beyond the highest values computed so far for the unworn UPMH and RMH (Table 1). Considering that the RET index average difference from unworn to wear stage 3 for both RMH and UPMH is about 0.80, it is reasonable to assume that if Cavallo-B would have worn down to a wear stage 3, it would provide a RET index of approximately 11. This value is still completely outside the Neanderthal range of variation and near the highest values computed for the unworn RMH. The result further supports strongly the affiliation of Cavallo-B as modern human rather than as Neanderthal.

Table 1. 2D enamel thickness of Cavallo-B and Cavallo-C compared with Neanderthal (N), Upper Paleolithic modern human (UPMH), recent modern human (RMH) dm^1 's and dm^2 's (SD in brackets)

| Tooth | Taxon | Wear stage ^a | <i>n</i> | AET ^b (mm) | | RET ^c (scale free) | |
|--------|-------------|-------------------------|----------|-----------------------|-----------|-------------------------------|-------------|
| | | | | Mean | Range | Mean | Range |
| dm^1 | Neanderthal | 3 | 6 | 0.40 (0.03) | 0.37-0.45 | 7.17 (0.54) | 6.61-7.93 |
| | UPMH | 3 | 2 | 0.51 (0.01) | 0.50-0.52 | 9.56 (0.13) | 9.47-9.66 |
| | RMH | 3 | 14 | 0.47 (0.03) | 0.43-0.52 | 9.12 (0.67) | 8.50-10.52 |
| | UPMH | unworn | 1 | 0.56 | | 10.36 | |
| | RMH | unworn-stage 1 | 8 | 0.51 (0.06) | 0.41-0.58 | 9.96 (0.96) | 8.66-11.36 |
| | Cavallo-B | unworn | | | 0.69 | | 11.80 |
| dm^2 | N | unworn-stage 1 | 9 | 0.63 (0.04) | 0.58-0.69 | 10.89 (0.84) | 9.60-12.39 |
| | UPMH | stage 1-stage 2 | 2 | 0.97 (0.15) | 0.86-1.07 | 17.93 (1.40) | 16.94-18.92 |
| | RMH | unworn-stage 3 | 23 | 0.73 (0.08) | 0.56-0.93 | 13.84 (1.53) | 11.43-18.00 |
| | Cavallo-C | stage 5 | | | 0.84 | | 14.28 |

^aBased on Smith²⁰; ^bAET = average enamel thickness index; ^cRET = relative enamel thickness index

With regard to the dm^2 's (Table 1), the Neanderthal RET indexes are significantly lower than those of RMH ($p < 0.001$). The UPMH specimens present the highest AET and RET indexes of the whole sample, RMH included. Cavallo-C is the most worn specimen within our dm^2 sample (wear stage 5), therefore the AET and RET indexes result in a rather lower value than could be expected for the unworn stage of the same tooth. Nonetheless, both indexes still rank

among the highest values obtained (Table 1). The cross-validation QDA of the dm^2 RET index classifies Cavallo-C as modern human with a $P_{\text{post}} > 0.90$ (Table S4).

New radiocarbon dating of the Uluzzian levels was undertaken to produce a more robust chronology. Previous dates from the site disclosed inconsistency due to incomplete decontamination and unsuitability of the dated samples (Supplementary Information). In the absence of collagen from bone at the site and the lack of charcoal samples collected at the time of the excavation, marine shell samples were the only alternative and were therefore selected for dating. The majority of the shells were transformed into beads, by snapping or piercing to produce personal ornaments generally held to be an indicator of symbolic and complex behaviour. Eight shells of *Dentalium* sp., *Nuculana* sp. and *Cyclope neritea* were dated by AMS radiocarbon dating following a novel methodological approach (Supplementary Information and Fig. S3). The new dates were incorporated into a Bayesian model using the OxCal programme (Supplementary Information) and calibrated against the INTCAL09 calibration curve²¹ (Figs. S4, S5; Tables S5, S6). Level E III was calculated by the model to date between 45,010—43,380 (68.2% prob.) and 47,530—43,000 (95.4% prob.) cal BP. The distribution falls within Greenland Interstadial (GIS) 12, a long warm phase following Heinrich Event 5, and most likely towards its latter part. A decrease in temperature has been inferred based on the faunal assemblage from EIII²². Muller et al.²³ have previously suggested a likely initial arrival of moderns during this post-HE5 interstadial. Level EII-I, associated with a shell date of 40,000 ¹⁴C BP, was modelled to date between 44,000—43,000 cal BP (68.2% prob.), a similar age to level EIII. Comparable chronometric results were obtained from Grotta di Fumane, another Uluzzian site in the Italian pre-Alps and the only other with reliable chronometric information, where the technocomplex is dated at 44,600-44,200 cal BP (68.2% prob.) (or $\approx 42,000$ -40,000 ¹⁴C BP)²⁴.

The new chronometric results show that the two deciduous molars from Grotta del Cavallo are the earliest European modern human fossils currently known. Since the Uluzzian technocomplex stratigraphically underlies the earliest Aurignacian in all instances where the two co-occur (e.g. Grotta di Castelcivita, Grotta della Cala, Grotta La Fabbrica and Grotta di Fumane)⁵, the arrival of the earliest modern humans at these sites must predate the Aurignacian. Furthermore, considering that Neanderthals are likely to have survived in most of continental Europe until at least $\approx 40,000$ cal BP²⁵, our results offer fossil evidence for a longer period of co-existence in Europe between Neanderthals and modern humans.



The re-attribution of the teeth of Grotta del Cavallo to modern human has implications for the interpretation of the Uluzzian technocomplex^{14,16}. The presence of personal ornaments in the form of marine shell beads, worked bone and colorants, including ochre and limonites, in the Uluzzian levels of Cavallo^{5,6} has been used as direct evidence for Neanderthals reaching behavioural modernity independent of, and prior to, modern humans reaching Europe^{1,26}. These attributes are all more typical of Upper Paleolithic industries. This multiple species model for the origin of fully modern behaviour has been considered by some to be an impossible coincidence²⁷ and a fervent debate has ensued among prehistorians on the behavioural and cognitive capabilities of the makers of the transitional industries found across Europe and the Levant. Our results show that the Uluzzian is not a Neanderthal industry.

Stratigraphically, the Uluzzian is always separated from the final Mousterian by sterile layers, volcanic ash (as in Cavallo), erosional discontinuities or depositional hiatuses, which would suggest that a period of time has elapsed between the two phases. In southern Italy, economic and cultural behaviour of the Uluzzian suggests a greater affinity with the succeeding Aurignacian (with marginally backed tools) than with the final Mousterian^{5,6,22}. These findings provide additional support for a modern human authorship of the Uluzzian. While we cannot extrapolate our conclusions to other transitional industries, our findings suggest caution should be applied in associating Neanderthals with them, particularly the Châtelperronian and Szeletian (see details of the ongoing debate on this topic in^{2-4,9,11,12}).

The association of the Uluzzian with modern humans implies much greater complexity and age-depth to the movement of moderns into Europe and may lend support to a southern Mediterranean route in their dispersal, similar to that identified by Mellars²⁷ for the spread of the Aurignacian. While it is during the Aurignacian that certain technological and behavioural innovations effloresce, such as blade and bladelet-dominated lithic assemblages, bone and ivory tools, art and personal ornaments, the initial appearance of these traits in southern Europe clearly predates this. This discovery has significant implications for our understanding of the earliest presence of modern humans in Europe, expands the period of overlap between moderns and Neanderthals and makes it much less likely that Neanderthals developed their own Upper Palaeolithic suite of behaviors prior to the arrival of moderns.



Methods Summary

The comparative dental sample for both the morphometric outline analyses and the 2D enamel thickness and dental tissue proportions analysis is provided in the Table S2.

Scans of all the specimens were undertaken by means of industrial and synchrotron-based μ CT scanners at isotropic voxel length between 15 and 55 μ m. The μ CT image stacks of each tooth were aligned with the cervical plane parallel to the xy-plane of the Cartesian coordinate system. The 3D digital surface models were created semi-automatically by threshold-based segmentation, contour extraction, and surface reconstruction.

For the outline analyses we considered the dm¹ crown outlines since Cavallo-B is unworn; conversely, we used the cervical outlines of the dm²s, since Cavallo-C shows both occlusal and interproximal wear. To identify the crown outline and the cervical outline we followed the procedures described in Benazzi et al.¹⁸, with some adjustment for our specific case (Method section).

For the analyses of the 2D enamel thickness and dental tissue proportions (Method section), the following measurements were recorded: the area of the enamel cap (mm²), the area of the coronal dentine (which includes the coronal pulp – mm²), the length of the enamel-dentine junction (EDJ – mm), the average enamel thickness (AET) index (the area of the enamel cap divided by the length of the EDJ; index in mm), and the RET index (the average enamel thickness divided by the square root of the coronal dentine area; scale free index)^{19,28}. The data was analyzed via software routines written in R²⁹ (Supplementary Information).

References

1. d'Errico, F., Zilhão, J., Julien, M., Baffier, D. & Pélegrin, J. Neanderthal acculturation in Western Europe? A critical review of the evidence and its interpretation. *Curr. Anthropol.* 39, 1-44 (1998).
2. Gravina, B., Mellars, P. & Ramsey, C.B. Radiocarbon dating of interstratified Neanderthal and early modern human occupations at the Châtelperronian type-site. *Nature* 438, 51-56 (2005).



3. Mellars, P., Gravina, B. & Bronk Ramsey C. Confirmation of Neanderthal/modern human interstratification at the Châtelperronian type-site. *Proc. Natl. Acad. Sci.* 104, 3657-62 (2006).
4. Zilhão, J. et al. Analysis of Aurignacian interstratification at the Châtelperronian-type site and implications for the behavioral modernity of Neandertals. *Proc. Natl. Acad. Sci.* 103, 12643-8 (2006).
5. Ronchitelli, A., Boscato, P. & Gambassini, P. in *La lunga storia di Neandertal. Biologia e comportamento* (eds Facchini, F. & Belcastro, G.M.) (Jaca Book, 2009).
6. d'Errico, F., Borgia, V. & Ronchitelli, A. Uluzzian bone technology and its implications for the origin of behavioural modernity. *Quat. Int.* In press. doi:10.1016/j.quaint.2011.03.039 (2011).
7. Lévêque, F. & Vandermeersch B.M. Découverte de restes humains dans un niveau castelperronien à Saint-Césaire (Charente-Maritime). *CR Acad. Sci. Paris* 291, 187-189 (1980).
8. Hublin, J.J., Spoor, F., Braun, M., Zonneveld, F. & Condemi, S. A late Neanderthal associated with Upper Palaeolithic artefacts. *Nature* 381, 224-226 (1996).
9. Harvati, K., Panagopoulou, E., Karkanas, P. First Neanderthal remains from Greece: the evidence from Lakonis. *J. Hum. Evol.* 45, 465-73 (2003).
10. Bailey, S.E. & Hublin, J.J. Dental remains from the Grotte du Renne at Arcy-sur-Cure (Yonne). *J. Hum. Evol.* 50, 485-508 (2006).
11. Bar-Yosef, O. & Bordes, J. G. Who were the makers of the Châtelperronian culture? *J. Hum. Evol.* 59, 586-593 (2010).
12. Higham, T. et al. Chronology of the Grotte du Renne (France) and implications for the context of ornaments and human remains within the Châtelperronian. *Proc. Natl. Acad. Sci.* 107, 20234-9 (2010).
13. Palma di Cesnola, A. & Messeri, M.P. Quatre dents humaines paléolithiques trouvées dans des cavernes de l'Italie Méridionale. *L'Anthropologie* 71, 249-262 (1967).
14. Churchill, S.E. & Smith, F.H. Makers of the early Aurignacian of Europe. *Am. J. Phys. Anthropol. Suppl* 31, 61-115 (2000).
15. Palma di Cesnola, A. L'Uluzzien: faciès italien du leptolithique archaïque. *L'Anthropologie* 93, 783-812 (1989).
16. Riel-Salvatore, J. in *Sourcebook of Paleolithic Transitions* (eds Camps, M. & Chauhan, P.) (Springer Science, 2009).
17. Messeri, P. & Palma di Cesnola, A. Contemporaneità di paleantropi e fanerantropi sulle coste dell'Italia meridionale. *Zephyrus* 26-27, 7-30 (1976).
18. Benazzi, S. et al. Comparison of dental measurement systems for taxonomic assignment of first molars. *Am. J. Phys. Anthropol.* 144, 342-54 (2011).
19. Olejniczak, A.J. et al. Dental tissue proportions and enamel thickness in Neanderthal and modern human molars. *J. Hum. Evol.* 55, 12-23 (2008).
20. Smith, B.H. Patterns of molar wear in hunter-gatherers and agriculturists. *Am. J. Phys. Anthropol.* 63, 39-56 (1984).



21. Reimer, P.J. et al. IntCal09 and Marine09 radiocarbon age calibration curves, 0–50,000 years cal BP. *Radiocarbon* 51, 1111–1150 (2009).
22. Boscato, P. & Crezzini, J. Middle-Upper Palaeolithic transition in Southern Italy: Uluzzian macromammals from Grotta del Cavallo (Apulia). *Quat. Int.* In press. doi:10.1016/j.quaint.2011.03.028 (2011).
23. Müller, U.C., Pross, J., Tzedakis, P.C., Gamble, C., Kotthoff, U., Schmiedl, G., Wulf, S. & Christanis, K. The role of climate in the spread of modern humans into Europe. *Quat. Sci. Rev.* 30, 273–279 (2011).
24. Higham, T. European Middle and Upper Palaeolithic radiocarbon dates are often older than they look: problems with previous dates and some remedies. *Antiquity* 85, 235–249 (2011).
25. Pinhasi, R., Higham, T.F., Golovanova, L.V., Doronichev, V.B. Revised age of late Neanderthal occupation and the end of the Middle Paleolithic in the northern Caucasus. *Proc. Natl. Acad. Sci.* 108, 8611–6 (2011).
26. Zilhão, J. in *Continuity and Discontinuity in the Peopling of Europe* (eds Condemni, S. & Weniger, G.C.) (Springer, 2011).
27. Mellars, P. The impossible coincidence: a single species model for the origins of modern human behavior in Europe. *Evol. Anthropol.* 14, 12–27 (2005).
28. Martin, L.B. Significance of enamel thickness in hominoid evolution. *Nature* 314, 260–263 (1985).
29. R Development Core Team. *R: a language and environment for statistical computing*. Vienna, Austria: R Foundation for Statistical Computing. <http://www.r-project.org>. (2008)

Supplementary Information is linked to the online version of the paper at www.nature.com/nature

Acknowledgements

We would like to thank the Soprintendenza per i Beni Archeologici della Puglia which facilitated the excavation of Grotta del Cavallo over the years. A special debt is due to M.A. Gorgoglione who supported and helped in the collection of samples for ^{14}C dating and encouraged the collaboration with the University of Siena for the study of the human fossil remains. P. Boscato, H. Klempererova, F. Ranaldo, S. Ricci have all helped in aspects of the research and are especially thanked. We are grateful to G. Gruppioni for providing the Italian modern human sample used in this work. We thank M. Francken, B. Trautmann, I. Trautmann, H. Scherf, M. Dockner and R. Ginner for technical assistance. We thank F.L. Bookstein for suggestions on statistics.



Access to the fossil specimens was made possible by the Croatian National History Museum, the French Musée National de Préhistoire, the French Muséum National d'Histoire Naturelle, Paleoanthropology, Eberhard Karls Universität Tübingen and the NESPOS (Neanderthal Studies Professional Online Service) Database 2011 (<https://www.nespos.org/display/openspace/Home>).

We acknowledge the Centre de Microtomographie (Université de Poitiers, France), the Vienna micro-CT Lab (University of Vienna, Austria), the Paleoanthropology High Resolution Computing Tomography Laboratory (Eberhard Karls Universität Tübingen, Germany), the European Synchrotron Radiation Facility beamline ID17, the AST-RX platform (French Muséum National d'Histoire Naturelle) and the Oxford Radiocarbon Accelerator Unit (ORAU). The authors would like to thank T. Higham and R.E.M. Hedges for their input in the radiocarbon dating part of the project, for important comments and proof-reading this manuscript. The radiocarbon dating was funded by the Natural Environment Research Council (NERC) NRCF programme. KD is part of the Ancient Human Occupation of Britain (AHOB) project, funded by the Leverhulme Trust. This work was supported by the NSF 01-120 Hominid Grant 2007, A.E.R.S. Dental Medicine Organisations GmbH FA547013, the Fondation Fyssen and the DFG INST 37/706-1 FUGG.

Author Contributions S.B., F.M., K.H. and G.W.W. initiated and organized the project. S.B., C.B., P.B., J.S., I.P., K.H., G.W.W. collected the fossils and modern human sample. S.B. and C.F. carried out the dental measurements. S.B. and M.C. analyzed the data. K.D. initiated and performed the radiocarbon dating project. S.B., K.D., C.F., O.K., M.C., S.C., A.R., K.H., G.W.W. discussed the results. S.B., K.D., C.F., M.C., S.C., A.R., K.H., G.W.W. wrote and edited the manuscript.

Author Information Reprints and permissions information is available at www.nature.com/reprints. The authors declare no competing financial interests. Correspondence should be addressed to S.B. (stefano.benazzi@univie.ac.at), Althanstrasse 14, 1090 Vienna, AUSTRIA. Phone: 0043 (01)-4277-54729; Fax: 0043 (01)-4277-9547



Methods

Scanning, segmentation and 3D reconstruction of the specimens. Microtomographic scans (μ CT) of all the specimens (Table S2) were undertaken by means of industrial and synchrotron-based μ CT scanners at isotropic voxel length between 15 and 55 μ m. The μ CT image stacks of each tooth were aligned to the best-fit plane computed at the cervical line (cervical plane) through Amira 5.3 (Mercury Computer Systems, Chelmsford, MA), and then rotated up to the cervical plane was parallel to the xy-plane of the Cartesian coordinate system. For the segmentation process, the half-maximum height (HMH) protocol was used to reconstruct 3D digital surface models of each μ CT-scanned tooth using Amira 5.3 (Supplementary Information).

Outline data. A further orientation of the dm^1 and dm^2 digital models in the Cartesian coordinate system was required previous to the outline analysis. The dm^1 oriented digital models were rotated around the z-axis to align the projection on the xy-plane of the intercept between the paracone and protocone cusp tips parallel to the y-axis of the Cartesian coordinate system. The crown outlines were then projected onto the xy-plane. The dm^2 digital models were oriented with the lingual side parallel to the x-axis. The best-fit plane of the cervical line identified the cervical outline. In one case (the Neanderthal specimen Engis 2), Computer-Aided Design (CAD) techniques were used to restore the dm^1 crown outline (Fig. S2).

All the outlines were represented by 24 landmarks obtained by equiangularly spaced radial vectors out of the centroid of their area¹⁸. These landmarks were superimposed through a Generalized Procrustes Analysis (GPA)³⁰. Since the outlines were oriented and centered on the centroid of their area¹⁸, GPA only entailed a uniform scaling of the landmark configurations to unit Centroid Size. This step removed size differences, except for static allometry.

Two-dimensional (2D) enamel thickness data. For the 2D enamel thickness assessment we followed the techniques developed by Martin²⁸, adapted to our specific case. A plane perpendicular to the cervical plane of the tooth and passing through two dentine horn tips was used for sectioning the dental crowns. The section passed through the dm^1 's paracone and protocone dentine horn tips, and through the dm^2 's paracone and metacone dentine horn tips

(Fig. 3). The dentine horn tips were identified as the highest points of the dentine in the central mammelon by scrolling apically through the oriented slices. For Cavallo-C (wear stage 5; based on Smith²⁰) and the comparative sample with wear stage 3, this approach was further verified by segmenting the whole crown dentine in order to check the continuity of the marginal ridges beside the dentine horns. For worn teeth, the EDJ length was truncated at the exposed edge of the occlusal dentine basins.

Cavallo-B shows a crack crossing the paracone mesiodistally (Fig. 3a). The area of the crack pertaining to the dentine was included in the dentine area, as well as the trait of the EDJ interested by the crack was calculated in the EDJ length. On the contrary, the missing area of the enamel cap was not reconstructed. Therefore, the computed RET index for Cavallo-B is slightly underestimated.

The segmentation process and the parameter measurements were carried out by two of us (SB and CF). The interobserver error was evaluated for the enamel and dentine area of three of the fossil specimens from our sample, and did not exceed 3% in each case.

The following measurements were recorded: the area of the enamel cap (mm^2), the area of the coronal dentine (which includes the coronal pulp – mm^2), the length of the enamel-dentine junction (EDJ – mm), the average enamel thickness (AET) index (the area of the enamel cap divided by the length of the EDJ; index in mm), and the RET index (the average enamel thickness divided by the square root of the coronal dentine area; scale free index)^{19,28}.

Statistical analysis. A Principal Component Analysis (PCA) of the matrix of Procrustes coordinates was carried out for the dm^1 crown outlines and dm^2 cervical outlines, separately. Since we aimed at assessing the dental outline shapes of the teeth from Grotta del Cavallo with respect to both the modern human and the Neanderthal outline shape variation, Cavallo-B and Cavallo-C spatial configurations were projected into the space built from the comparative sample only. In the Supplementary Information we show that the first PC of dm^1 crown outlines PCA and the first two PCs of dm^2 cervical outlines PCA are the only informative ones.

We did not regress the part of radial size correlated with the diameters, diagonals, and area out of the crown and cervical outline data (as already suggested by Benazzi et al.¹⁸ for the first



permanent molars), because size information related to static allometry is an important factor for the separation of Neanderthal and modern human dm^2 s.

The differences between Neanderthal and RMH' AET and RET indexes, were tested via a permutation test ($n = 1000$) on group mean and variance.

Finally, we used leave-one-out cross-validation Quadratic Discriminant Analysis (QDA) for the taxonomic classification of Cavallo-B and Cavallo-C. We built up QDA models leaving out the data from the Cavallo specimens. The computation of the posterior probabilities (P_{post}) was made with an equal prior probability (P_{prior}) of 0.5 for Neanderthal and modern human groups (UPMH plus RMH). The threshold for taxonomic determination was a $P_{post} \geq 0.90$. The taxonomic analyses are summarized in the Supplementary Information. The data was processed and analyzed through software routines written in R²⁹.

30. Rohlf, F.J. & Slice, D.E. Extensions of the Procrustes method for the optimal superimposition of landmarks. *Syst. Zool.* 39, 40-59 (1990).

Supplementary Methods

GROTTA DEL CAVALLO

Description of the site and history of excavations

Grotta del Cavallo (40°9'18.85"N, 17° 57' 37.27"E) is situated on the rocky coast of the Bay of Uluzzo, Nardò, around 90 km south of the town of Taranto in Apulia, SE Italy. It is located within a low Mesozoic limestone plateau, about 15m above the present day shore, with a large, 5 m wide by 2.5 m high opening facing NW and an approximately circular shape, about 9 m in diameter³¹. Cavallo was discovered in 1960 and was initially investigated in 1961 by A. Palma di Cesnola. Official excavations took place between 1963–1966³¹⁻³⁴, and again between 1986–2008 focusing on the Mousterian parts of the sequence^{35,36}. In the interlude between the two series of excavations, looters severely disturbed the central part of the deposits, removing much of the Upper Palaeolithic layers. In the light of this damage, salvage excavations were conducted by the University of Siena (P. Gambassini and colleagues) for four seasons in the late 1970s/early 1980s and a metal gate was installed at the entrance of the cave. In the process of installing it, the standing sections were cleaned and some free-standing

deposits at the entrance of the cave were carefully removed and correlated to the original stratigraphy.

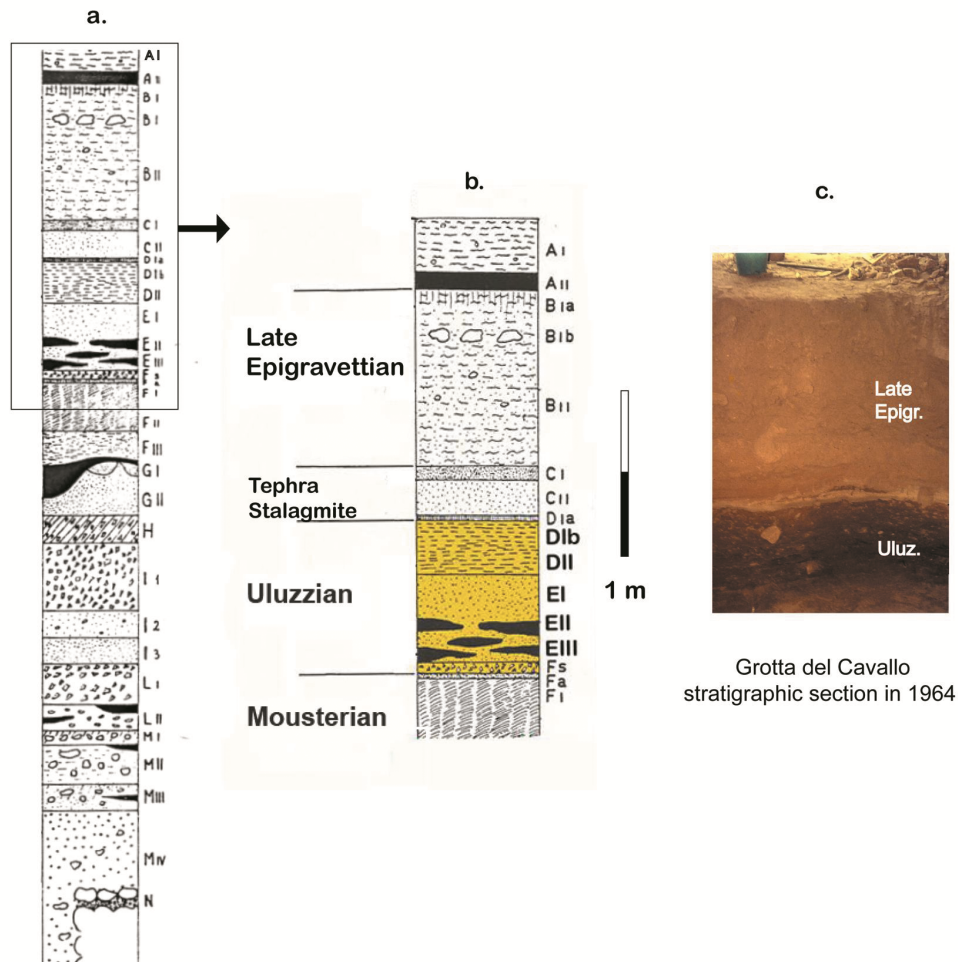


Figure S1: Section drawing of the Palaeolithic sequence of Grotta del Cavallo. **a**, The entire stratigraphic section of Cavallo Cave, after Palma di Cesnola³⁸; **b**, detail of the section showing only the late Mousterian and UP layers; **c**, the section photograph illustrates the clear distinction between the very dark Uluzzian deposits from the lighter-coloured sediments of the later UP layers at the site.

Stratigraphy

The site preserves a long stratigraphic succession comprising about 7 m of archaeological deposits directly based on a marine interglacial beach conglomerate (layer N) (Fig. S1). The archaeological sequence of Cavallo is dominated by Middle Palaeolithic layers (MIV-F I),

capped by a thin layer of green volcanic ash (F α), which separates Mousterian from the overlying Uluzzian layers (E-DIb) (Fig. S1).

The Uluzzian deposits, about 80-85 cm thick, were excavated both in the 1960s and in the late 1970s/early 1980s at separate sections of the site. A correlation is given in Table S1.

Table S1: Cross-correlation of Uluzzian layers at Cavallo, revealed in the original excavations of Palma di Cesnola (1963-1966) and in the subsequent rescue operations in the late 1970s and early 1980s.

| Layers (1963-1966) | Spits (1978-1984) |
|--------------------|-------------------|
| DIb | D1–D2 |
| DII | D3–D4 |
| E-D | E 1 |
| EII-I | E2–E4 |
| EIII | E5–E7 |

These layers are divided into Archaic Uluzzian (E III), Evolved Uluzzian (EII-I) and Final Uluzzian (D II – D Ib)³⁷⁻⁴⁰. They are separated from the upper part of the sequence by a stalagmitic crust (D Ia) and two sterile layers of volcanic ash (C II and C Ia-b). The tephra in layer C has been traditionally assigned to the Campanian Ignimbrite eruption⁴¹ on empirical grounds and by comparison to other sequences (e.g. Castelcivita), but no geochemical characterisation has been attempted. Directly superimposed are Epigravettian horizons B II- B I (Romanellian and Epiromanellian *facies*), of much younger age (\approx 11,000 yr BP).

The Uluzzian layers of Cavallo comprise the most complete stratified sequence of the technocomplex ever revealed.

DENTAL MORPHOMETRIC ANALYSIS

Comparative sample

Table S2 shows the comparative sample used for the morphometric analyses. The whole corpus, except for the UPMH specimen Brillenhöhle, was used for outline analysis. For enamel thickness and dental tissue proportions, only individuals with wear stage equal or lower than 3 (based on Smith⁴²) were selected. Nonetheless, the different wear stage of the fossil sample forced us to follow different solutions for dM¹ and dM². The fossil dM¹ sample

is almost completely dominated by wear stage 3. Accordingly, a modern human comparative sample of similar wear stage was created. Additionally, since Cavallo-B is unworn, we collected also an unworn modern human sample to figure out the hypothetical 2D AET and 2D RET indexes that Cavallo-B could have in wear stage 3. For the dM² Neanderthal sample, because almost all individuals are unworn or slightly worn, specimens with wear stage 3 were not considered to measure the enamel thickness and dental tissue proportions. Conversely, in the modern human sample specimens with wear stage 3 were included to create the worst scenario in support to the attribution of Cavallo specimen to *H. sapiens*. Namely, the AET and RET indexes obtained for the modern human sample are slightly underestimated.

Table S2: List of Neanderthal (N) and modern human (UPMH and RMH) dM¹s and dM²s

| Taxon | dM ¹ | | | | dM ² | | | |
|-------------------|--|--------------------------------------|---------------------|-------------------------|--|---------------------------------------|---------------------|-------------------------|
| | Specimen | Country | Source | Wear stage ^d | Specimen | Country | Source | Wear stage ^d |
| N | Engis 2 ^e | Belgium | NESPOS ^a | stage 4 | Krapina d185 | Croatia | NESPOS ^a | unworn |
| | Krapina d181 | Croatia | NESPOS ^a | stage 3 | Krapina d186 | Croatia | NESPOS ^a | unworn |
| | Krapina d183 | Croatia | NESPOS ^a | stage 3 | Krapina d187 ^e | Croatia | NESPOS ^a | stage 3 |
| | Pech-de-l'Azé I-R | France | Original data | stage 3 | Krapina d188 | Croatia | NESPOS ^a | unworn |
| | Pech-de-l'Azé I-L | France | Original data | stage 3 | Krapina d189 ^e | Croatia | NESPOS ^a | stage 3 |
| | Roc de Marsal 1-R | France | NESPOS ^a | stage 3 | Krapina d190 | Croatia | NESPOS ^a | stage 1 |
| | Roc de Marsal 1-L | France | NESPOS ^a | stage 3 | Pech-de-l'Azé I-R | France | Original data | stage 1 |
| | Subalyuk 2-R ^c | Hungary | Original data | stage 3 | Pech-de-l'Azé I-L | France | Original data | stage 1 |
| | | | | | Roc de Marsal 1-R | France | NESPOS ^a | unworn |
| | | | | | Roc de Marsal 1-L | France | NESPOS ^a | unworn |
| | | | | Subalyuk 2-L | Hungary | Original data | stage 1 | |
| UPMH ^b | Brillenhöhle ^f | Germany | Original data | stage 3 | Dolni Vestonice 36-3 | Czech Republic | Original data | stage 1 |
| | Dolni Vestonice 36-2 | Czech Republic | Original data | unworn | La Rochette | France | Original data | stage 2 |
| | La Rochette | France | Original data | stage 3 | Pavlov 6 ^e | Czech Republic | Original data | stage 4 |
| | | | | | Pavlov 12 ^e | Czech Republic | Original data | stage 6 |
| RMH ^c | From Medieval and contemporary samples | France: 2 Germany: 11 Italy: 9 | Original data | Unworn: 5 | From Medieval and contemporary samples | France: 2 Germany: 10 Italy: 11 | Original data | Unworn: 5 |
| | | | | Stage 1: 3 | | | | Stage 1: 9 |
| | | | | Stage 2: 0 | | | | Stage 2: 6 |
| | | | | Stage 3: 14 | | | | Stage 3: 3 |
| | | | | | | | | |

^aNESPOS Database 2011/ www.nespos.org/display/openspace/Home; ^bUPMH= Upper Paleolithic modern human; ^cRMH= recent modern human; ^dbased on Smith⁴²; ^eused only for crown outline analysis; ^fused only for 2D enamel thickness and dental tissue proportions; ^gused only for cervical outline analysis

Scanning of the specimens and segmentation

The original specimens used in this study were scanned at the Vienna Micro-CT Lab, Department of Anthropology, University of Vienna (Viscom X8060 μ CT scanner using the following scan parameters: 130kV, 100mA, isotropic voxel size=25 μ m), at the Paleoanthropology High Resolution CT laboratory, Senckenberg Center for Human Evolution and Paleoecology, Eberhard Karls Universität Tübingen (v|tome|x s 240 μ CT from GE

Phoenix, using the following scan parameters: 130kV, 100mA, isotropic voxel size ranging from=15-26 μ m), and at the AST-RX platform (Accès Scientifique à la Tomographie à Rayons X) at the Muséum national d'Histoire naturelle (using the following scan parameters:150 kV, 220 mA, isotropic voxel size=33.62 μ m). Details about the scanning procedure of the other specimens can be found in NESPOS (Neanderthal Studies Professional Online Service) Database 2011.

For the segmentation process, the half-maximum height (HMH) protocol⁴³ was used to reconstruct 3D digital surface models for the dentine and the enamel of each CT-scanned tooth using the software package Amira 5.3 (Mercury Computer Systems, Chelmsford, MA). This protocol samples the Hounsfield values on either side of the transition between two adjacent tissues and takes the value halfway between them as the threshold value. When voxels were located on the boundary between two tissues with similar Hounsfield values and the automatic threshold could not distinguish the differences (for example, for the presence of cracks or small decays), manual corrections were conducted.

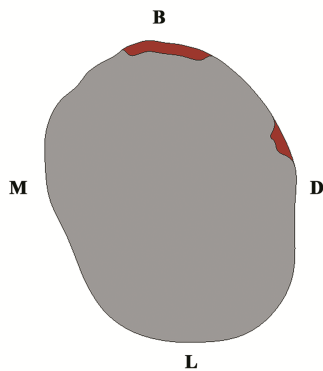


Figure S2: 2D virtual reconstruction of Engis 2 dM¹ crown outline. The crown outline of the original tooth is in grey; the reconstructed portions are shown in red. B=buccal; D=distal; L=lingual; M=mesial.

Digital reconstruction of Engis 2 dM¹ crown outline

Computer-Aided Design (CAD) techniques in RapidForm XOR2 (INUS Technology, Inc.) were used to restore the dM¹ crown outline of the Neanderthal specimen Engis 2 (Fig. S2; the reconstructed regions in red). At the distal side, the small part of the outline missing was reconstructed by using a spline (namely, a curve interpolation). At the buccal side, the enamel is chipped away due to a post-mortem fracture, which reveals the dentine. This missing region

of the enamel outline was restored virtually by offset of the corresponding dentine outline. In particular, the dentine outline exposed was duplicated and translated towards the enamel outline of 0.39 mm (length equal to the enamel thickness measured in the fracture). Finally, that segment was fused to the rest of the outline.

Table S3: 2D enamel thickness of Cavallo-B and Cavallo-C compared with Neanderthal (N), Upper Paleolithic modern human (UPMH), recent modern human (RMH) dM¹s and dM²s (SD in brackets)

| Tooth | Taxon | Wear stage ^a | n | Enamel area (mm ²) | Coronal dentine area (mm ²) | EDJ ^b length (mm) | AET ^c (mm) | RET ^d (scale free) |
|-----------------|-----------|-------------------------|----|--------------------------------|---|------------------------------|-----------------------|-------------------------------|
| dM ¹ | N | 3 | 6 | 7.02 (0.69) | 31.76 (2.10) | 17.36 (0.42) | 0.40 (0.03) | 7.17 (0.54) |
| | UPMH | 3 | 2 | 7.26 (1.10) | 28.16 (0.84) | 14.28 (1.75) | 0.51 (0.01) | 9.56 (0.13) |
| | RMH | 3 | 12 | 7.28 (0.65) | 26.62 (1.51) | 15.38 (0.78) | 0.47 (0.03) | 9.19 (0.70) |
| | UPMH | unworn | 1 | 9.63 | 29.14 | 17.22 | 0.56 | 10.36 |
| | RMH | unworn-stage 1 | 8 | 8.39 (1.26) | 26.18 (1.73) | 16.39 (0.73) | 0.51 (0.06) | 9.96 (0.96) |
| | Cavallo-B | unworn | | 12.64 | 34.14 | 18.33 | 0.69 | 11.80 |
| dM ² | N | unworn-stage 1 | 9 | 12.14 (1.23) | 33.85 (5.10) | 19.25 (1.39) | 0.63 (0.04) | 10.89 (0.84) |
| | UPMH | stage 1-stage 2 | 2 | 16.75 (3.14) | 28.93 (4.23) | 17.30 (0.64) | 0.97 (0.15) | 17.93 (1.40) |
| | RMH | unworn-stage 3 | 20 | 12.33 (1.61) | 28.36 (2.32) | 16.83 (0.93) | 0.73 (0.09) | 13.78 (1.63) |
| | Cavallo-C | stage 5 | | 13.4 | 34.59 | 15.96 | 0.84 | 14.28 |

^aBased on Smith⁴²; ^bEDJ= enamel-dentine junction; ^cAET = average enamel thickness index; ^dRET = relative enamel thickness index

Statistical analysis

The data was analyzed via software routines written in R⁴⁴. Table S3 shows the complete descriptive statistic for dM¹ and dM² enamel thickness and dental tissue proportions.

Principal Component Analysis (PCA)

The PCA of the matrix of Procrustes coordinates was carried out on the sample of the dM¹ crown and the dM² cervical outlines respectively. We applied Anderson's formula to test the deviation from joint equality of any sequence of consecutive eigenvalues^{45,46}. When the formula is applied to a single pair of consecutive eigenvalues, it states that the distribution of $2N \log(a/g)$ is that of an ordinary chi-square on two degrees of freedom. Here N is the sample size (Cavallo's teeth excluded), a is the arithmetic mean of the pair of consecutive eigenvalues, and g is the geometric mean of this same pair of eigenvalues. The expected value of the chi-square is two (its degrees of freedom), and so no PC (eigenvector) should be



considered for interpretation if, when its eigenvalue is compared with the next eigenvalue, $2N \log(a/g)$ does not exceed two, as their ordination most probably accounts only for noise.

PCA of the dM^1 and dM^2 outlines

When applying Anderson's formula⁴⁵ to test PC2 and PC3 from the PCA of the dM^1 s, of eigenvalues of 0.083 and 0.072, we obtain the value of 0.644 ($N=32$) — clearly below the expected value of a chi-square on two degree of freedom. Likewise for the PCA of the dM^2 s, PC3 and PC4, of eigenvalues 0.083 and 0.070, Anderson's value is equal to 1.097 ($N=38$). The eigenvalues of PC2 and PC3 from the PCA of the dM^1 s and those of PC3 and PC4 from the PCA of the dM^2 s are nearly equal, and hence cannot be considered for either interpretation or further statistical analyses.

Quadratic Discriminant Analysis (QDA)

The leave-one-out cross-validation QDA was used for the taxonomic classification of Cavallo-B and Cavallo-C. We built up QDA models on RET, AET and subsets of PCs of the outline analysis, leaving out the data from the Cavallo specimens. The use of QDA is justified as the results show that the variances of the dental variables are significantly different between Neanderthals and modern humans. The computation of the posterior probabilities (P_{post}) was made with an equal prior probability ($P_{\text{prior}} = 0.5$) for the Neanderthal and modern human groups (UPMH+RMH). Taxonomic determination is accepted with a P_{post} equal or superior to 0.90. The performance of the QDA models is defined by the percentage of specimens which taxon is determined with a $P_{\text{post}} \geq 0.90$ (correctly and incorrectly classified) and by the percentage of specimens correctly classified (accuracy). Cavallo's teeth have been tested through all the iterations of leave-one-out cross-validation QDAs. The accuracy of the classification was also computed as the number of iterations for which Cavallo's teeth were classified with a $P_{\text{post}} \geq 0.90$ either as modern human or Neanderthal.

QDA of dM^1 and dM^2 PCs, RET and AET

Table S4 summarizes the analysis. The performance of the QDA models is high for the tooth outlines (dM^1 : PC1 scores, dM^2 : PC1 and PC2 scores) and RET with a high accuracy ranging from 96.3% to 100% and percentage of specimens classified superior to 82%. For both dM^1 and dM^2 , although the accuracy is high, the QDA models based on AET have a low power of

classification when the threshold of decision $P_{\text{post}} \geq 0.90$. Therefore, they are not used for the classification of Cavallo-B and Cavallo-C. According to the QDA models based on outline and RET data, Cavallo-B and Cavallo-C are classified as modern humans with a $P_{\text{post}} > 0.90$ and with an accuracy of 100%.

Table S4: Summary of the leave-one-out cross validation Quadratic Discriminant Analysis (QDA)

| Tooth | Parameter | n | Classified $P_{\text{post}} \geq 0.90$ | | Indetermined $0.10 < P_{\text{post}} < 0.90$ | Missclassified $P_{\text{post}} \geq 0.90$ | Taxa % | Accuracy % |
|-----------------|-----------|----|--|---------|---|---|--------|------------------|
| | | | MH | N | | | | |
| dM ¹ | Outline | 32 | 20 (24) | 7 (8) | 5 | 1 | 84.4 | 96.3 |
| | RET | 31 | 23 (24) | 4 (7) | 4 | 0 | 87.1 | 100 |
| | AET | 31 | 14 (24) | 3 (7) | 14 | 0 | 54.8 | 100 |
| | Cavallo-B | | $P_{\text{post}} = 0.98^a$ | | | | | 100 ^c |
| dM ² | Outline | 38 | 25 (27) | 11 (11) | 2 | 0 | 94.7 | 100 |
| | RET | 34 | 21 (25) | 7 (9) | 6 | 0 | 82.3 | 100 |
| | AET | 34 | 13 (25) | 0 (9) | 21 | 0 | 38.2 | 100 |
| | Cavallo-C | | $P_{\text{post}} = 0.99^a$ | | | | | 100 ^c |
| | | | $P_{\text{post}} = 0.99^b$ | | | | | 100 ^c |

P_{post} = posterior probability; n = sample size; () = original group sample size; MH = modern human (UPMH and RMH); N = Neanderthal. AET = average enamel thickness index; RET = relative enamel thickness index; Species % = percentage of specimens for which a taxon is determined with $P_{\text{post}} \geq 0.90$ after cross validation; Accuracy % = percentage of specimens correctly classified after cross-validation; ^a P_{post} based on outline data; ^b P_{post} based on RET data; ^c Percentage of iterations (during cross validation) for which Cavallo's tooth is classified as modern human with a $P_{\text{post}} \geq 0.90$.

RADIOCARBON DATING

Previous chronology

Since the first identification of the technocomplex in 1963 by Palma di Cesnola^{33,34} and for four decades afterwards, the chronology of the Uluzzian of Cavallo was based on an infinite conventional radiocarbon date, RM-352: $>31,000$ ¹⁴C yr bp (yr BP)³⁹. The sample comprised a piece of charcoal recovered from layers E II-I excavated in 1966.

More recently, four new radiocarbon determinations (AA-66812: $34,900 \pm 1900$ yr BP, AA-66813: $32,300 \pm 2700$ yr BP, AA-66814: $36,510 \pm 2300$ yr BP, AA-66819: $36,600 \pm 2300$ yr BP) were reported by Ronchitelli et al.⁴⁷ and Kuhn et al.⁴⁸. They belong to a series of ten AMS dates made on burnt bone from layer E III ranging from 21,000–36,000 yr BP with no

age-depth consistency⁴⁹. This is not surprising because burnt bone is an unreliable material for AMS dating⁵⁰. It consists of pyrolysed collagen, often with sediment carbon and non-autochthonous material within it, and has a tendency to produce ages that often underestimate the true age, especially of Palaeolithic-aged samples.

These previous dates, therefore, can only serve as a minimum estimate of the real age of layer EIII, and should be set to one side.



Figure S3: Marine shells from the Uluzzian layers of Grotta del Cavallo used for AMS dating. *Dentalium* sp. (Cvl 3, 4, 5, 8, 11), *Nuculana* sp. (Cvl 2), *Cyclope neritea* (Cvl 10) and bivalve fragment (Cvl 6).

New radiocarbon chronology

Material

More recent chronometric work has been undertaken by one of us (KD) as part of a D. Phil. project at the University of Oxford⁵¹, supervised by Prof. R.E.M. Hedges. Two shells from the uppermost layers D II and D I of the original 1963 excavations³¹ were selected for dating from the *Soprintendenza per i Beni Archeologici della Puglia* in Taranto. In addition, six

shells from the salvage fieldwork in the 1970s and 1980s were sampled from the collection housed at the University of Siena. All dated shells are shown in Fig. S3.

The *Dentalium* sp. shells (Cvl 3, 4, 5, 8, 11) are of smooth morphology and have been snapped transversely to create regular tube-shaped beads. The *Nuculana* sp. shell (Cvl 2) is a relatively uncommon species in Upper Palaeolithic ornamental assemblages and was one of eight similarly perforated small valves from the same context.

Table S5: New radiocarbon determinations for the Uluzzian layers in Grotta del Cavallo

| Sample | OxA | ¹⁴ C yr BP | ± | Layer-Spit | Species | Calibrated (95.4%) yr BP | | Aragonite-Calcite % |
|--------|-----------|-----------------------|-----|------------|------------------------|--------------------------|--------|---------------------|
| | | | | | | from | to | |
| Cvl 10 | 21072 | 19,685 | 75 | D I | <i>Cyclope neritea</i> | 23,380 | 22,470 | 100-0 |
| Cvl 10 | Dupl. | 19,235 | 75 | D I | <i>Cyclope neritea</i> | 23,220 | 22,060 | 100-0 |
| Cvl 2 | 19254 | 35,080 | 230 | D 1=D Ib | <i>Nuculana</i> sp.? | 40,450 | 38,860 | 100-0 |
| Cvl 4 | 19255 | 36,260 | 250 | D 2=D Ib | <i>Dentalium</i> sp. | 41,570 | 40,390 | 100-0 |
| Cvl 11 | 20631 | 36,780 | 310 | D II | <i>Dentalium</i> sp. | 42,010 | 40,880 | 99.8-0.2 |
| Cvl 6 | 19257 | 42,360 | 400 | D 3=D II | Bivalve fragm. | 45,990 | 44,640 | 100-0 |
| Cvl 8 | 19258 | 36,000 | 400 | D 8=D II? | <i>Dentalium</i> sp. | 41,570 | 39,560 | 100-0 |
| Cvl 5 | 19256 | 39,060 | 310 | E 1=E-D | <i>Dentalium</i> sp. | 43,510 | 42,350 | 99.7-0.3 |
| Cvl 5 | X-2280-16 | 38,300 | 400 | E 1=E-D | <i>Dentalium</i> sp. | 43,380 | 42,080 | 100-0 |
| Cvl 3 | 19242 | 39,990 | 340 | E 4=E II-I | <i>Dentalium</i> sp. | 44,300 | 43,000 | 50-50 |

Conventional ages are expressed in ¹⁴C years BP, after Stuiver and Polach³⁹. Note that layer assignation for Cvl 10 and Cvl 11 follows that of the original excavations³¹. The rest of the shells were recovered during rescue excavations in subsequent years and follow different assignation system. The correlation of the two series is based on field documentation. Percentages of aragonite to calcite are listed in the right hand column based on high precision XRD analysis.

Pretreatment methods

All new radiocarbon dates in this paper were produced at the Oxford Radiocarbon Accelerator Unit (ORAU), University of Oxford. Ten determinations were obtained from eight shells – Cvl 10 and 5 were dated twice for methodological reasons or as internal laboratory checks.

Part of each shell was cleaned using an air-abrasive system with aluminum oxide until the surface was removed and the inner shell structure was exposed. A small fragment of the carbonate was sawn off and crushed in an agate mortar and pestle to a fine powder. Approximately 30mg of powdered sample was reacted with 5ml of 80% phosphoric acid (H₃PO₄) for 12h at 60°C, under vacuum. The CO₂ evolved via this process was extracted



through a manifold and cryogenically purified while passing through a liquid N₂-methanol cooled trap that removes less volatile impurities (H₂O and phosphoric acid vapour). The gas was injected through an automated elemental analyzer connected to a continuous flow isotope-ratio-monitoring mass spectrometer (EA-CF-IRMS) system where it was measured isotopically. The CO₂ remaining from the process was transferred to a graphitization rig and was reduced to graphite with H₂ at 560 °C for 6h, in the presence of ≈2 mg of a Fe⁺ catalyst. The graphite was pressed into a target holder prior to accelerator mass spectrometry (AMS).

Results

The raw determinations and sample details are given in Table S5. The majority of the new radiocarbon dates (OxA-19242, OxA-19256, OxA-19258, OxA-20631, OxA-19255, OxA-19254) are consistent with respect to the stratigraphic position of the samples.

Only OxA-19257 from horizon D II is too old for its context. This is *not* an ornament but a small, indeterminate fragment of a bivalve shell (Fig. S3; Cvl 6). Its preservation state was poor and the sample surface showed alteration and a chalky appearance. Given that the rest of the shells are much better preserved and with a very low degree of fragmentation a possible explanation may be that Cvl 6 is an old shell, either collected on purpose, or accidentally brought to the site. Bivalve shells are found in lower layers of Cavallo and the breaking pattern, the small dimensions and the old age of Cvl 6, in contrast with the rest of the shell Uluzzian assemblage, supports the suggestion of an old or redeposited specimen.

In contrast, OxA-21072 (and its duplicate) was obtained from a *Cyclope neritea* shell, discovered during the original excavation of Palma di Cesnola in 1963 in layer D I on the top of the Uluzzian sequence. The material was stored in Taranto since the 1960s separately from the other dated samples. These dates are surprising young, especially since there has been no other archaeological material of a similar age discovered in Cavallo Cave.

Infiltration of younger Epigravettian material to the uppermost Uluzzian layer D I would require passing through the stalagmitic crust and the volcanic ash layers (see Fig. S1). However, according to the excavator's observations the ash and the stalagmite crust formed a continuous layer. While we suspect several reasons might be responsible for this younger age,



we cannot prove them. What is certain, however, is that the sample does not truly relate to the Uluzzian layers. Other similarly young material has not been discovered in the Uluzzian layers and the few Aurignacian-like elements observed at the uppermost Uluzzian layer D I were considered by Palma di Cesnola to belong to a transitional, Terminal Uluzzian phase, before the arrival of the Protoaurignacian in the region⁴⁰.

XRD analyses

Prior to chemical pretreatment, all samples were mineralogically characterized using X-Ray Diffraction (XRD), following the optimized methods described by Douka et al.⁵² which allow detection and quantification of very low amounts of calcite in binary mixtures with aragonite. With the exception of Cvl 3, all shells appeared well-preserved and largely unaffected by diagenesis (Table S5 shows the percentage of calcite present in the naturally aragonitic shell samples).

Cvl 3 contained large amounts of calcite ($\approx 50\%$) in the originally aragonite structure. The sample was examined microscopically and no evidence of mineral overgrowth or other form of alteration was observed. It is very likely that the formation of calcite was caused by exposure to high temperature (over 230°C) which readily alters biogenic aragonite to calcite. This would not incorporate a shift in the radiocarbon age. OxA-19242 is in very good agreement with the rest of the dates from overlying spits of layers E and D (see below).

Cvl 5 was also dated twice as part of an experimental project where the effect of surface cleaning (by abrasion) was examined. The results of the two methods are statistically indistinguishable, but the first determination (OxA-19256) is preferred over the second date (OxA-X-2280-16), given that the fraction used for the latter was not thoroughly cleaned.

Bayesian model

In an attempt to place the two human teeth, Cavallo-B and Cavallo-C, within their most likely age and palaeoclimatic context, the new radiocarbon determinations were incorporated into a Bayesian model built with OxCal 4.1.7⁵³ and calibrated using the INTCAL Marine09 curve⁵⁴. This is an interim curve and will be refined as additional datasets become available and are incorporated into it.

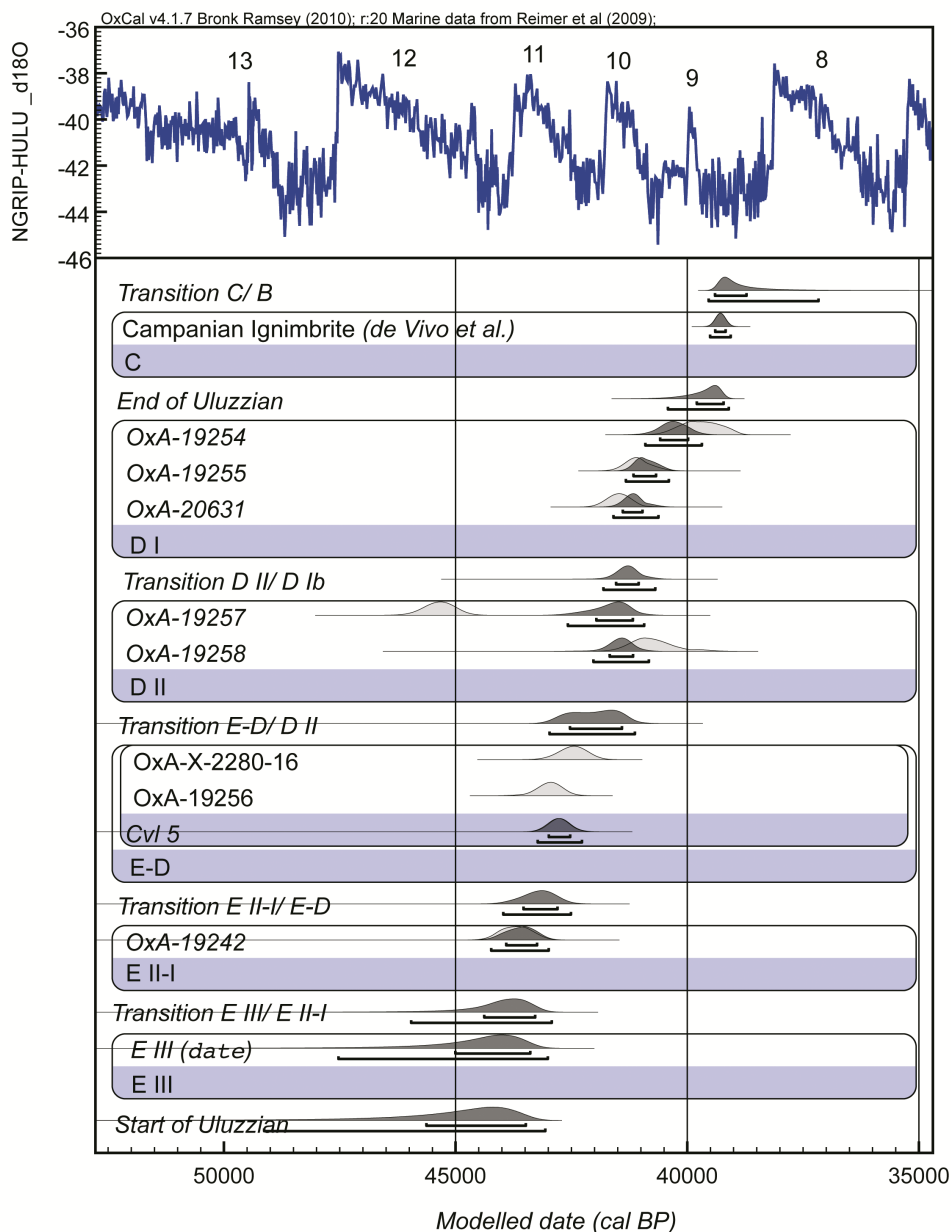


Figure S4: Bayesian model of the calibrated radiocarbon dates obtained on shell material from the Uluzzian layers of Cavallo. The radiocarbon dates are calibrated using the INTCAL Marine09 curve⁵⁴ with resolution set at 20. The NGRIP $\delta^{18}\text{O}$ record is shown^{56,57} tuned with the U/Th chronology for the Hulu Cave speleothem⁵⁸. Individual likelihoods are shown with lighter shaded distributions. Posterior probability distributions are in black outline. OxA-19257 is an outlier (100% chances for being an outlier) and most probably corresponds to an 'old' or redeposited shell (see text). The rest of the determinations demonstrate a consistent trend of decreasing age until the time of the inferred CI eruption. OxA-19254 is in perfect agreement with this age. The very young dates from Cvl 10 (OxA-21072 and duplicate) are not included in the figure since they certainly do not relate to the Uluzzian occupation (see text). Cvl 5 was dated twice. Figure generated using OxCal 4.1.7⁵³.



The Bayesian model (Fig. S4) includes prior stratigraphic information as observed at the site during excavation, as well as the presence of the tephra on top of the Uluzzian sequence, here taken as the CI ($\approx 39,300 \pm 55$ yr BP)⁵⁵. This age estimate has been produced from an average of 36 $^{40}\text{Ar}/^{39}\text{Ar}$ measurements from twelve proximal deposits. Since there is no chemical identification of the tephra capping the Uluzzian deposits in Cavallo, the probability distribution for the CI is only tentatively placed on top of the Bayesian plot. An outlier detection analysis was used to assess outliers in the model. This showed two outliers of significance: OxA-21072 and its duplicate date (not shown in Fig. S4) and OxA-19257.

The earliest Uluzzian phase of layer E III, in which Cavallo-B was found, was not dated directly due to the lack of suitable samples. Using the Date function in OxCal, however, we calculated a probability distribution function (PDF) for the likely age of the human fossil within this phase. This PDF corresponds to a range between 45,010—43,380 (68.2% prob.) and 47,530—43,000 (95.4% prob.) cal yr BP with respect to INTCAL Marine09 (Fig. S5). The longer tail of the distribution and wider uncertainty is caused because it is unconstrained by chronometric data below the Uluzzian layers. Further work is needed to refine this estimate for the age of the layer.

The oldest radiocarbon determination from the site comes from E II-I and places the evolved Uluzzian –and the age of Cavallo-C– at about 40,000 ^{14}C yr BP or 43,000 cal yr BP. This date also acts a *terminus ante quem* for Cavallo-B and the arrival of modern humans in the cave. The PDF for the age of Cavallo B determined using the Date function in OxCal ranges between 43,970—43,060 (68.2% prob.) and 44,910—42,660 (95.4% prob.) cal yr BP.

The two age estimates overlap significantly, although the PDF for EIII is by definition older than that of EII-I (Fig. S5).

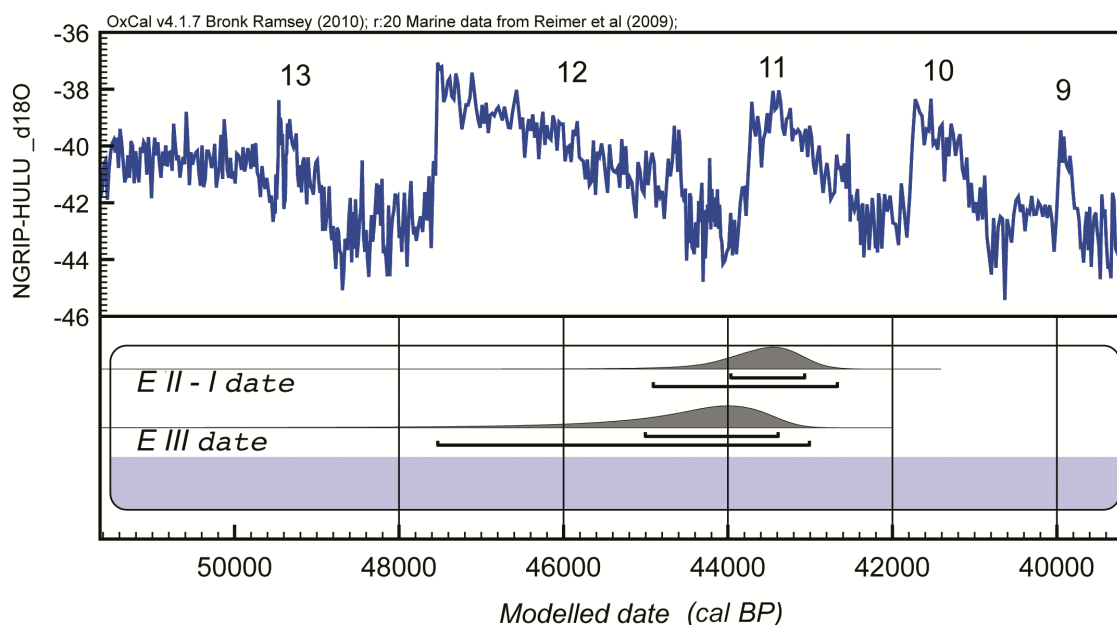


Figure S5: Age estimates for the human remains found in Cavallo layers EIII and EII-I. These ages are Date estimates, no direct measurements, which provide probability distribution functions (PDFs) for the likely age for the human teeth in layers EIII and EII-I. The NGRIP $\delta^{18}\text{O}$ record is shown^{56,57}, tuned with respect to the U/Th chronology for the Hulu Cave speleothem⁵⁸. The relevant Greenland interstadials (GI) are given. Figure generated using OxCal 4.1.7⁵³.

We compare these data tentatively against the NGRIP $\delta^{18}\text{O}$ record^{56,57} tuned with respect to the Hulu Cave U-series chronology (following Weninger and Jöris⁵⁸) (Figs. S4, S5). The PDF for EIII fits within the latter part of GIS 12 on this timescale, while the PDF for EII-I is slightly later (Fig. S5). Overall, the radiocarbon determinations from Grotta del Cavallo agree with the stratigraphic position of the majority of the samples and the presence of the CI ash. This is the first time the Uluzzian of the type-site of Grotta del Cavallo has been dated reliably since its discovery in 1963.

Confirmation of the age of the La Rochette and Brillenhöhle specimens

We checked the age of these two comparative human specimens by redating the samples to confirm their antiquity (Table S6).

Table S6: Radiocarbon determinations from La Rochette and Brillenhöhle

| Specimen | OxA | ¹⁴ C yr BP | ± | Used (mg) | Yield (mg) | %Yld | %C | δ ¹³ C (‰) | δ ¹⁵ N (‰) | C:N atomic ratio |
|--------------|-------|-----------------------|-----|-----------|------------|------|------|-----------------------|-----------------------|------------------|
| La Rochette | 11053 | 23,630 | 130 | 710 | 34.2 | 4.8 | 45.8 | -17.1 | 11.7 | 3.3 |
| | 23413 | 23,400 | 110 | na | 23.84 | 3.4 | 42.9 | -17.2 | 11.9 | 3.1 |
| Brillenhöhle | 11054 | 12,470 | 65 | 600 | 34.7 | 5.8 | 44.7 | -19.2 | 8.5 | 3.3 |
| | 23414 | 12,535 | 50 | na | 22.67 | 3.8 | 42.5 | -19.5 | 8.5 | 3.1 |

Conventional ages are expressed in years BP, after Stuiver and Polach⁵⁹. Stable isotope ratios are expressed in ‰ relative to vPDB with a mass spectrometric precision of ±0.2‰. Gelatin yield represents the weight of gelatin or ultrafiltered gelatin in milligrams. %Yld is the percent yield of extracted collagen as a function of the starting weight of the bone analysed. %C is the carbon present in the combusted gelatin. CN is the atomic ratio of carbon to nitrogen and is acceptable if it ranges between 2.9–3.5. The new AMS dates are reultrafiltered gelatin sample extracted from the first pretreatment chemistries undertaken. This was done as a check on the original filtration chemistry. You can see that the results are statistically identical and confirm the original measurements.

Supplementary References

31. Palma Di Cesnola, A. Prima campagna di scavi nella Grotta del Cavallo presso Santa Caterina (Lecce). *Riv. Sc. Preist.* **18**, 41-74 (1963).
32. Palma di Cesnola, A. Seconda campagna di scavo nella grotta del Cavallo. *Riv. Sc. Preist.* **19**, 23-39 (1964).
33. Palma di Cesnola, A. Notizie preliminari sulla terza campagna di scavi nella Grotta del Cavallo (Lecce). *Riv. Sc. Preist.* **20**, 291-302 (1965a).
34. Palma di Cesnola, A. Gli scavi nella Grotta del Cavallo (Lecce) durante il 1966. *Riv. Sc. Preist.* **21**, 289-302 (1966a).
35. Sarti, L., Boscato, P. & Lo Monaco, M. Il Musteriano finale di Grotta del Cavallo nel Salento, studio preliminare. *Origini* **22**, 45-109 (1998-2000).
36. Sarti, L., Boscato, P., Martini, F. & Spagnoletti, A.P. Il Musteriano di Grotta del Cavallo - strati H e I : studio preliminare. *Riv. Sc. Preist.* **52**, 21-110 (2002).
37. Palma di Cesnola, A. Il Paleolitico superiore arcaico (facies uluzziana della Grotta del Cavallo, Lecce). *Riv. Sc. Preist.* **20**, 33-62 (1965b).
38. Palma di Cesnola, A. Il Paleolitico superiore arcaico (facies uluzziana) della Grotta del Cavallo, Lecce (continuazione). *Riv. Sc. Preist.* **21**, 3-59 (1966b).
39. Palma di Cesnola, A. Datazione dell'Uluzziano col Metodo del C-14. *Riv. Sc. Preist.* **24**, 341-348 (1989).
40. Palma di Cesnola, A. *Il Paleolitico superiore in Italia* (Garlatti e Razzai, 1993).
41. Giaccio, B., Hajdas, I., Peresani, M., Fedele, F.G. & Isaia, R. in *When Neanderthals and Modern Humans Met* (ed. Conard, N.J.) (Kerns Verlag, Tubingen, 2006).
42. Smith, B.H. Patterns of molar wear in hunter-gatherers and agriculturists. *Am. J. Phys. Anthropol.* **63**, 39-56 (1984)
43. Spoor, F., Zonneveld, F. & Macho, G.A. Linear measurements of cortical bone and dental enamel by computed tomography: applications and problems. *Am. J. Phys. Anthropol.* **91**, 469-484



- (1993).
44. R Development Core Team. R: a language and environment for statistical computing. Vienna, Austria: R Foundation for Statistical Computing. <http://www.r-project.org>. (2008).
 45. Anderson, T.W. Asymptotic Theory for Principal Component Analysis. *Ann. Math. Statist.* **34**, 122-148 (1963).
 46. Coquerelle, M. et al. Sexual dimorphism of the human mandible and its association with dental development. *Am. J. Phys. Anthropol.* **145**, 192-202 (2011).
 47. Ronchitelli, A., Boscatto, P. & Gambassini, P. in La lunga storia di Neandertal. Biologia e comportamento (eds Facchini, F. & Belcastro, G.M.) (Jaca Book, 2009).
 48. Kuhn, S.L. et al. Radiocarbon Dating Results for the Early Upper Paleolithic of Klissoura 1 Cave. *Euras. Prehist.* **7** (2), 37-46 (2010).
 49. Riel-Salvatore, J. The Uluzzian and the Middle-Upper Paleolithic Transition in Southern Italy. Unpublished Ph.D. dissertation, School of Human Evolution and Social Change, Arizona State University (2007).
 50. Van Strydonck, M., Boudin, M. & De Mulder, G. ¹⁴C dating of cremated bones: the issue of sample contamination. *Radiocarbon* **51**, 553-568 (2009).
 51. Douka, K. *Investigating the Chronology of the Middle to Upper Palaeolithic Transition in Mediterranean Europe by Improved Radiocarbon Dating of Shell Ornaments*. Unpublished D.Phil in Archaeological Science, University of Oxford (2011).
 52. Douka, K., Hedges, R.E.M., Higham, T.F.G., 2010. Improved AMS ¹⁴C dating of shell carbonates using high-precision X-Ray Diffraction (XRD) and a novel density separation protocol (CarDS). *Radiocarbon* **52** (2): 735–751.
 53. Bronk Ramsey, C. Bayesian analysis of radiocarbon dates. *Radiocarbon* **51**, 337-360 (2009).
 54. Reimer, P.J. et al. IntCal09 and Marine09 radiocarbon age calibration curves, 0–50,000 years cal BP. *Radiocarbon* **51**, 1111-1150 (2009).
 55. De Vivo, B., Rolandi, G., Gans, P.B., Calvert, A., Bohrson, W.A., Spera, F.J. & Belkin, H.E. New constraints on the pyroclastic eruptive history of the Campanian volcanic Plain (Italy). *Mineral. Petrol.* **73**, 47–65 (2001).
 56. Andersen, K.K. et al. The Greenland ice core chronology 2005, 15-42 ka. Part 1: constructing the time scale. *Quat. Sci. Rev.* **25**, 3246-3257 (2006).
 57. Svensson, A. et al. The Greenland ice core chronology 2005, 15-42ka. Part 2: Comparison to other records. *Quat. Sci. Rev.* **25**, 3258-3267 (2006).
 58. Weninger, B., Jöris, O. A ¹⁴C age calibration curve for the last 60 ka: the Greenland-Hulu U/Th timescale and its impact on understanding the Middle to Upper Paleolithic transition in Western Eurasia. *Journal of Human Evolution* **55**, 772–781 (2008).
 59. Stuiver, M. & Polach, H.A. Discussion: Reporting of ¹⁴C Data. *Radiocarbon* **19**, 355-363 (1977).

Journal of Human Evolution

Vol. 82 pp. 190 - 196, doi: 10.1016/j.jhevol.2015.03.001



News and Views

A human deciduous molar from the Middle Stone Age (Howiesons Poort) of Klipdrift shelter, South Africa

Katerina Harvati^{a,*}, Catherine C. Bauer^a, Frederick E. Grine^b, Stefano Benazzi^{c,d}, Rebecca Rogers Ackermann^e, Karen L. van Niekerk^f, Christopher S. Henshilwood^{f,g}

^a*Paleoanthropology, Senckenberg Center for Human Evolution and Paleoenvironment, Eberhard Karls Universität Tübingen, Rümelinstrasse 23, Tübingen 72070, Germany*

^b*Departments of Anthropology and Anatomical Sciences, Stony Brook University, Stony Brook 11794-4364, New York, USA*

^c*Department of Cultural Heritage, University of Bologna, Via degli Ariani 1, 48121 Ravenna, Italy*

^d*Department of Human Evolution, Max Planck Institute for Evolutionary Anthropology, Deutscher Platz 6, D-04103 Leipzig, Germany*

^e*Department of Archaeology, University of Cape Town, Rondebosch 7701, South Africa*

^f*Institute for Archaeology, History, Culture and Religious Studies, University of Bergen, Øysteinsgate 3, N-5007 Bergen, Norway*

^g*Evolutionary Studies Institute, University of the Witwatersrand, 1 Jan Smuts Avenue, Braamfontein 2000, Johannesburg, South Africa*

**Corresponding author:*

E-mail address: katerina.harvati@ifu.uni-tuebingen.de (K. Harvati)

Keywords: Hominin dental remains, microCT, Morphometrics, Modern human origins

Introduction

Klipdrift Shelter (hereafter KDS) is part of a cave complex situated in the De Hoop Nature Reserve, southern Cape, South Africa (Figure 1). The complex (34°27.0963'S 20°43.4582'E) is a single wave cut platform with a quartzite promontory in the centre, located in a steep quartzite cliff approximately 12-15 m from the Indian Ocean and ~19 m above current sea level. The complex is divided into a western and eastern section with the west forming a cave and the east a shelter. Approximately 7 m² of surface area of the shelter containing archaeological deposits were excavated from 2011 to 2013. The deposits span the time period between c. 66-52 ka dated by single grain optically stimulated luminescence (Henshilwood et al., 2014).

Anthropogenically sterile layers at the base of the excavation have an age of c. 72 ka. The lithic assemblage in layers PCA to PAY, with ages ranging from 65.5±4.8 ka to 59.4±4.6 ka, is consistent with that of the Howiesons Poort (HP). The HP is a Middle Stone Age (MSA) techno-tradition geographically confined to southern Africa (Henshilwood and Dubreuil, 2011). Artefacts associated with the HP are regarded as highly innovative and indicative of early advances in the technology of *Homo sapiens* (Henshilwood and Marean, 2003), for example backed stone segments (crescents) that were mounted on arrows launched by bow (Wadley and Mohapi, 2008). Some of the earliest examples of material culture associated with symbolically mediated behaviour are linked to the HP including engraved ostrich eggshell (Henshilwood et al., 2014; Texier et al., 2013) and formal bone tools (Backwell et al., 2008).

Other materials recovered from the HP layers at KDS include ochre, ostrich eggshell, marine shells, terrestrial and aquatic macro and microfauna, organic materials and numerous hearths and ash lenses. Ochre is ubiquitous in all layers in the form of chunks, 'crayons' and powder. Ostrich eggshell is common throughout the sequence and more than 100 pieces are engraved with geometric designs, similar to those reported from the pre-HP and HP levels at Diepkloof (Texier et al., 2010, 2013) in the western Cape and Apollo II in Namibia (Vogelsang et al., 2010).

In 2011 a hominin lower deciduous second molar (hereafter dm₂), labeled KDS, 23-02-11, S29b, PBE (hereafter KDS PBE), was recovered in the HP layer PBE (Figure 2). The base of this layer where the tooth was found, and in adjacent quadrats, is characterized by a layer of

ochre fragments and powder. The specimen itself was covered with ochre, possibly from the powder and tiny pieces found throughout the base of the unit. KDS PBE is the only complete dm_2 crown known from the South African later Pleistocene human fossil record (a fragmentary and worn dm_2 was recovered from Klasies River Mouth; Grine, 2012; see also Rightmire and Deacon, 2001). Here we present the description and comparative analysis of this specimen.

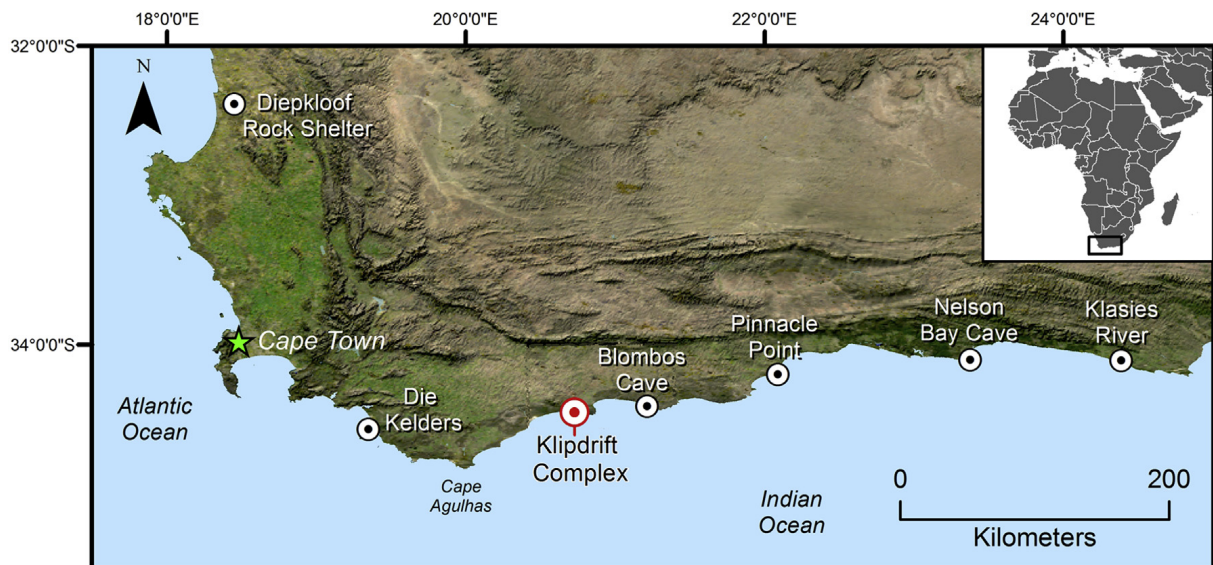


Figure 1. Map of southern Africa showing the location of the Klipdrift Cave Complex and other MSA sites. Adapted from Henshilwood et al. (2014).

Materials and methods

The detailed morphological description of the KDS PBE crown follows standard terminology (e.g. Scott and Turner, 1997). Mesiodistal (MD) and buccolingual (BL) diameters of the crown were recorded using digital calipers by one of us (FG) and compared with measurements collected from the literature for dm_2 s of recent and fossil *Homo* specimens, representing *H. heidelbergensis* from Europe and the Near East (HH), *H. neanderthalensis* (NEA), early *H. sapiens* from the Near East and North Africa (EHS), Upper Paleolithic European specimens (UPHS), and recent human samples from Europe and Africa (Moss and Chase, 1966; Grine, 1984, 1986; Toussaint et al., 2010; Hershkovitz et al., 2011; Benazzi et al., 2011b; Table 1). KDS PBE was also scanned in the Tübingen Paleoanthropology High Resolution CT Laboratory, and three further comparative analyses were undertaken on the

basis of the scan: analysis of the crown outline shape, lateral dentine and pulp chamber volume, and lateral crown height (lateral in this instance is defined as relating to the sides of the tooth crown in 3-D minus the occlusal surface, following Toussaint et al. [2010]). The latter two measurements were gathered from the center region of the tooth crown, which is defined by removing the occlusal surface (thus removing occlusal wear) and the root (see methods below). Therefore, only the lateral aspect of the crown dentine (and the enclosed pulp) was considered (Toussaint et al., 2010; Benazzi et al., 2011b). The comparative sample consisted of 68 scans of dm_2 s of recent and fossil *Homo*, including NEA, EHS, UPHS, as well as Holocene South Africans (Khoesan; RSAF), and recent Europeans (REU) (SOI Table 1). Different numbers of specimens, depending on the availability of CT scans and state of preservation of each tooth, were used for each analysis.

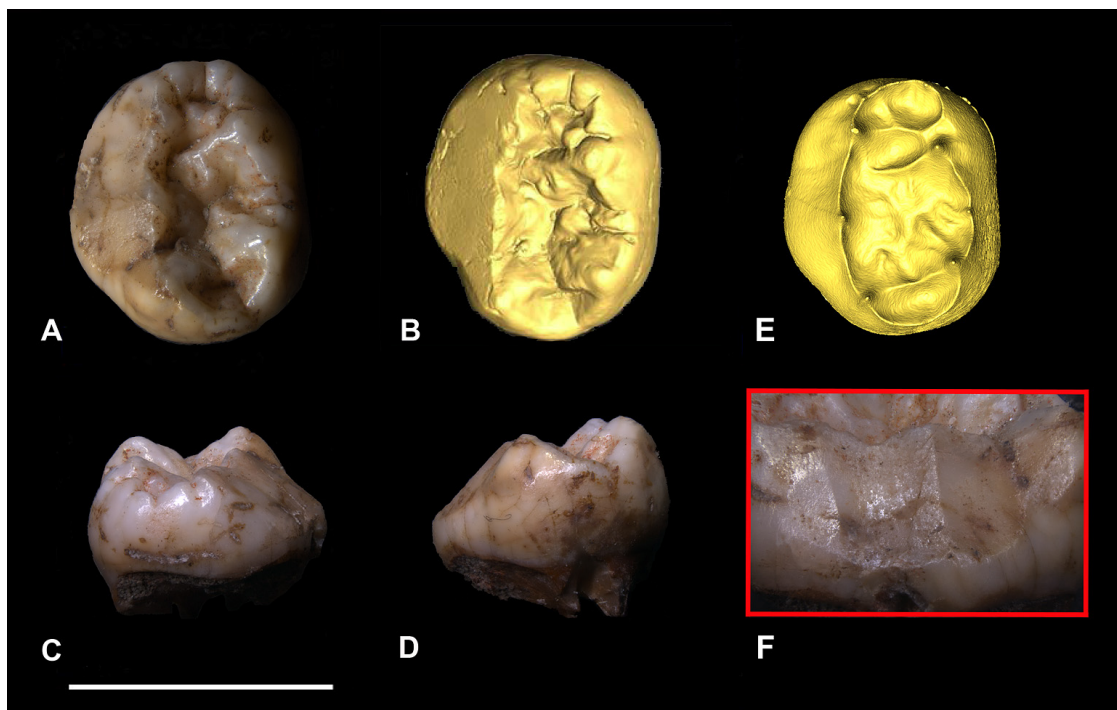


Figure 2. The KDS PBE left dm_2 . **A:** Occlusal view, mesial to the top and buccal to the left. **B:** Occlusal view of the isosurface reconstruction of the microCT scan of the specimen used in the analyses. **C:** Mesial view. **D:** Distal view. **E:** Enamel-dentine junction surface of KDS PBE, derived from the high resolution CT scan of the specimen. Mesial to the top. **F:** Closeup image of the atypical wear surface on the buccal aspect of the KDS PBE crown, showing subdivisions into smaller facets. Mesial to the left. Scale bar 1/4 1 cm. Photographs were taken by CB with the multi focus microscope of the Geosciences Laboratory, University of Tübingen (courtesy P. Bons).

Table 1. KDS PBE crown dimensions and summary statistics for MD and BL crown measurements (in mm) for fossil and modern human samples.

| Sample | Sex | n | MD ± SD | MD range | BL ± SD | BL range | Reference |
|---------------------------|-----|--------------------|--------------|-----------|-------------|------------|--|
| Klipdrift (KDS PBE) | | 1 | 10.3 | | 8.5 | | This paper |
| Klasies River O1/C1/SMB | | | – | | 8.3 | | Grine, 2012 |
| HH | | 3 | 10.83 ± 0.45 | 10.4–11.3 | 9.50 ± 0.10 | 9.4– 9.6 | Toussaint et al., 2010; Hershkovitz et al., 2011 |
| NEA | | 40 | 10.34 ± 0.59 | 9.2–11.5 | 9.29 ± 0.47 | 8.0– 10.2 | Toussaint et al., 2010 |
| EHS | | 10 | 10.92 ± 0.54 | 9.9–11.4 | 9.71 ± 0.73 | 8.6– 10.7 | Toussaint et al., 2010 |
| UPHS | | 10 | 10.57 ± 0.54 | 9.9–11.5 | 9.33 ± 0.41 | 8.5– 10.0 | Toussaint et al., 2010; Benazzi et al., 2011b |
| Recent European | | 50 | 10.07 ± 0.48 | 9.10–11.1 | 8.87 ± 0.45 | 8.20– 9.70 | Toussaint et al., 2010 |
| Recent African (Liberian) | | 20 | 10.09 ± 0.51 | 8.3–10.0 | 8.86 ± 0.45 | 8.2– 10.0 | Moss and Chase, 1966b |
| Recent South African | M | 18 | 10.39 ± 0.44 | 9.5–11.2 | 9.03 ± 0.37 | 8.2– 9.7 | Grine, 1986 |
| Recent South African | F | 17 | 10.13 ± 0.57 | 8.9–10.9 | 8.76 ± 0.39 | 8.0– 9.3 | Grine, 1986 |
| Recent African (San) | M | 54/56 ^a | 10.06 ± 0.49 | 8.9–11.2 | 8.68 ± 0.41 | 7.8– 9.7 | Grine, 1984 |
| Recent African (San) | F | 41/45 ^a | 9.88 ± 0.45 | 9.0–10.9 | 8.48 ± 0.39 | 7.6– 9.5 | Grine, 1984 |

^a Different sample size (n) for MD/BL

Scanning procedures: 3D- μ CT scans of all specimens were obtained using industrial and synchrotron-based μ CT scanners at isotropic voxel length between 15 and 65 μ m. The only exception is the UPHS sample from Grotta Paglicci, for which a white-light surface scanning system was used (see Benazzi et al., 2012). The EHS and part of the REU samples were scanned with a General Electric Phoenix v|tome|x micro-CT at the Department of Paleoanthropology of the University of Tübingen. The RSAF sample was scanned with a General Electric Phoenix v|tome|x micro-CT located at the Stellenbosch University CT Scanner Facility (near Cape Town, South Africa). Scan settings varied between 130 kV/100 μ A and 180 kV/140 μ A depending on the state of preservation and/or fossilization. Details about the μ CT scanning procedure for the NEA, UPHS and remaining RHS samples can be found in Toussaint et al. (2010), Benazzi et al. (2011a; 2012), the NESPOS (Neanderthal Studies Professional Online Service) Database 2011 and the ESRF Paleontological Database (Smith et al., 2010).

Data processing: The REU, RSAF and EHS samples scanned in Tübingen and in Cape Town were added to the dm₂ dataset of Benazzi et al. (2012). Because KDS PBE is a lower left deciduous molar, all teeth were regarded as left dm₂s, with right dm₂ specimens mirror imaged before data processing and analysis. To ensure that all specimens were correctly oriented for data collection we followed the procedures described in Benazzi et al. (2011a, 2012) using AVIZO® 7.0 (VSG, Visualization Sciences Group) and Amira® 5.2 software (Mercury Computer Systems, Chelmsford, USA). The Tübingen and Cape Town samples were segmented following the half-maximum height protocol by Spoor et al. (1993) to assign voxels of different grey values to different dental material and to obtain 3D digital models of the teeth.

Crown outline analysis: All 68 comparative specimens could be included in the outline shape analysis (SOI Table 1), following Benazzi et al. (2011b, 2012) and using Rhino® 5.0 (Robert McNeel & Associates, Seattle, WA). The crown silhouette (in occlusal view) was projected onto the cervical plane and all outlines were centered by a superimposition of their individual centroids. They were represented by 16 pseudolandmarks obtained by equiangularly spaced radial vectors out of the centroid (see Benazzi et al., 2011b, 2012). To remove size information from the oriented and centered outlines, the pseudolandmarks were uniformly scaled to unit centroid size in Morphologika (O'Higgins & Jones, 2006). Because of the importance of size reduction in the discussion of morphological modernity, crown outline centroid size was examined separately. A between-group Principal Component Analysis (PCA) on shape coordinates of the outline was carried out to explore the shape differences between groups (NEA, EHS, UPHS, REU, RSAF) and the relationship of KDS PBE to them (Mitteroecker and Bookstein, 2011; Baab et al., 2013). For this analysis the PC axes were calculated from the covariance matrix obtained from means of these groups. KDS PBE and all other individual specimens were then projected onto these axes. Overall outline shape similarities among individual specimens were further assessed by the Procrustes distances (the square root of the sum of squared distances between two fitted landmark configurations) among specimens and mean Procrustes distances between KDS PBE and our samples. Statistical analyses were performed using the SAS software package (SAS Institute, 1999-2001), and figures were prepared in PAST 3.01 (Hammer et al., 2001). Shape differences between the crown outline of KDS PBE and the mean crown outlines of the comparative samples were visualized in Morpheus (Java version 1.8.0_25; Slice, 2005).

Lateral Dentine & Pulp Chamber Volume and Lateral Crown Height analyses: Lateral Dentine and Pulp Chamber Volume (LDPV) measurements were recorded for 44 specimens of our total sample (including KDS PBE), whereas 45 specimens were measured for lateral crown height (LCH; SOI Table 1). As the sample that underwent LDPV and LCH analysis greatly overlaps with the sample used for crown outline analysis, digital models of the aligned and separated crown (as mentioned above, the separation of the crown from the root as based on the cervical plane) could be re-used for these analyses without any further data preparation. Procedures followed Benazzi et al. (2011b) using the Avizo® 7.0 software.

Interobserver error: To control for observer error, two of us (SB and CB) compared measurements on five specimens (REU) from this study, reorienting them twice (allowing

several days between the samplings). For each group of observations, the Euclidian Distances to the mean were computed and used for analysis of variance (ANOVA) and a permutation test. No statistically significant deviation was found between the measurements of the two observers (ANOVA: F-value = 0.333, $p = 0.801$; permutation test: $p = 0.32$).

Description

KDS PBE is a very nearly complete crown of an isolated human left mandibular deciduous second molar (Ldm_2) (Figure 2), measuring 10.3 mm MD and 8.5 mm BL (Table 1). The root is broken just below the cervical margin, which is slightly damaged buccally and mesially, but mostly intact lingually. There is no occlusal wear visible on the lingual cusps, the mesial or distal marginal ridges, or the occlusal basin. An atypical, large wear surface dominates the buccal aspect of the crown, making assessment of normal occlusal wear to the buccal cusps difficult. This facet measures 8.0 mm mesiodistally by 3.5 mm in height, and extends from the mesiobuccal aspect of the protoconid and crosses the hypoconid to include the mesiobuccal aspect of the hypoconulid. It presents a nearly planar aspect that is angled at about 41° to the horizontal (as defined by the crown cervix). The surface is subdivided into five semi-discrete facets set to one another at different angles, whose orientation appears to be dictated largely by the natural surface of the crown (Figure 2F). We interpret this facet as likely the result of "scissor bite." In this condition the mandibular dentition is contained within the maxillary during occlusion, resulting in occlusion between the buccal side of the buccal cusps of the lower molars and the lingual side of the lingual cusps of the upper molars (Yun et al., 2007). This malocclusion thus produces contact on the buccal aspect of mandibular molars rather than on the occlusal surface itself. A small, extremely faint mesial interproximal contact facet is located just below the occlusal margin (measuring 1.3 mm in height by 1.7 mm BL). The individual represented by KDS PBE was therefore older than c. 18 months, the age of eruption of this tooth among modern human children (Ash, 1993), and the lack of a distal interproximal facet suggests it was younger than c. 6 years of age. However, because of the unusual occlusion in this specimen, this age estimate can be regarded only as tentative.

The crown of KDS PBE (Figure 2A) shows five well-developed principal cusps, the largest of which is the metaconid. A thick distal trigonid ridge from the metaconid contacts the base of

the hypoconid, producing a clear Y occlusal pattern. The mesial marginal ridge is multicuspidate, with the individual cusplids separated from one another and the apices of the metaconid and protoconid by short, distinct fissures. A continuous "mid-trigonid" ridge (the epicristid of Hershkovitz [1971] or the mid-trigonid crest of Korenhof [1978; 1982]) courses from the apex of the metaconid to the remnant of the protoconid tip. It walls a short, BL transverse mesial trigonid furrow between it and the mesial marginal ridge, which forms (with the mesial-most portion of the tooth crown) an anterior fovea. The apex of the metaconid is separated from both the mesial marginal and mid-trigonid ridges by a narrow furrow that courses around the tip to end as a small triangular depression on the distolingual side of the cusp tip. A small postmetaconulid that forms an incipient tuberculum intermedium (C7) is wedged between and separated equally from the metaconid and entoconid. The entoconid and hypoconulid are connected by a robust, obliquely oriented transverse ridge (clearly visible in the EDJ; Fig. 2E) that is shallowly incised in its middle. It forms the mesial wall of a comparatively capacious and deep posterior fovea. The distal marginal ridge is thick, but lower than the mesial wall of the posterior fovea; it is crossed in its middle by a slight groove. There is no tuberculum sextum (C6). There is no evidence of pathology, enamel hypoplasia or dental calculus.

Comparisons

KDS PBE is comparable to both archaic Pleistocene and recent human samples in retaining the likely primitive cusp number and occlusal crown configuration. The presence of a C7 and the absence of a C6 are not unusual among fossil samples nor among recent San and South Africans (Grine, 1986, 1990). On the other hand, the presence of a mid-trigonid crest on the dm_2 , while not unknown among modern San and South African populations, is comparatively rare (at some 3 – 8%) (Grine, 1986, 1990). A mid-trigonid crest on the dm_2 is also reported for Asian Holocene populations, with a high frequency among the Neolithic Jomon and Aeneolithic Tanegashima Yogui populations (50,9 and 37,5 % respectively), but much lower occurrence in the more recent samples examined (2,4 – 10,8 %; Kitagawa, 2000). This feature is variable among Late Pleistocene humans from the Levant, with Qafzeh 10 showing a continuous, but low crest (grade 2, scored from the CT scan following Bailey et al., 2011),

while Skhul 1 and Qafzeh 15 show a non-continuous crest (grade 1, scored from the CT scan following Bailey et al., 2011). Although it is observed on Neanderthal dm_2 s (e.g. Bailey and Hublin, 2006), its presence on KDS PBE cannot be taken as indicating any special relationship with this group.

The MD and BL diameters of the KDS PBE crown fall within the values reported for modern human samples from Europe and Africa (with the exception of the Liberian sample for the MD dimension). In particular, the BL dimension closely matches that reported for the fragmentary dm_2 from Klasies River Mouth (Table 1). Nevertheless, crown dimensions appear to be limited in their ability to discriminate among groups, as KDS PBE is also consistent with some of the other fossil samples, and overlap exists between recent humans and fossil taxa (Table 1). Centroid size was also calculated for the samples for which outline data were available. Here KDS PBE falls within the lower part of the modern European and African range of variation, and below that of all the fossil samples (SI Figure 1).

In the between-group PCA of the crown outline, PC1 separated the modern human samples, with REU falling on the negative end and RSAF on the positive end of the axis. Early modern humans (UPHS and EHS) fell more centrally on PC1, overlapping with REU (in the case of the UPHS) and with both the REU and the RSAF (in the case of the EHS). PC2 showed a separation between Neanderthals and all modern humans, with small overlap with the range of EHS and, to a lesser extent, those of UPHS and RSAF. Early and Upper Paleolithic *H. sapiens* plotted in a central position on PC2, overlapping largely with RHS and, to a lesser extent, with Neanderthals. KDS PBE fell on the modern human side of PC2 and centrally on PC1, outside the ranges of either recent samples, at the border of the UPHS range and within the EHS convex hull.

KDS PBE was closest in Procrustes Distance, and therefore in total crown outline shape, to one of the RSAF specimens (PD = 0,219) and to the Skhul 1 specimen (PD = 0,232). It was most dissimilar to the Scladina Neanderthal specimen (PD = 0,717). When the KDS PBE crown outline was compared to the mean outlines of the comparative samples it was also most similar to that of the EHS (Figure 3B-F).

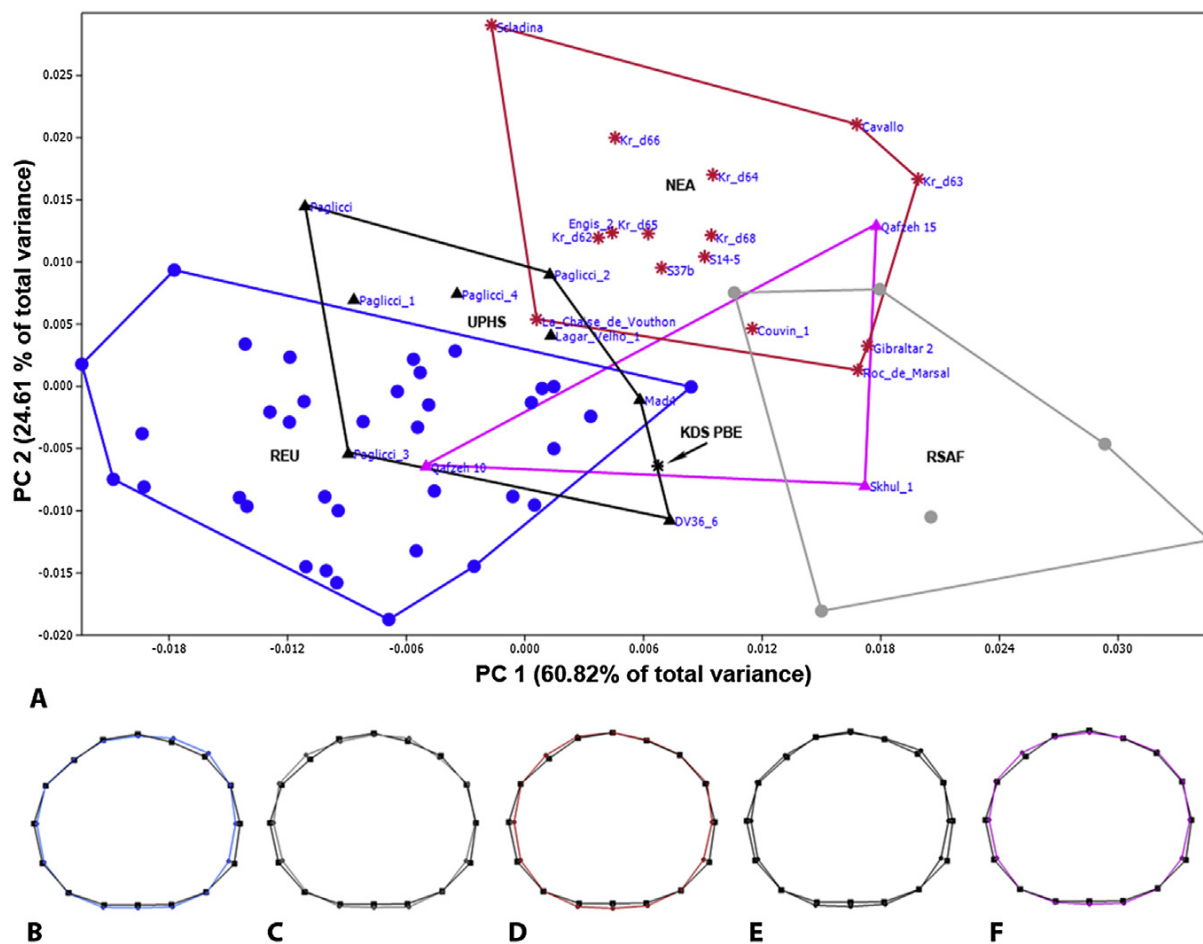


Figure 3. A: Between-group principal components analysis, PC1 plotted against PC2. NEA (red stars); EHS (purple triangles); UPHS (black triangles); REU (blue dots); RSAF (grey dots); KDS PBE (black star). Lines indicate convex hulls for NEA (red), EHS (purple), UPHS (black), REU (blue), and RSAF (grey). Fossil specimens are individually labeled in the plot. **B-F:** Crown outline comparison between KDS PBE (black squares) and comparative samples (B: KDS PBE vs. REU; C: KDS PBE vs. RSAF; D: KDS PBE).

In our analyses of LDPV and LCH, KDS PBE fell close to the lower limit of the range of variation of our REU sample for these metrics, and outside the range of the NEA, EHS, UPHS and RSAF samples (Tables 2 and 3). The UPHS and EHS specimens, as well as the RSAF sample, showed mean values and ranges within the upper part of the REU range, and overlapped more with the NEA range. However, our sample sizes for these groups were very small and their range of variation is probably underestimated.

Table 2. Lateral Dentine and Pulp Chamber Volume value for KDS PBE and descriptive statistics for the groups included in the analysis^a.

| LDPV (mm ³) | | | | | |
|-------------------------|----|------------------------------|----------------------------|----------------------------|--------|
| KDS PBE | | | | | |
| 106.70 | | | | | |
| Group | n | Mean LDPV (mm ³) | Maximum (mm ³) | Minimum (mm ³) | St Dev |
| REU | 23 | 130.20 | 159.03 | 99.72 | 18.94 |
| RSAF | 6 | 144.30 | 200.98 | 118.65 | 31.63 |
| UPHS | 2 | 157.54 | 168.48 | 146.60 | 15.47 |
| EHS | 1 | 134.70 | — | — | — |
| NEA | 11 | 185.28 | 227.20 | 132.84 | 27.30 |

^a REU: recent European *H. sapiens*; RSAF: recent S. African *H. sapiens*; UPHS: Upper Paleolithic *H. sapiens*; NEA: *H. neanderthalensis*; EHS: early *H. sapiens* (Qafzeh/Skhul).

Table 3. Lateral crown height for KDS PBE and descriptive statistics for the groups included in the analysis^a.

| Crown Height (mm) | | | | | |
|-------------------|----|------------------------|--------------|--------------|--------|
| KDS PBE | | | | | |
| 2.22 | | | | | |
| Taxon | n | Crown Height Mean (mm) | Maximum (mm) | Minimum (mm) | St Dev |
| REU | 23 | 2.47 | 2.88 | 2.01 | 0.26 |
| RSAF | 6 | 2.67 | 3.19 | 2.34 | 0.28 |
| UPHS | 2 | 2.83 | 2.90 | 2.76 | 0.10 |
| EHS | 3 | 2.59 | 2.80 | 2.43 | 0.19 |
| NEA | 10 | 3.04 | 3.41 | 2.56 | 0.26 |

^a Labels as in Table 2.

Discussion

The human fossil record from South African MSA contexts is for the most part poorly preserved and often consists of isolated teeth or fragmentary skeletal elements. This poor state of preservation, as well as, in some cases, questions about provenance (see Millard, 2008), have hampered the full assessment of their affinities and have resulted in an incomplete view of the South African MSA populations, limiting our understanding of the association between the evolution of behavioral and anatomical modernity (e.g. Klein, 2008), the possible role of South African MSA people as a source population for the origin of modern humans (e.g. Grine et al., 2007; Henn et al., 2011), and the pattern of population subdivision and early modern human dispersals within Africa (e.g. Gunz et al., 2009; Harvati et al., 2011b). The discovery and analysis of additional human remains, especially specimens found in association with the crucial archaeological context of early behavioral modernity, such as that of Klipdrift Shelter, can help further illuminate the evolutionary processes leading to anatomical modernity in South Africa (see e.g. Verna et al., 2013).

The degree of modernity and possible affinities of the MSA South African populations with archaic hominins have been widely discussed (see e.g. Grine, 2000; Verna et al., 2013). The numerous isolated dental remains show dimensions and morphology that are not diagnostic for late Pleistocene human taxa, although their relatively small size has been argued to infer modernity (Henshilwood et al., 2001; Grine & Henshilwood, 2002; Marean et al., 2004; Grine, 2012). The known MSA cranial and postcranial remains have been described as showing a combination of archaic and modern-like features, as well as a range of sexual dimorphism that exceeds that of recent humans (e.g. Rightmire & Deacon, 1991; Pearson and Grine, 1996; Rightmire et al., 2006; Bräuer, 2008; Royer et al., 2009).

Our analysis of the newly discovered KDS PBE dm_2 is limited by its status as an isolated tooth, and by the lack of dental homologues from either South African MSA contexts (with the exception of the worn and incomplete dm_2 from Klasies River Mouth) or Middle-Late Pleistocene sub-Saharan Africa. Direct comparisons with human remains from relevant South African sites, or from other penecontemporaneous sub-Saharan African sites, are therefore impossible, greatly complicating the interpretation of this specimen. The KDS PBE crown is characterized by some primitive features (e.g. cusp number and crown configuration) compatible with either archaic or modern humans. Like other dental remains from the South African MSA, KDS PBE shows crown dimensions that are within the modern human range of variation. However, they also overlap with (or fall close to the edges of) the ranges of all the fossil samples examined here with the exception of *H. heidelbergensis*. The crown outline analysis differentiated among the fossil and recent samples more clearly. Here KDS PBE was found to cluster with the Skhul-Qafzeh and Upper Paleolithic samples. Its overall outline shape as reflected by inter-individual Procrustes distances was most similar to a Holocene South African Khoesan specimen and to Skhul 1. When the mean Procrustes distances were considered, KDS PBE was most similar to the EHS group, followed by the RSAF sample. Furthermore, the centroid size of KDS PBE, as derived from the crown outline, was relatively small and overlapped only with the recent human samples. In the two additional parameters examined, the lateral crown height and the lateral dentine and pulp chamber volume, KDS PBE shows very low values. These fall well below the means of all comparative samples, including the modern human ones, and within the range only of the recent European specimens included here. While KDS PBE has lower LDPV and crown height values than the minimum values obtained for RSAF, UPHS and EHS, it must be noted that the latter samples

were rather limited in the number of specimens that could be included in this study (see Tables 2 and 3).

KDS PBE therefore retains some features common in early *H. sapiens* populations and even archaic *Homo* species (crown outline shape; crown features; possibly the midtrigonid crest), but is more similar to recent humans in other respects (e.g., relatively small overall crown size; lateral crown height; lateral dentine and pulp chamber volume). This mosaic morphology is consistent with similar results reported for other human remains associated with the South African MSA indicating a population with variable expressions of archaic and modern morphologies. Although further evaluation of possible relationships with both penecontemporaneous and recent southern African populations must await future research, our results show that KDS PBE fits well within the pattern of morphological variation described for MSA humans, consistent with their interpretation as a modern human population chronologically intermediate between the earliest *H. sapiens* and recent modern humans.

Acknowledgments

This research was supported by the European Research Council Starting Grant PaGE No. 283503. The Tübingen Paleoanthropology High Resolution CT Laboratory was funded by a major instrumentation grant from the Deutsche Forschungsgemeinschaft (DFG INST 37/706-1). Financial support for the KDS project was provided to CSH by a European Research Council Advanced Grant, TRACSYMBOLS No. 249587, awarded under the FP7 programme at the University of Bergen, Norway and by a National Research Foundation/Department of Science and Technology funded Chair at the University of the Witwatersrand, South Africa. Additional funding for the KDS excavations in 2013 was provided by the National Geographic Expeditions Council, grant number EC0592-12. CT scans of RSAF sample funded through a grant to RRA by the National Research Foundation of South Africa. We would like to extend thanks to the board of Cape Nature, and especially Tierck Hoekstra and Callum Beattie, for access to the Klipdrift Complex and the facilities at Potberg. We thank Israel Hershkovitz and Rachel Sarig for allowing access to and enabling the HRCT scanning of the Qafzeh and Skhul specimens included in our analyses, Wendy Black of Iziko Museums of South Africa in Cape Town for access to the Holocene Khoesan material, Anton du Plessis

for facilitating scanning at Stellenbosch University, Michael Francken and Sireen El Zaatari for valuable help and comments, and Paul Bons for allowing access to microscope facilities.

References

- Ash, M.M., 1993. Wheeler's Dental Anatomy, Physiology and Occlusion, seventh ed., W. B. Saunders, Philadelphia.
- Baab, K., McNulty, K., Harvati, K. 2013. *Homo floresiensis* Contextualized: A Geometric Morphometric Comparative Analysis of Fossil and Pathological Human Samples. PLoS ONE 8(7), e69119.
- Backwell, L., d'Errico, F., Wadley, L. 2008. Middle Stone Age bone tools from the Howiesons Poort Layers, Sibudu Cave, South Africa. *J. Archaeol. Sci.* 35, 1566–1580.
- Bailey, S. E., Hublin, J.-J. 2006. Did Neanderthals make the Chatelperronian assemblage from La Grotte du Renne (Arcy-sur-Cure, France)? In: Harvati, K., Harrison, T., (Eds.), *Neanderthals Revisited: New Approaches and Perspectives*. Dordrecht: Springer, pp. 191-210.
- Bailey, S.E., Skinner, M.M., Hublin, J.-J. 2011. What lies beneath? An evaluation of lower molar trigonid crest patterns based on both dentine and enamel expression. *Am. J. Phys. Anthropol.* 145, 505-518.
- Benazzi, S., Douka, K., Fornai, C., Bauer, C.C, Kullmer, O., Svoboda, J., Pap, I., Mallegni, F., Bayle, P., Coquerelle, M., Condemi, S., Ronchitelli, A., Harvati, K., Weber, G.W., 2011a. Early dispersal of modern humans in Europe and implications for Neanderthal behaviour. *Nature* 479, 525–528.
- Benazzi, S., Fornai, C., Bayle, P., Coquerelle, M., Kullmer, O., Mallegni, F., Weber, G.W., 2011b. Comparison of dental measurement systems for taxonomic assignment of Neanderthal and modern human lower second deciduous molars. *J. Hum. Evol.* 61, 320–32.
- Benazzi, S., Coquerelle, M., Fiorenza, L., Bookstein, F., Katina, S., Kullmer, O., 2011c. Comparison of Dental Measurement Systems for Taxonomic Assignment of First Molars. *Am. J. Phys. Anthropol.* 144, 342-54.
- Benazzi S., Fornai, C., Buti, L., Toussaint, M., Mallegni, F., Ricci, S., Gruppioni, G., Weber, G.W., Condemi, S., Ronchitelli, A., 2012. Cervical and Crown Outline Analysis of Worn Neanderthal and Modern Human Lower Second Deciduous Molars. *Am. J. Phys. Anthropol.* 149, 537-546.
- Benazzi, S., Bailey, S.E., Peresani, M., Mannino, M.A., Romandini, M., Richards, M.P., Hublin, J.-J., 2014. Middle Paleolithic and Uluzzian human remains from Fumane Cave, Italy. *J. Hum. Evol.* 70, 61-68.
- Bräuer, G., 2008. The origin of modern anatomy: By speciation or intraspecific evolution? *Evol. Anthropol.* 17, 22-37.
- Grine, F.E., 1984. Comparison of the deciduous dentition of African and Asian hominids. *Cour Forsch-Inst Senckenberg* 69, 69–82.

- Grine, F.E., 1986. Anthropological aspects of the deciduous teeth of South African blacks. In: Singer, R., Lundy, J.K. (Eds.), *Variation, Culture and Evolution in African Populations: Papers in Honour of Professor Hertha de Villiers*, pp. 47-83. Johannesburg: Witwatersrand University Press.
- Grine, F.E., 1990. Deciduous dental features of Kalahari San: comparison of non-metrical traits. In: Sperber, G.H. (Ed.), *From Apes to Angels: Essays in Honor of Phillip V. Tobias*, pp. 153-169. New York: Wiley-Liss.
- Grine, F.E., 2000. Middle Stone Age human fossils from Die Kelders Cave 1, Western Cape Province, South Africa. *J. Hum. Evol.* 38, 129-145.
- Grine, F.E., Henshilwood, C.S., 2002. Additional human remains from Blombos Cave, South Africa: (1999–2000 excavations). *J. Hum. Evol.* 42, 293-302.
- Grine, F. E., Bailey, R.M., Harvati, K., Nathan, R.P., Morris, A.G., Henderson, G.M., Ribot, I., Pike, A.W.G., 2007. Late Pleistocene Human Skull from Hofmeyr, South Africa and Modern Human Origins. *Science* 315, 226-229
- Grine, F.E., 2012. Observations on Middle Stone Age human teeth from Klasies River Main Site, South Africa. *J. Hum. Evol.* 63, 750-758.
- Gunz, P., Bookstein, F.L., Mitteroecker, P., Stadlmayr, A., Seidler, H., Weber, G.W., 2009. Early modern human diversity suggests subdivided population structure and a complex out-of-Africa scenario. *Proc. Nat. Acad. Sci.* 106, 6094-6098.
- Hammer, Ø., Harper, D.A.T., Ryan, P.D., 2001. PAST: Paleontological Statistics software package for education and data analysis. *Palaeontologia Electronica* 4(1), 9.
- Harvati, K., Hublin, J.-J., Gunz, P. 2010. Evolution of Middle-Late Pleistocene human cranio-facial form: A 3-D approach. *J. Hum. Evol.* 59, 445-464
- Harvati, K., Stringer, C., Karkanas, P., 2011a. Multivariate analysis and classification of the Apidima 2 cranium from Mani, Southern Greece. *J. Hum. Evol.* 60, 246-250.
- Harvati, K., Stringer, C., Grün, R., Aubert, M., Allsworth-Jones, P., 2011b. The Later Stone Age calvaria from Iwo Eleru, Nigeria: Morphology and chronology. *PLoS ONE* 6(9), e24024.
- Henn, B.M., Gignoux, C.R., Jobin, M., Granka, J.M., Macpherson, J.M., Kidd, J.M., Rodríguez-Botigué, L., Ramachandran, S., Hon, L., Brisbin, A., Lin, A.A., Underhill, P.A., Comas, D., Kidd, K.K., Norman, P.J., Parham, P., Bustamante, C.D., Mountain, J.L., Feldman, M.W., 2011. Hunter-gatherer genomic diversity suggests a southern African origin for modern humans. *Proc. Nat. Acad. Sci.* 108, 5154-5162.
- Henshilwood, C.S., Sealy, J.C., Yates, R., Cruz-Uribe, K., Goldberg, P., Grine, F.E., Klein, R.G., Poggenpoel, C., van Niekerk, K., Watts, I., 2001. Blombos Cave, Southern Cape, South Africa: Preliminary Report on the 1992–1999 Excavations of the Middle Stone Age Levels. *J. Archaeol. Sci.* 28, 421–448.
- Henshilwood, C.S., d’Errico, F., Yates, R., Jacobs, Z., Tribolo, C., Duller, G.A.T., Mercier, N., Sealy, J.C., Valladas, H., Watts, I., Wintle, A.G., 2002. Emergence of modern human behavior: Middle Stone Age engravings from South Africa. *Science* 295, 1278–1280.
- Henshilwood, C.S., & Marean, C.W. 2003. The origin of modern human behavior: A review and critique of the models and their test implications. *Cur. Anthropol.* 44, 627–651.

- Henshilwood, C.S., Dubreuil, B. 2011. The Still Bay and Howiesons Poort, 77–59 ka. *Cur. Anthropol.* 52, 361–400.
- Henshilwood, C.S., van Niekerk, K.L., Wurz, S., Delagnes, A., Armitage, S., Rifkin, R., Douze, K., Keene, P., Haaland, M., Reynard, J., Discamps, E., Mienies, S., 2014. Klipdrift Shelter, southern Cape, South Africa: Preliminary report on the Howiesons Poort levels. *J. Archaeol. Sci.* 45: 284–303.
- Hershkovitz, P., 1971. Basic crown patterns and homologies of mammalian teeth. In: Dahlberg, A.A. (Ed.), *Dental Morphology and Evolution*. University of Chicago Press, Chicago, pp. 95-149.
- Hershkovitz, I., Smith, P., Sarig, R., Quam, R., Rodríguez, L., García, R., Arsuaga, J.L., Barkai, R., Gopher, A., 2011. Middle pleistocene dental remains from Qesem Cave (Israel), *Am. J. Phys. Anthropol.* 144, 575-592.
- Kitagawa, Y., 2000. Nonmetric morphological characters of deciduous teeth in Japan: Diachronic evidence of the past 4000 years. *Int. J. Osteoarchaeol.* 10, 242 – 253.
- Klein, R.G., 2008. Out of Africa and the Evolution of Human Behavior. *Evol. Anthropol.* 17, 267-281.
- Korenhof, C.A.W., 1978. Remnants of the trigonid crests in medieval molars of man of Java. In: Butler, P.M., Joysey, K.A. (Eds.), *Development, Function and Evolution of Teeth*. Academic Press, New York, pp. 157-169.
- Korenhof, C.A.W., 1982. Evolutionary Trends of the Inner enamel anatomy of deciduous molars from Sangiran (Java, Indonesia). In: Kurten, B. (Ed.) *Teeth: Form, Function and Evolution*. Columbia University Press, New York, pp. 350-365.
- Marean, C.W., Nilssen, P.J., Brown, K., Jerardino, A., Stynder, D., 2004. Paleoanthropological investigations of Middle Stone Age sites at Pinnacle Point, Mossel Bay (South Africa): Archaeology and human remains from the 2000 field season. *PaleoAnthropology* 2004.05.02, 14–83.
- Marean, C.W., Bar-Matthews, M., Bernatchez, J., Fisher, E., Goldberg, P., Herries, A.I.R., Jacobs, Z., Jerardino, A., Karkanas, P., Minichillo, T., Nilssen, P., Thompson, E., Watts, I., Williams, H.M., 2007. Early human use of marine resources and pigment in South Africa during the Middle Pleistocene. *Nature* 449, 905-908.
- Millard, A.R., 2008. A critique of the chronometric evidence for hominid fossils: I. Africa and the Near East 500-50 ka. *J. Hum. Evol.* 54, 848-874.
- Mitteroecker, P., Bookstein, F., 2011. Linear discrimination, ordination, and the visualization of selection gradients in modern morphometrics. *Evol. Biol.* 38, 100–114.
- Moss, M.L., Chase, P.S., 1966. Morphology of Liberian Negro deciduous teeth. I. Odontometry. *Am. J. Phys. Anthropol.* 24, 215–229.
- O’Higgins, P., Jones, N., 2006. *Morphologika 2.5. Tools for shape analysis*. Hull York Medical School, University of York. <http://www.york.ac.uk/res/fme>.
- Pearson, O.M., Grine, F.E., 1996. Morphology of the Border Cave hominid ulna and humerus. *S. Afr. J. Sci.* 92, 231–236.
- Rightmire, G.P., Deacon, H.J., 1991. Comparative studies of Late Pleistocene human remains from Klasies River Mouth, South Africa. *J. Hum. Evol.* 20, 131-156.

- Rightmire, G.P., Deacon, H.J., 2001. New human teeth from Middle Stone Age deposits at Klasies River, South Africa. *J. Hum. Evol.* 41, 535–544.
- Rightmire, P.G., Deacon, H.J., Schwartz, J.H., Tattersall, I., 2006. Human foot bones from Klasies River main site, South Africa. *J. Hum. Evol.* 50, 96-103.
- Rightmire, G.P., 2009. Out of Africa: Modern Human Origins Special Feature: Middle and later Pleistocene hominins in Africa and Southwest Asia. *Proc. Nat. Acad. Sci.* 106, 16046-16050.
- Royer, D.F., Lockwood, C.A., Scott, J.E., Grine, F.E., 2009. Size variation in early human mandibles and molars from Klasies River, South Africa: Comparison with other Middle and Late Pleistocene assemblages and with modern humans. *Am. J. Phys. Anthropol.* 140, 312-323.
- SAS Institute, (1999-2001). SAS System for Windows V8. The SAS Institute.
- Scott, G.R., Turner II, C.G. 1997. *The Anthropology of Modern Human Teeth. Dental Morphology and its Variation in Recent Human Populations.* Cambridge University Press, Cambridge.
- Slice, D.E. 2005. Platform-Independent software for morphometric analysis.
- Smith, T.M., Tafforeau, P., Reid, D.J., Pouech, J., Lazzari, V., Zermeno, J.P., Guatelli-Steinberg, D., Olejniczak, A.J., Hoffman, A., Radović, J., Makaremi, M., Toussaint, M., Stringer, C., Hublin, J.J. 2010. Dental evidence for ontogenetic differences between modern humans and Neanderthals. *Proc. Nat. Acad. Sci.* 107, 20923-20928.
- Spoor, C.F., Zonneveld, F.W., Macho, G.A., 1993. Linear Measurements of Cortical Bone and Dental Enamel by Computed Tomography: Applications and Problems. *Am. J. Phys. Anthropol.* 91, 469 – 484.
- Texier, P.J., Porraz, G., Parkington, J., Rigaud, J.P., Poggenpoel, C., Miller, C., Tribolo, C., Cartwright, C., Coudenneau, A., Klein, R., Steele, T., Verna, C., 2010. A Howiesons Poort tradition of engraving ostrich eggshell containers dated to 60,000 years ago at Diepkloof Rock Shelter, South Africa. *Proc. Nat. Acad. Sci.* 107, 6180-6185.
- Texier, P.J. Porraz, G., Parkington, J., Rigaud, J.-P., Poggenpoel, C., Tribolo, C., 2013. The context, form and significance of the MSA engraved ostrich eggshell collection from Diepkloof Rock Shelter, Western Cape, South Africa. *J. Archaeol. Sci.* 40, 3412-3431.
- Toussaint, M., Olejniczak, A., El Zaatari, S., Cattelain, P., Flas, D., Letourneux, C., Pirson, S., 2010. The Neandertal lower right deciduous second molar from Trou de l'Abime at Couvin, Belgium. *J. Hum. Evol.* 58, 56-67.
- Verna, C., Texier, P.J., Rigaud, J.P., Poggenpoel, C., Parkington, J., 2013. The Middle Stone Age human remains from Diepkloof Rock Shelter (Western Cape, South Africa). *J. Archaeol. Sci.* 40, 3532-3541.
- Vogelsang, R., Richter, J., Jacobs, Z., Eichhorn, B., Linseele, V., Roberts, R., 2010. New excavations of Middle Stone Age Deposits at Apollo 11 Rockshelter, Namibia: Stratigraphy, Archaeology, Chronology and Past Environments. *J. Afr. Archaeol.* 8, 185-218.
- Wadley, L., Mohapi, M. 2008. A segment is not a monolith: Evidence from the Howiesons Poort of Sibudu, South Africa. *J. Archaeol. Sci.* 35, 2594–2605.
- Yun, S.W., Lim, W.H., Chong, D.R., Chu, Y.S., 2007. Scissors-bite correction on second molar with a dragon helix appliance. *Am. J. Orthod. Dentofac.* 132, 842-847.

Supplementary Online Information

Scanning procedures

3D- μ CT scans of all specimens were obtained using industrial and synchrotron-based μ CT scanners at isotropic voxel length between 15 and 65 μ m. The only exception is the UPHS sample from Grotta Paglicci, for which a white-light surface scanning system was used (see Benazzi et al., 2012). The EHS and part of the REU samples were scanned with a General Electric Phoenix v|tome|x micro-CT at the Department of Paleoanthropology of the University of Tübingen. The RSAF sample was scanned with a General Electric Phoenix v|tome|x micro-CT located at the Stellenbosch University CT Scanner Facility (near Cape Town, South Africa). Scan settings varied between 130 kV/100 μ A and 180 kV/140 μ A depending on the state of preservation and/or fossilization. Details about the μ CT scanning procedure for the NEA, UPHS, and remaining RHS samples can be found in Toussaint et al. (2010), Benazzi et al. (2011a, 2012), the NESPOS (Neanderthal Studies Professional Online Service) Database 2011, and the ESRF Paleontological Database (Smith et al., 2010).

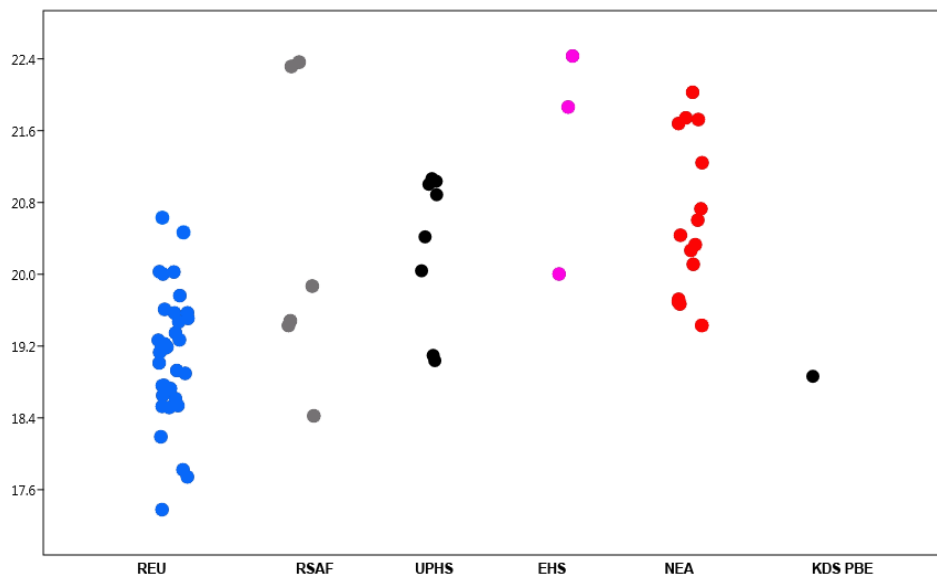
Data processing

The REU, RSAF, and EHS samples scanned in Tübingen and in Cape Town were added to the dm₂ dataset of Benazzi et al. (2012). Because KDS PBE is a lower left deciduous molar, all teeth were regarded as left dm₂s, with right dm₂ specimens mirror imaged before data processing and analysis. To ensure that all specimens were correctly oriented for data collection we followed the procedures described in Benazzi et al. (2011a, 2012) using AVIZO® 7.0 (VSG, Visualization Sciences Group) and Amira® 5.2 software (Mercury Computer Systems, Chelmsford, USA). The Tübingen and Cape Town samples were segmented following the half-maximum height protocol by Spoor et al. (1993) to assign voxels of different grey values to different dental material and to obtain 3D digital models of the teeth.

SOM Table 1. Fossil and recent comparative samples used in the crown outline shape, LDPV, and CH analyses. Taxa labeled as in the text.

| Taxon | Specimen | Origin | Source | Outline | LDPV | LCH |
|----------------|--------------------------------------|------------------------------------|--|---------|------|-----|
| NEA | Abri Suard S42 | France | NESPOS (μ CT) ^a | X | X | X |
| | Abri Suard S37 | France | NESPOS (μ CT) ^a | X | X | X |
| | Abri Suard S14-5 | France | NESPOS (μ CT) ^a | X | X | X |
| | Cavallo A | Italy | Benazzi et al., 2011a (μ CT) | X | X | X |
| | Couvin | Belgium | Toussaint et al., 2010 (μ CT) | X | X | |
| | Engis 2 | Belgium | Toussaint et al., 2010 (μ CT) | X | X | |
| | Gibraltar 2 | Gibraltar | ESRF Paleontological Database (Smith et al., 2010) | X | X | X |
| | Krapina d62 | Croatia | NESPOS (μ CT) ^a | X | X | X |
| | Krapina d63 | Croatia | NESPOS (μ CT) ^a | X | X | X |
| | Krapina d64 | Croatia | NESPOS (μ CT) ^a | X | X | X |
| | Krapina d65 | Croatia | NESPOS (μ CT) ^a | X | | |
| | Krapina d66 | Croatia | NESPOS (μ CT) ^a | X | | |
| | Krapina d68 | Croatia | NESPOS (μ CT) ^a | X | | X |
| | Roc de Marsal 1 | France | NESPOS (μ CT) ^a | X | X | X |
| Scladina 4A-13 | Belgium | Toussaint et al., 2010 (μ CT) | X | | | |
| EHS | Skhul_1 | Israel | Original data (μ CT) University of Tuebingen | X | X | X |
| | Qafzeh 10 | Israel | Original data (μ CT) University of Tuebingen | X | | X |
| | Qafzeh 15 | Israel | Original data (μ CT) University of Tuebingen | X | | X |
| UPHS | Dolni Vestonice 36-6 | Czech Republic | Benazzi et al., 2012 | X | | |
| | La Madeleine 4 | France | NESPOS (μ CT) ^a | X | X | X |
| | Paglicci 38 | Italy | Benazzi et al., 2012 (surface scan of the cast) | X | | |
| | Paglicci 39 | Italy | Benazzi et al., 2012 (surface scan of the cast) | X | | |
| | Paglicci 40 | Italy | Benazzi et al., 2012 (surface scan of the cast) | X | | |
| | Paglicci 41 | Italy | Benazzi et al., 2012 (surface scan of the cast) | X | | |
| REU | Paglicci 42 | Italy | Benazzi et al., 2012 (surface scan of the cast) | X | | |
| | Lagar Velho 1 | Portugal | NESPOS (μ CT) ^a | X | X | X |
| | From medieval and recent individuals | Germany & Luxemburg: 5 | Original data (μ CT) University of Tübingen | 36 | 23 | 23 |
| | | Austria: 14 | Original data (μ CT) Bayle et al., 2010 NESPOS (μ CT) | | | |
| | France: 7 | Original data (μ CT) | | | | |
| | Italy: 10 | | | | | |
| RSAF | Holocene | South Africa | Original data (Cape Town) | 6 | 6 | 6 |

^a NESPOS (Neanderthal Studies Professional Online Service) digital internet archive, www.nespos.org

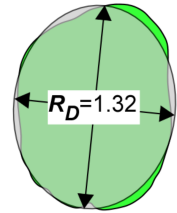


SOM Figure 1. Crown centroid sizes, as calculated from the crown outline pseudolandmarks. REU: blue; RSAF: gray; UPHS: black; EHS: purple; NEA: red.

SOM References

- Benazzi, S., Douka, K., Fornai, C., Bauer, C.C, Kullmer, O., Svoboda, J., Pap, I., Mallegni, F., Bayle, P., Coquerelle, M., Condemi, S., Ronchitelli, A., Harvati, K., Weber, G.W., 2011a. Early dispersal of modern humans in Europe and implications for Neanderthal behaviour. *Nature* 479, 525–528
- Benazzi, S., Coquerelle, M., Fiorenza, L., Bookstein, F., Katina, S., Kullmer, O., 2011c. Comparison of dental measurement systems for taxonomic assignment of first molars. *Am. J. Phys. Anthropol.* 144, 342–534.
- Benazzi S., Fornai, C., Buti, L., Toussaint, M., Mallegni, F., Ricci, S., Gruppioni, G., Weber, G.W., Condemi, S., Ronchitelli, A., 2012. Cervical and crown outline analysis of worn Neanderthal and modern human lower second deciduous molars. *Am. J. Phys. Anthropol.* 149, 537–546.
- Benazzi, S., Bailey, S.E., Peresani, M., Mannino, M.A., Romandini, M., Richards, M.P., Hublin, J.-J., 2014. Middle Paleolithic and Uluzzian human remains from Fumane Cave, Italy. *J. Hum. Evol.* 70, 61–68.
- Smith, T.M., Tafforeau, P., Reid, D.J., Pouech, J., Lazzari, V., Zermeno, J.P., Guatelli-Steinberg, D., Olejniczak, A.J., Hoffman, A., Radović, J., Makaremi, M., Toussaint, M., Stringer, C., Hublin, J.-J., 2010. Dental evidence for ontogenetic differences between modern humans and Neanderthals. *Proc. Natl. Acad. Sci.* 107, 20923–20928.
- Spoor, C.F., Zonneveld, F.W., Macho, G.A., 1993. Linear measurements of cortical bone and dental enamel by computed tomography: applications and problems. *Am. J. Phys. Anthropol.* 91, 469–484.
- Toussaint, M., Olejniczak, A., El Zaatari, S., Cattelain, P., Flas, D., Letourneux, C., Pirson, S., 2010. The Neanderthal lower right deciduous second molar from Trou de l’Abime at Couvin, Belgium. *J. Hum. Evol.* 58, 56–67.

American Journal of Physical Anthropology



Resubmitted after revision

Technical Note

Using elliptical best fits to characterize dental shapes

Catherine C. Bauer^{1*}, Paul D. Bons², Stefano Benazzi^{3,4} and Katerina Harvati¹

¹Paleoanthropology, Senckenberg Center for Human Evolution and Paleoenvironment, Eberhard Karls Universität Tübingen, Rümelinstrasse 23, Tübingen 72070, Germany

²Mineralogy and Geodynamics, Department of Geosciences, Eberhard Karls Universität Tübingen, Wilhelmstrasse 56, Tübingen 72074, Germany

³Department of Cultural Heritage, University of Bologna, Via degli Ariani 1, 48121 Ravenna, Italy

⁴Department of Human Evolution, Max Planck Institute for Evolutionary Anthropology, Deutscher Platz 6, D-04103 Leipzig, Germany

*Corresponding author:

E-mail address: catherine.bauer@ifu.uni-tuebingen.de (C. Bauer)

Keywords: Geometric morphometrics, *Homo sapiens*, *Homo neanderthalensis*, Dental morphology

Because of their physical properties dental remains are disproportionately preserved, and indeed isolated teeth are often the only specimens recovered from paleontological and archaeological settings. Dental tissues preserve a strong genetic signal because they are formed early in development and are not subject to remodeling and environmental factors during an individual's lifetime. As a result, teeth play an important role in the interpretation of the human fossil record and their study is useful for taxonomic and phylogenetic purposes (e.g. Suwa et al. 1994, 1996; Irish 1998; Irish and Guatelli-Steinberg 2003; Bailey 2006; Martín-Torres et al. 2006, Gómez-Robles et al. 2008, 2011, Benazzi et al. 2011a, b, 2012, 2013, 2014; Fornai et al. 2014; Harvati et al. 2015).

Beyond the basic measurements of crown bucco-lingual and mesio-distal dimensions, dental morphology can be characterized using non-metric traits and trait frequencies (e.g. Bailey, 2006), as well as through geometric morphometric approaches (e.g. Bailey and Lynch, 2005; Martín-Torres et al., 2006; Braga et al., 2010; Gómez-Robles et al, 2011; Harvati et al. 2015). Both approaches depend upon adequate preservation of the teeth, for wear and abrasion can damaged or obliterate the cusps and grooves required to define traits or landmarks (Benazzi et al., 2011c, 2012). This problem can be avoided with high-resolution micro-CT scanning, which allows the analysis of, for example, the morphology of the dentine surface (e.g. Skinner et al. 2008, 2009; Braga et al., 2010; Bailey et al. 2011; Benazzi et al., 2013, 2014). However, even characteristic cusps or spines on the dentine surface may be affected by dental wear. Furthermore, the full segmentation required to define the dentine surface of a tooth at a sufficiently high resolution is a time-consuming and cumbersome task, making large comparative sample sizes difficult to achieve. Finally, high-resolution CT scans are not always available, with databases such as NESPOS (www.nespos.org) in some cases only providing surface outlines for dental remains.

We propose here that elliptical fits (Bookstein, 1979; Mulchrone and Choudhury, 2004) to dental outlines, or, when available, internal tissue outlines, are efficient descriptors of dental morphology. This approach may prove to be a useful addition to the current range of morphometric methods, especially in cases where teeth are worn or difficult to orient teeth.

MATERIALS AND METHODS

Teeth from two different tooth classes, dm^2 and the M^3 , were used for this study. For the dm^2 analysis we used all specimens for which both the cervical and crown outlines were included in the sample of Benazzi et al. (2011a). These include two Upper Paleolithic Modern Humans (UPMH, Dolni Vestonice 3, Cavallo C), eight Neanderthals (NEA, six specimens from Krapina and two from Roc de Marsal), and 15 European Recent Modern Humans (RMH). The reader is referred to Benazzi et al. (2011a) for details of origin and scanning procedure of the specimens. The cervical line of each 3D digital tooth model was first aligned parallel to the xy -plane of the Cartesian coordinate system. The teeth were subsequently rotated around the z -axis to align the lingual wall of the crown parallel to the x -axis. All teeth from the right side were mirror-imaged and treated as teeth from the left side.

The samples for the M^3 analysis included eight NEA from Krapina, Croatia (Radovčić et al. 1988), and 25 RMH specimens (seven Neolithic Egyptians, six Bronze-Age Tunisians, seven medieval Germans, and five recent specimens from Oceania). The Krapina M^3 remains were obtained from the NESPOS online database, while the remaining comparative sample was scanned at the Tübingen Paleoanthropology high-resolution computed tomography lab at a resolution of 26-100 μm . The different resolution of the scans is depending on the size of each specimen (i.e. isolated teeth vs maxillary fragments). Similar to the dm^2 sample, all M^3 s from the left side were mirror-imaged and treated as teeth from the right side.

Bitmaps of dental tissue outlines were created at ~ 40 -60 pixel/mm. The shape of an outline is defined by a set of x and y coordinates of the pixels on the outline. The aforementioned outlines are approximately convex and close to elliptical. A first-order shape descriptor for such a shape is thus an ellipse. An ellipse that is centered on the origin of a rectangular coordinate system can be described as (Bookstein, 1979):

$$ax^2 + bxy + cy^2 - 1 = 0 \quad (1)$$

The shape and size of the ellipse are thus defined by three parameters, a , b and c (see Table 1 for symbols used). These parameters can be estimated with standard least-squares techniques (Bookstein, 1979; Erslev and Ge, 1990) that minimize the sum of the squared errors (δ_i) for each i -th data point, using:

$$ax_i^2 + bx_iy_i + cy_i^2 - 1 = \delta_i \quad (2)$$

TABLE 1. List of symbols and subscripts used, as well as list of parameters used for each tooth class.

| Symbol | Description |
|---------------------|--|
| a, b, c | Ellipse parameters [mm ²] |
| δ | Error in least-squares best fit procedure [-] |
| L_{max}, L_{min} | Long and short axis of best-fit ellipse [mm] |
| β | Orientation of long axis of best-fit ellipse [°] |
| R | Axial ratio of best-fit ellipse ($R=L_{max}/L_{min}$) [-] |
| ΔP | Ratio of perimeters of the shape and its best-fit ellipse [-] |
| A | Area of shape [mm ²] |
| $\Delta\beta_{X,Y}$ | Difference in orientation of best-fit ellipse of shape X and Y [°] |
| Subscripts | |
| Cr | Crown outline |
| C | Outline in the cervical plane |
| E | Outline of the enamel in the EDJ-plane |
| D | Outline of the dentine and pulp chamber in the EDJ-plane |
| Tooth class | Parameters used |
| dm^2 | R_{Cr}, R_C, β_{Cr} and β_C |
| M^3 | $\Delta\beta_{E,D}, \Delta\beta_{C,D}, (A_E/A_D)^{1/2}, (A_C/A_D)^{1/2}, R_E/R_D, R_C/R_D, \Delta P_E, \Delta P_C$ |

This least-squares conical fit suffices as the tooth outlines are approximately elliptical and data points (edge pixels of the shape) are distributed regularly on the surface of the outline. This avoids complications and pitfalls related to conical fits when these requirements are not met (see e.g. Rosin, 1993; Ahn et al., 2001; Mulchrone and Choudhury 2004). The above requires the ellipse to be centered on the origin. The center of area of the outline can be chosen as the origin. Alternatively, or in case of an incomplete outline, an iterative routine can be used to find the origin that results in the smallest summed error. The latter approach is used here.

It should be noted that elliptical best fits can be performed in various ways (Mulchrone and Choudhury, 2004) of which the conical best fit used here is only one. We compared our best-fit ellipses with those calculated from the second moments of the entire shape, using the free software ImageJ (Rasband, 1997-2014) and found no significant difference.

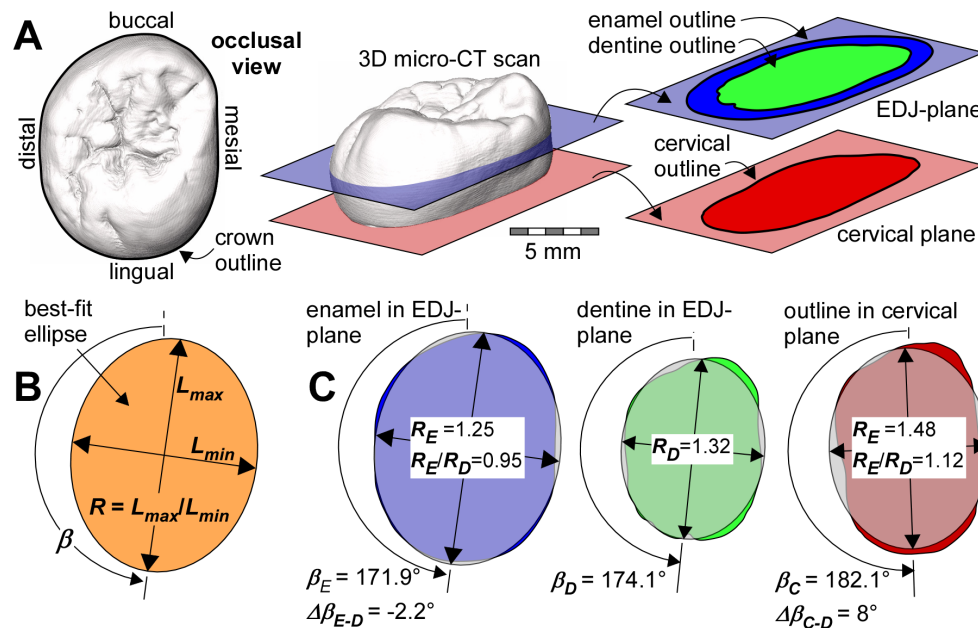


Fig. 1. Definition of (A) the various outlines and (B) the parameters L_{max} , L_{min} , R and b that define shape and orientation of an ellipse (C) Three ellipses were fitted to outlines of one M³, here illustrated with a Neanderthal M³ (Krapina d163).

Instead of using the parameters a , b and c , an ellipse can be defined by its size (area), how elongate it is and its orientation. The elongation of an ellipse is usually defined by its eccentricity or by its axial ratio, which is the shape parameter used here. The axial ratio (R) is the ratio of the lengths of the long (L_{max}) and short (L_{min}) principal axes ($R = L_{max}/L_{min}$) that are, by definition, orthogonal. R is unity for a circle and increases in value for more elongate ellipses. The orientation of an ellipse is defined here as the orientation of its long axis (β) relative to a reference. As a reference we use the bucco-lingual direction (Fig. 1). Advantages of an elliptical fit are that it is done on the complete outline shape and thus obviates the need to select landmarks. A further parameter to be used is the quality of the fit, which can be expressed in various ways. Both a circle and a square have the same axial ratio of one. However, the ratio ΔP of their perimeter and that of their best-fit ellipse will be different: one for a circle and >1 for a square. ΔP will thus be used as a measure of how close to an ellipse a shape is. An additional parameter that is readily available when conducting the above analysis is the area (A) enclosed by an outline.

Crown (subscript Cr) and cervical (subscript C) plane outlines were analyzed for the dm^2 (Fig. 1A). We measured the orientations (β_{Cr} and β_C) and the axial ratios (R_{Cr} and R_C). Outlines in

the cervical plane (the best-fit plane of the cervical line), as well as those of enamel (subscript E) and dentine (subscript D) in the EDJ-plane (a plane, parallel to the cervical plane, passing through the lowest point of the enamel in the occlusal basin) were analyzed for the M^3 (Fig. 1C). M^3 outlines are more variable in shape, even within a species, compared to those of dm^2 . This hampers accurate orientation and the orientations ($\Delta\beta_{E-D}=\beta_E-\beta_D$ and $\Delta\beta_{C-D}=\beta_C-\beta_D$) relative to that of the best-fit ellipse to the dentine outline in the EDJ-plane were therefore used instead of absolute orientations. The dentine outline was chosen as reference, as it is least affected by wear or other damage. Relative areas $(A_E/A_D)^{1/2}$ and $(A_C/A_D)^{1/2}$ were normalized to that of the dentine outline in the EDJ-plane to exclude size in the analysis. A square root was taken as area is in mm^2 . As axial ratios of different outlines within a single tooth tend to correlate well, we also normalized the axial ratios R_E and R_C to R_D . The dentine outline in the EDJ plane can be smooth, but also serrate, especially at the lingual side. Because this has a relatively strong effect on ΔP_D , we only used ΔP_E and ΔP_C . For the M^3 , we thus obtained a total of eight size- and orientation-independent parameters (Table 1). A principal component analysis of correlations was carried out with the software JMP, version 11.1.1, for both datasets.

RESULTS

The best-fit ellipses of the dm^2 -outlines, using the least-squares method, have axial ratios ranging between about 1.12 to 1.24 for crown outlines and about 1.25 to 1.5 for cervical outlines (Fig. 2). Although there is a tendency for NEA outlines to be slightly more elliptical, value ranges for each outline overlap between NEA and RMH. The orientations of the long axes, however, show a clear taxonomic differentiation. If, as in this case, the teeth can be oriented accurately, the orientation of the best-fit ellipse of either the dm^2 crown or cervical outline suffices to distinguish between the two species. Dolni Vestonice 3 and Cavallo C clearly plot with RMH. Combining the orientations of the ellipses of both outlines gives an even clearer separation (Fig. 2C). A PCA of all four measured parameters (Table 1) confirms that the orientations of the best-fit ellipses are the main discriminators between the species, dominating PC1, which represents 58.7% of total variance. In summary, best-fit ellipses are useful shape descriptors to separate RMH from NEA in case of dm^2 . The analysis supports the classification of Cavallo C as an UPMH by Benazzi et al. (2011a).

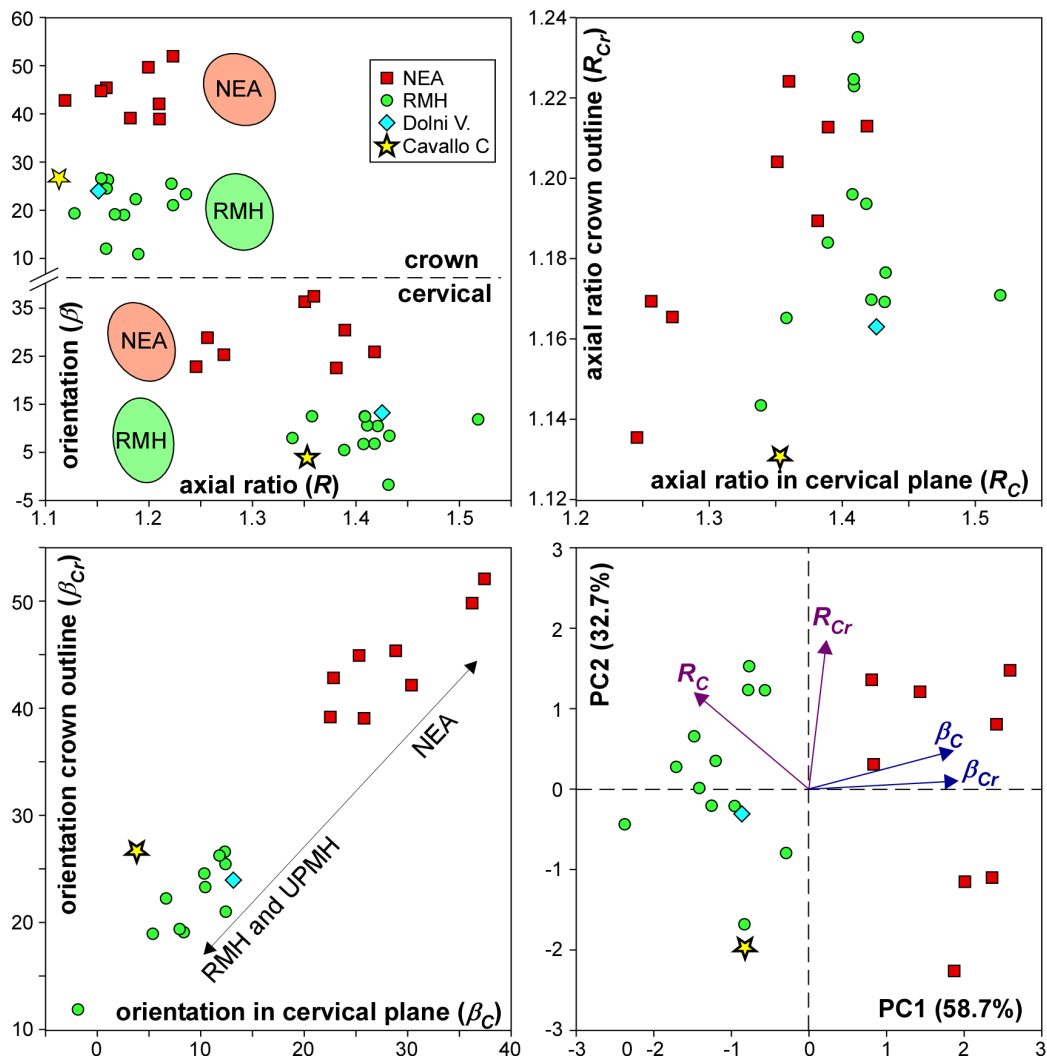


Fig. 2. Results for the analyses of dm^2 crown and cervical outlines. **(A)** Orientation (β) of long axis of best-fit ellipse versus R for crown outlines (top) and cervical outlines (bottom), together with mean best-fit ellipses for NEA and RMH. **(B)** Ellipse axial ratios of crown versus cervical outlines. **(C)** Ellipse orientation of crown versus cervical outlines. **(D)** PCA of the four parameters.

Unlike our results for the dm^2 , a plot of orientation versus axial ratio of a single M^3 outline shows no separation between Neanderthals and modern humans (compare fig. 3A with fig. 2A). This is likely due to the variability in shape and the difficulty to consistently orient the teeth. Relative orientations ($\Delta\beta_{E-D}$ and $\Delta\beta_{C-D}$) show a more consistent pattern (Fig. 3B). NEA enamel outlines tend to be rotated clockwise ($\Delta\beta_{E-D} < 0^\circ$) relative to the dentine outline, whereas this rotation varies for the RMH specimens ($-8^\circ < \Delta\beta_{E-D} < 7^\circ$). The cervical outline is usually rotated clockwise relative to the dentine outline, but generally stronger in RMH (-

$1^\circ < \Delta\beta_{C,D} < 16^\circ$) than in NEA specimens ($0^\circ < \Delta\beta_{C,D} < 8^\circ$). The normalized axial ratios (R_E/R_D and R_C/R_D ; Fig. 3C) plot in a narrow range for the NEA specimens. Data for the RMH specimens lie on a trend that is, with the exception of two specimens, distinct from the NEA individuals. Relative areas of outlines in the cervical and dentine in the EDJ-plane vary over the same range for both RMH and NEA (Fig. 3D). There is a weak tendency for NEA to have a relatively low ratio of enamel and dentine area in the EDJ-plane, indicating that their enamel tends to be relatively thin. The plot of ΔP_E versus ΔP_C shows that the NEA outlines tend to be closer to elliptical in shape than those of most of the RMH specimens (Fig. 3E).

Combining the eight size- and orientation-free parameters (Table 1) in a PCA results in a partial separation between NEA and RMH (Fig. 3F). NEA specimens plot in the range of negative PC2, mostly owing to their close-to-elliptical shape of the outlines (ΔP) and their relative outline orientations ($\Delta\beta$). Oceania specimens plot in a distinct group in the negative PC1 and positive PC2 range, mostly because their enamel outline is distinctly less elliptical ($R_E < R_D$) than that of the dentine in the EDJ-plane (Fig. 3C) and a mostly small relative area of the cervical outline, $(A_C/A_D)^{1/2}$.

DISCUSSION AND CONCLUSIONS

It must be noted that our results are preliminary and limited by the small sample sizes available for this study. Nevertheless, they show that elliptical fits are potentially useful for a first-order description of outlines of dental tissue. The example of the application to dm^2 shows that a single outline may suffice if the teeth can be accurately oriented. However, M^3 are difficult to orient owing to their highly variable outline shapes. This seriously hinders the use of pseudolandmarks, as these rely on a correct and consistent orientation of the shape to be analyzed (Benazzi et al., 2011a,c, 2012, 2014). If multiple outlines are available, the absolute orientation can be removed by using relative orientations of the different outlines. By additionally using relative areas enclosed by the different outlines, the method becomes fully independent of absolute size and orientation of the specimens.

This approach can be successfully applied to surface scans if no micro-CT scans are available, as was shown in the application to dm^2 . However, internal tissue outlines, such as the dentine outline in the EDJ plane, can be used as well, and can help increase the usefulness of the

method, as in our application to the M^3 . Only one or a few slices of a 3D micro-CT scan need to be segmented, which constitutes an enormous time saving advantage compared to methods that require the segmentation of a complete tooth or the whole volume between the cervical and EDJ-plane.

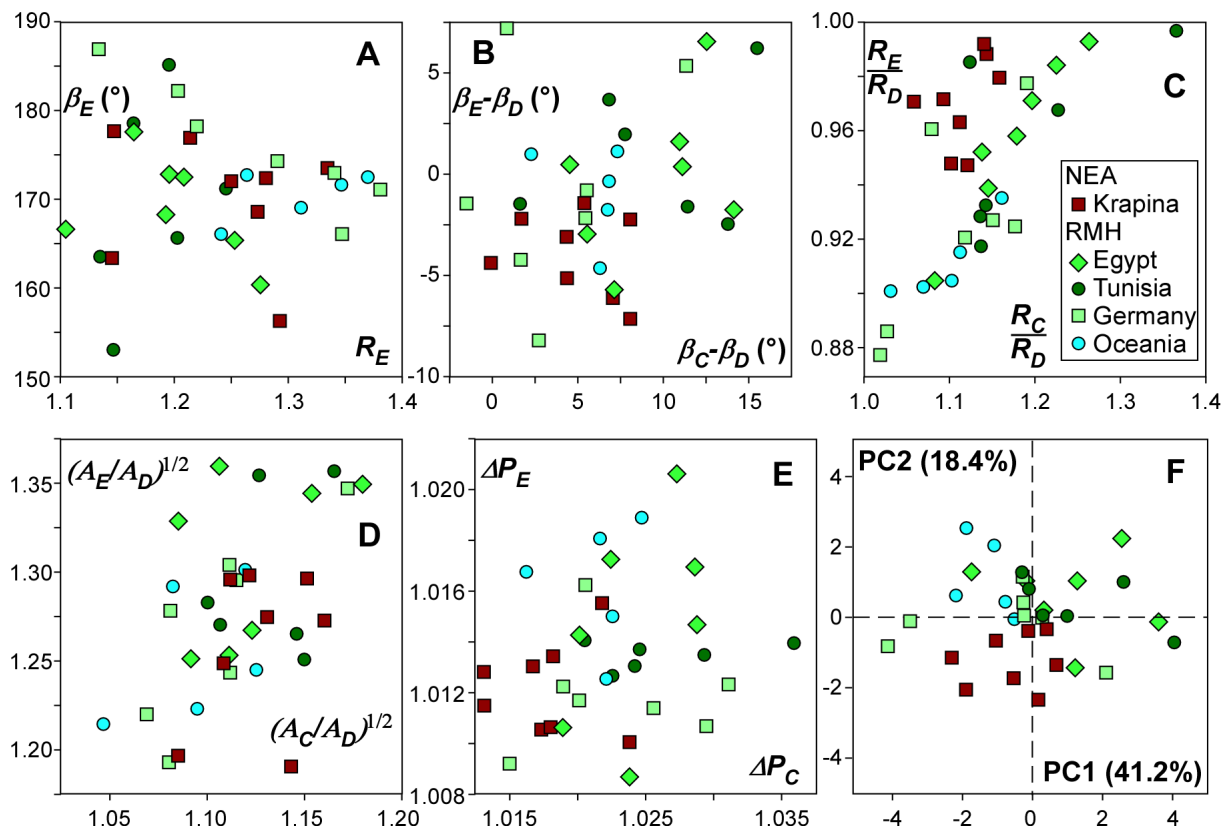


Fig. 3. Results for the analysis of M^3 outlines in the cervical plane, as well as enamel and dentine outlines in the EDJ-plane. **(A)** Absolute orientation versus axial ratio of enamel in the EDJ-plane. **(B)** Orientations relative to that of the dentine outline in the EDJ-plane. **(C)** Axial ratios and **(D)** areas normalized to that of the dentine outline in the EDJ-plane. **(E)** Perimeters relative to that of the best-fit ellipse. **(F)** PCA based on the eight size and orientation-free parameters listed in the main text.

In summary, our first application of elliptical best fits to two tooth classes suggests that it may be a robust additional method for dental shape analysis. It may prove to be particularly useful where dental wear or highly variable dental morphologies make the determination of real or pseudolandmarks difficult or impossible. Further work on increased samples and additional tooth classes will help validate our results.

ACKNOWLEDGMENTS

This study was supported by the European Research Council Starting Grant PaGE, No. 283503. The Tübingen Paleoanthropology High-Resolution CT Laboratory is funded through a major-instrumentation grant by the Deutsche Forschungsgemeinschaft (DFG INST 37/706-1 FUGG). We thank two anonymous reviewers and the Associate Editor of the journal for their helpful comments and criticism.

LITERATURE CITED

- Ahn SJ, Rauh W, Warnecke HJ. 2001. Least-squares orthogonal distances fitting of circle, sphere, ellipse, hyperbola, and parabola. *Pattern Recognit Lett* 34:2283-2303.
- Bailey SE. 2006. Beyond Shovel-Shaped Incisors: Neandertal Dental Morphology in a Comparative Context. *Period Biol* 108:253-267.
- Bailey SE, Lynch JM. 2005. Diagnostic differences in mandibular P4 shape between Neandertals and Anatomically Modern Humans. *Am J Phys Anthropol* 126:268-277.
- Bailey SE, Skinner MW, Hublin JJ. 2011. What Lies Beneath? An Evaluation of Lower Molar Trigonid Crest Patterns Based on Both Dentine and Enamel Expression. *Am J Phys Anthropol* 145:505-518.
- Benazzi S, Fornai C, Buti L, Toussaint M, Mallegni F, Ricci S, Gruppioni G, Weber GW, Condemi S, Ronchitelli A. 2012. Cervical and Crown Outline Analysis of Worn Neandertal and Modern Human Lower Second Deciduous Molars. *Am J Phys Anthropol* 149:537-546.
- Benazzi S, Douka K, Fornai C, Bauer CC, Kullmer O, Svoboda J, Pap I, Mallegni F, Bayle P, Coquerelle M, Condemi S, Ronchitelli A, Harvati K, Weber GW. 2011a. Early dispersal of modern humans in Europe and implications for Neandertal behaviour. *Nature* 479:525 – 528.
- Benazzi S, Fornai C, Bayle P, Coquerelle M, Kullmer O, Mallegni F, Weber GW. 2011 b. Comparison of dental measurement systems for taxonomic assignment of Neandertal and modern human lower second deciduous molars. *J Hum Evol* 61 (3):320 – 326.
- Benazzi S, Coquerelle M, Fiorenza L, Bookstein F, Katina S, Kullmer O. 2011c. Comparison of Dental Measurement Systems for Taxonomic Assignment of First Molars. *Am J Phys Anthropol* 144: 342-354.
- Benazzi S, Bailey SE, Mallegni F. 2013. A morphometric analysis of the Neandertal upper second molar Leuca I. *Am J Phys Anthropol* 152:300-305.
- Benazzi S, Bailey SE, Peresani M, Mannino MA, Romandini M, Richards MP, Hublin JJ. 2014. Middle Paleolithic and Uluzzian human remains from Fumane Cave, Italy. *J Hum Evol* 70:61-68.
- Bookstein FL. 1979. Fitting conic sections to scattered data. *Comput Vision Graph* 9:56-71.

- Braga J, Thackeray JF, Subsol G, Kahn JL, Maret D, Treil J, Beck A. 2010. The enamel–dentine junction in the postcanine dentition of *Australopithecus africanus*: intra-individual. *J Anat* 216:62-79.
- Erslev EA, Ge H. 1990. Least-squares center-to-center and mean object ellipse fabric analysis. *J Struct Geol* 12:1047-1059.
- Fornai C, Benazzi S, Svoboda J, Pap I, Harvati K, Weber GW. 2014. Enamel thickness variation of deciduous first and second upper molars in modern humans and Neanderthals. *J Hum Evol* 76:83 – 91.
- Gómez-Robles A, Martínón-Torres M, Bermúdez de Castro JM, Prado-Simón L, Arsuaga JL. 2011. A geometric morphometric analysis of hominin upper premolars. Shape variation and morphological integration. *J Hum Evo* 61:688 – 702.
- Gómez-Robles A, Martínón-Torres M, Bermúdez de Castro JM, Prado L, Sarmiento S, Arsuaga JL. 2008. Geometric morphometric analysis of the crown morphology of the lower first premolar of hominins, with special attention to Pleistocene *Homo*. *J Hum Evo* 55:627 – 638.
- Harvati K, Bauer CC, Grine FE, Benazzi S, Ackerman RR, van Niekerk KL, Henshilwood CS. 2015. A human deciduous molar from the Middle Stone Age (Howiesons Poort) of Klipdrift Shelter, South Africa, *J Hum Evo* <http://dx.doi.org/10.1016/j.jhevol.2015.03.001>
- Irish JD, Guatelli-Steinberg D. 2003. Ancient teeth and modern human origins: An expanded comparison of African Plio-Pleistocene and recent world dental samples. *J Hum Evol* 45 (2):113 - 144.
- Irish JD. 1998. Ancestral Dental Traits in recent Sub-Saharan Africans and the origin of modern humans. *J Hum Evol* 34 (1):81 - 98.
- Martinón-Torres M, Bastir M, Bermúdez de Castro JM, Gómez A, Sarmiento S, Muela A, Arsuaga JL. 2006. Hominin lower second premolar morphology: evolutionary inferences through geometric morphometric analysis. *J Hum Evo* 50:523 – 533.
- Mulchrone KF, Choudhury KR. 2004. Fitting an ellipse to an arbitrary shape: implications for strain analysis. *J Struct Geol* 26:143-153.
- Rosin PL. 1993. A note on the least squares fitting of ellipses, *Pattern Recognit Lett* 14:799-808.
- Radovčić J, Smith FH, Trinkaus E, Wolpoff MH. 1988. *The Krapina Hominids: An Illustrated Catalog of Skeletal Collection*. Mladost, Zagreb.
- Rasband, W.S., 1997-2014. ImageJ, U. S. National Institutes of Health, Bethesda, Maryland, USA, <http://imagej.nih.gov/ij/>.
- Skinner MM, Wood BA, Hublin, JJ. 2009. Protostylid expression at the enamel-dentine junction and enamel surface of mandibular molars of *Paranthropus robustus* and *Australopithecus africanus*. *J Hum Evol* 56 (1):76 – 85.
- Skinner MM, Wood BA, Boesch C, Olejniczak AJ, Rosas A, Smith TM, Hublin JJ. 2008. Dental trait expression at the enamel-dentine junction of lower molars in extant and fossil hominoids. *J Hum Evol* 54 (2):173 – 186.
- Suwa G, White TD, Clark Howell F. 1996. Mandibular postcaninedentition from the Shungura Formation, Ethiopia: Crown morphology, taxonomic allocations, and Plio-Pleistocene hominid evolution. *Am J Phys Anthropol* 101 (2):247 - 282.



Suwa G, Wood BA, White TD. 1994. Further analysis of mandibular molar crown and cusp areas in Pliocene and early Pleistocene hominids. *Am J Phys Anthropol* 93 (4):407 - 426.

American Journal of Physical Anthropology

Manuscript close to submission²



Geometric morphometric analysis and internal structure measurements of the Neanderthal lower fourth premolars from Kalamakia, Greece

Catherine C. Bauer^{1*}, Stefano Benazzi^{2, 3}, Andreas Darlas⁴ and Katerina Harvati¹

¹*Paleoanthropology, Senckenberg Center for Human Evolution and Paleoenvironment, Eberhard Karls Universität Tübingen, Rümelinstrasse 23, Tübingen 72070, Germany*

²*Department of Cultural Heritage, University of Bologna, Via degli Ariani 1, 48121 Ravenna, Italy*

³*Department of Human Evolution, Max Planck Institute for Evolutionary Anthropology, Deutscher Platz 6, D-04103 Leipzig, Germany*

⁴*Ephoreia of Paleanthropology and Speleology, Ardittou 34 b, 11636 Athens, Greece*

**Corresponding author:*

E-mail address: catherine.bauer@ifu.uni-tuebingen.de (C. Bauer)

² The final submitted manuscript may deviate slightly from the version included in this thesis

ABSTRACT

During excavations at the Middle Paleolithic cave site of Kalamakia, Southern Greece, from 1993 – 2006, several Neanderthal remains were found. Among them were two lower second premolars, KAL6 and KAL9, which are investigated in this study together with other Neanderthal, early modern human and recent modern humans that serve as a comparative sample. Geometric morphometric analyses show that both Kalamakia specimens have crown outline shapes, in occlusal view, that are typical for Neanderthals. However, the analyses showed some overlap of the species, as well as a large variability of the outline shapes, in particular for recent modern humans. Our analyses of internal dental features, such as the enamel-dentine junction surface area and the lateral dentine and pulp chamber volume, show a significant difference between Neanderthals and modern humans. Crown height, instead, appears to be less useful for taxonomic differentiation. This study aims to improve our knowledge about lower second premolar shape and size variability, both between and within species, in particular for geographically distributed groups. Our results highlight the need for further investigation of μ CT-based analyses of fossil and recent dental remains.

INTRODUCTION

The site of Kalamakia is formed in a limestone cliff on the western shoreline of the Mani Peninsula (Fig. 1). During excavations on the site from 1993 – 2006, conducted by the Ephoreia of Paleoanthropology and Speleology and the Musée National d'Histoire Naturelle, Paris, numerous Middle Paleolithic remains dating from 100 ka to >39 ka were recovered (de Lumley et al. 1994, Darlas and de Lumley 2004, Harvati et al., 2013). These include stone tools, abundant faunal remains, as well as fourteen fragments of human remains (isolated teeth, postcranial remains and a small cranial fragment; Harvati et al., 2013). Among these specimens, ten teeth, representing different tooth classes, were uncovered: two upper incisors (KAL10 and KAL11), four upper and lower premolars (KAL2, KAL5, KAL6 and KAL9), two upper molars (KAL3 and KAL8), as well as two deciduous upper incisors (KAL12 and KAL13). Harvati et al. (2013) investigated non-metric features of the specimens, as well as their mesio-distal and bucco-lingual diameters. In addition, analyses of the occlusal fingerprint and occlusal microwear texture were undertaken for one specimen (KAL3). Although not all specimens from Kalamakia show clear Neanderthal features, the observation

of Neanderthal characteristics in most of the material, the absence of modern human features, and the association of the remains with Middle Paleolithic lithic assemblages led to the assignment of the Kalamakia human fossils to Neanderthals (Harvati et al., 2013). The Kalamakia site therefore joins Lakonis and Apidima, the other Middle Paleolithic sites preserving Neanderthal remains from the region of Mani (see Harvati et al., 2003; 2011).

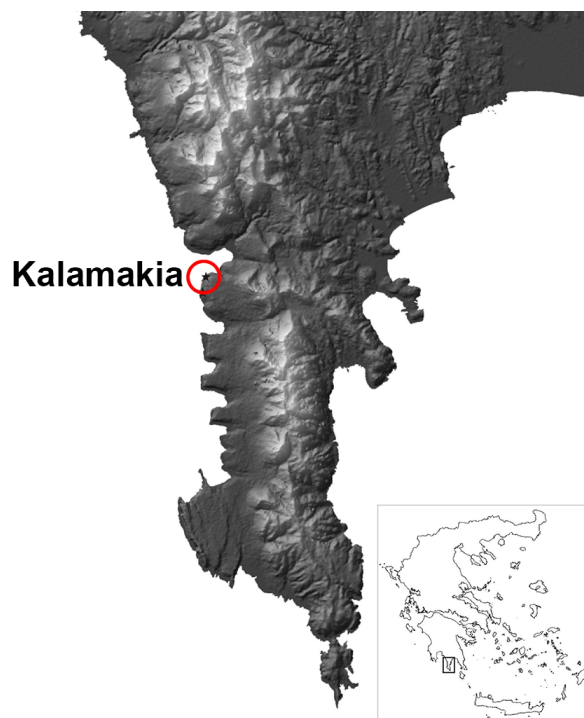


Fig. 1. Map of Greece showing the location of the Kalamakia middle Paleolithic cave site (adapted from Harvati et al., 2013).

The focus of this study is on the two Kalamakia lower fourth premolars (hereafter P₄) KAL6 and KAL9 (Fig. 2). Both were recovered from the lower part of stratigraphic unit IV of the site, at a depth of 270 and 273 cm respectively. KAL6 is substantially worn (dental attrition stage 4 [Molnar, 1971]). However, distinctive Neanderthal features can be identified on its crown, including a slight asymmetry and a transverse crest between the metaconid and protoconid, a trait combination typical for Neanderthals. It is relatively small, with crown dimensions that fall at the lower end of the Neanderthal range and well within that of Upper Paleolithic modern humans (Harvati et al., 2013). KAL9 is less worn (dental attrition stage 3 [Molnar, 1971]), and shows marked crown asymmetry, a well-developed transverse crest, multiple lingual cusps and a mesially placed metaconid, a trait combination highly

characteristic for Neanderthals. The dimensions of KAL9 are larger than those of KAL6. They fall well within the range of variation of early Neanderthals, Neanderthals and early modern humans and are larger than the values reported for Upper Paleolithic modern humans (Harvati et al., 2013).

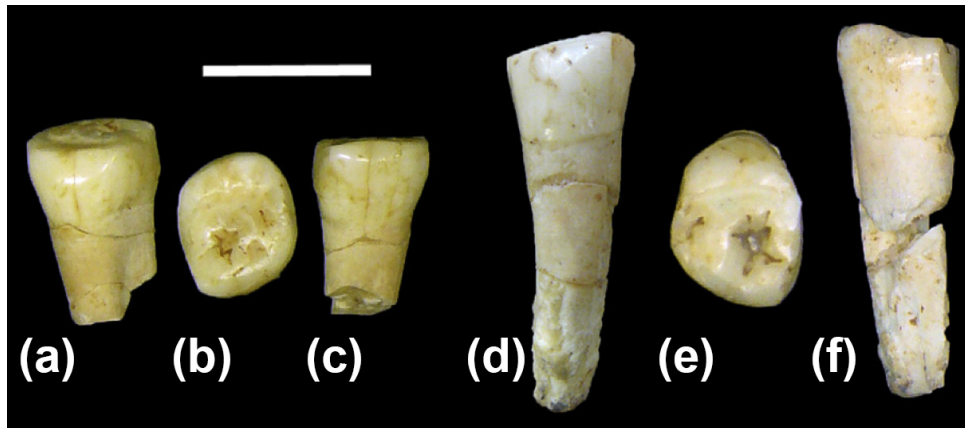


Fig. 2. The KAL 6 (left) and the KAL 9 specimens in (a,d) buccal, (b,e) occlusal and (c,f) lingual view. Scale bar 1 cm (adapted from Harvati et al., 2013).

Although Neanderthal P_4 s show a combination of features (e.g., taurodontism, a strong transverse crest, asymmetry in the lingual bulge of the crown and the mesial position of the metaconid) that distinguish them from modern humans, therefore allowing for their taxonomic attribution (Bailey and Lynch 2005), several recent contributions have emphasized the need to include digital morphometric analysis to support dental taxonomic discrimination (e.g. Le Cabec et al. 2013; 2015; Smith et al. 2012; Gómez-Robles et al. 2011; Benazzi et al. 2011a,b,c; 2012; 2013; 2014; Olejniczak 2008). Nevertheless, relatively few contributions have focused on digital analyses of lower premolars until now. Existing studies have focused mostly on anatomical landmarks, for example the cusp tips and the position of foveas, in combination with sliding semi-landmarks along the outline of the tooth crown or elliptic Fourier analyses of crown outlines (Bailey and Lynch, 2005; Martín-Torres et al. 2006; Gómez-Robles et al. 2008; 2011). Anatomical landmark-based studies require distinctive anatomical features, such as the tips of the dental cusps, which therefore excludes the analysis of even moderately worn teeth. Moreover, with only few exceptions (Bailey and Lynch 2005), existing studies did not focus on a distinction between Neanderthals and early /recent *Homo*

sapiens in particular, and mostly included more species (e.g. Australopithecines, *Paranthropus*, *H. antecessor*) in their analyses (Martinón-Torres et al., 2006; Gómez-Robles et al., 2008; 2011), ultimately leading to an overlap between Neanderthals and recent *Homo sapiens*. However, Bailey and Lynch (2005) only analyzed crown outline shape, using Elliptic Fourier analysis, and did not take internal structure measurements into account.

Here we present a digital morphometric analysis of the two lower second premolars from Kalamakia, KAL6 and KAL9. Using 3D μ CT scan data, we examined external features (i.e. the outline shape of the crown in occlusal view), as well as internal dental parameters (lateral crown height of the dentine or LCH; the lateral dentine and pulp chamber volume, LDPV; and the area of the contact surface of the dentine with the enamel, EDJ), following the procedures described in Benazzi et al. (2011 a,b,c; 2012; see also Harvati et al., 2015). Our goals are two-fold: 1. to better explore and document the morphology of the Kalamakia assemblage, and 2. to contribute to the understanding of taxonomic and geographical variation in human P₄ external and internal anatomy.

TABLE 1. Specimens used in the study and in the different types of analyses.

| Taxon | Specimen | Origin | Source | Outline | LDPV | LCH | EDJ |
|-------|--|---|---|--|------|-----|-----|
| NEA | KAL6 | Greece | Original data (μ CT) University of Tuebingen | X | X | X | X |
| | KAL9 | Greece | Original data (μ CT) University of Tuebingen | X | X | X | X |
| | Krapina d26 | Croatia | NESPOS (μ CT) ¹ | X | X | X | X |
| | Krapina d31 | Croatia | NESPOS (μ CT) ¹ | X | X | X | X |
| | Krapina d32 | Croatia | NESPOS (μ CT) ¹ | X | X | X | X |
| | Krapina d35 | Croatia | NESPOS (μ CT) ¹ | | X | X | X |
| | Krapina d50 | Croatia | NESPOS (μ CT) ¹ | X | X | X | X |
| | Krapina d113 | Croatia | NESPOS (μ CT) ¹ | X | | X | |
| | Krapina d118 | Croatia | NESPOS (μ CT) ¹ | X | | X | |
| | Abri Bourgeois Delaunay BD9 | France | NESPOS (Surface Scan) ¹ | X | | | |
| | Weimar-Ehringsdorf G1_1049 | Germany | NESPOS (Surface Scan) ¹ | X | | | |
| | Spy 12B | Belgium | NESPOS, courtesy of P. Semal | X | | | |
| | EHS | Qafzeh 10 | Israel | Original data (μ CT) University of Tuebingen | X | X | X |
| RHS | From Neolithic, Bronze Age, medieval and recent individuals | Egypt: 11 Tunisia: 10 Germany: 8 Oceania: 5 Khoi San: 5 | Original data (μ CT) University of Tübingen Original data (μ CT) University of Cape Town | 39 | 39 | 39 | 39 |

MATERIALS AND METHODS

Sample and scanning procedures

In addition to the two Kalamakia premolars, our comparative sample comprises 50 P₄s, including 10 Neanderthal (NEA), one early *Homo sapiens*, (Qafzeh 10; EHS) and 39 recent *Homo sapiens* (RHS) specimens. The latter range from the Neolithic to the present time and represent European, North African, Sub-Saharan African and New Guinean populations (Table 1). Most of the comparative sample was scanned at the Tübingen Paleoanthropology High-Resolution Computer Tomography lab. Scan settings varied between 100 kV – 170 kV and 100 μ A – 130 μ A with a 0.1 – 0.3 Cu-filter applied. The resolution ranges from 11 – 73 μ m depending on specimen size (i.e. entire mandibles or isolated teeth). Some fossil specimens were obtained from the NESPOS database (Neanderthal Studies Professional Online Service). The South African sample was kindly provided by Prof. B.R. Ackermann, and was scanned at a resolution: 0.065 μ a. Different numbers of specimens were used for each analysis (see below, Table 1), depending on their state of preservation. Each specimen was regarded as a right P₄. Specimens from the left side were mirrored and treated as teeth from the right side.

Data processing and outline analysis

After scanning, the cervical plane of each tooth was determined as the plane that fits multiple digitized points on the cervical line (following Benazzi et al., 2011a,b; 2012), using Avizo® 7.0 software (VSG, Visualization Sciences Group) (Fig. 3). Each scan was realigned to orient all slices parallel to that cervical plane and then segmented into their enamel and dentine tissue according to the half-maximum-height protocol of Spoor et al. (1993), again using the Avizo® 7.0 software. Each specimen was rotated around the z-axis, with Rhino® 5.0 software (Robert McNeel and Associates, Seattle, WA) until the projection on the cervical plane of both mid-points of the lingual and the buccal side were aligned to the y-axis (Fig. 3). With the same software, the crown outline for each specimen was obtained in occlusal view and 16 pseudo-landmarks, representing equiangularly spaced radial vectors out of the centroid, were created (Benazzi et al. 2011a; 2012). The first vector points toward the buccal direction and further landmarks were collected anticlockwise at intervals of 22.5° (Fig. 3). Pseudo-

landmarks were used to overcome limitations in case of worn teeth, where anatomical landmarks cannot easily be recognized on the crown. Even though crown outline pseudo-landmarks simplify crown morphology they are less sensitive to resolution of the outline and damage or dental wear. Relatively worn teeth can thus still be included in an analysis. The landmark datasets, shifted to a common centroid, were then imported into the software package Morphologika (O’Higgins & Jones, 2006). With the landmark datasets already oriented (i.e., rotated and superimposed to the centroid of each outline), only scaling to unit centroid size was applied with Morphologika. Subsequently, we performed a between-group Principal Components Analysis (PCA) on the matrix of the Procrustes coordinates using the PAST software (Hammer et al., 2001). The following groups were defined: NEA, EHS, and for the RHS specimens Egypt, Germany, Khoi San, Oceania and Tunisia. We also reported Procrustes distances (PD; a measure of total shape similarity) between the two KAL specimens and all the fossils, as well as the group mean configurations of all the comparative samples.

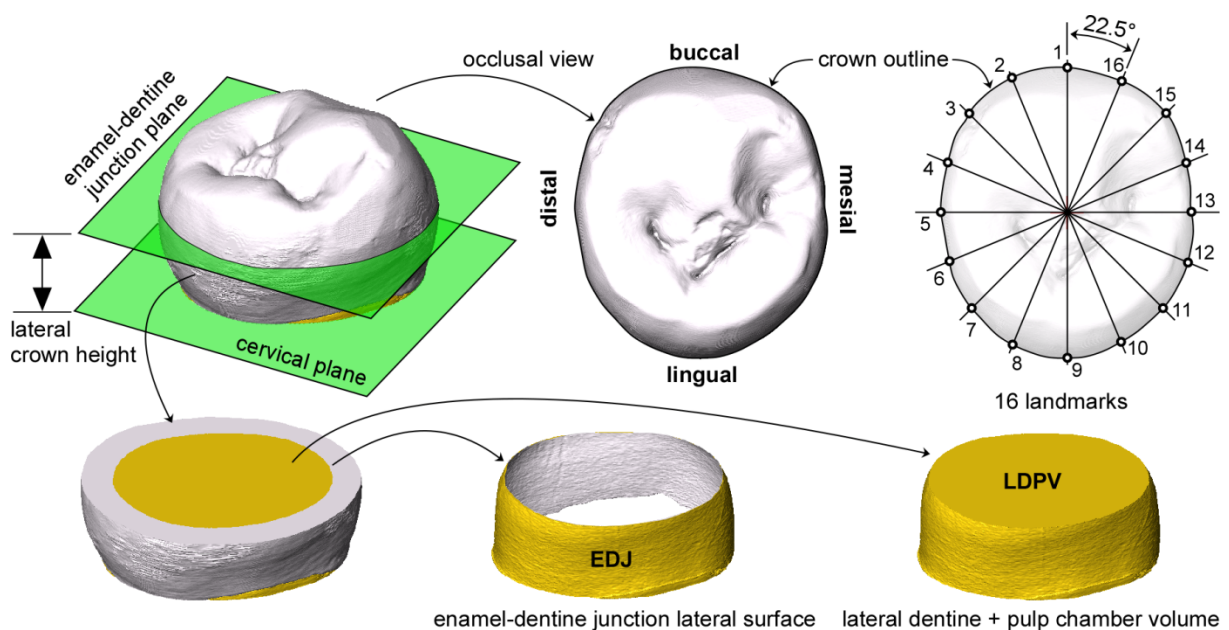


Fig. 3. Definition and alignment of the cervical and enamel-dentine junction plane, the 16 pseudo-landmarks, as well as the crown height, EDJ surface and LDPV, using the specimen CH_TUN8 as an example.

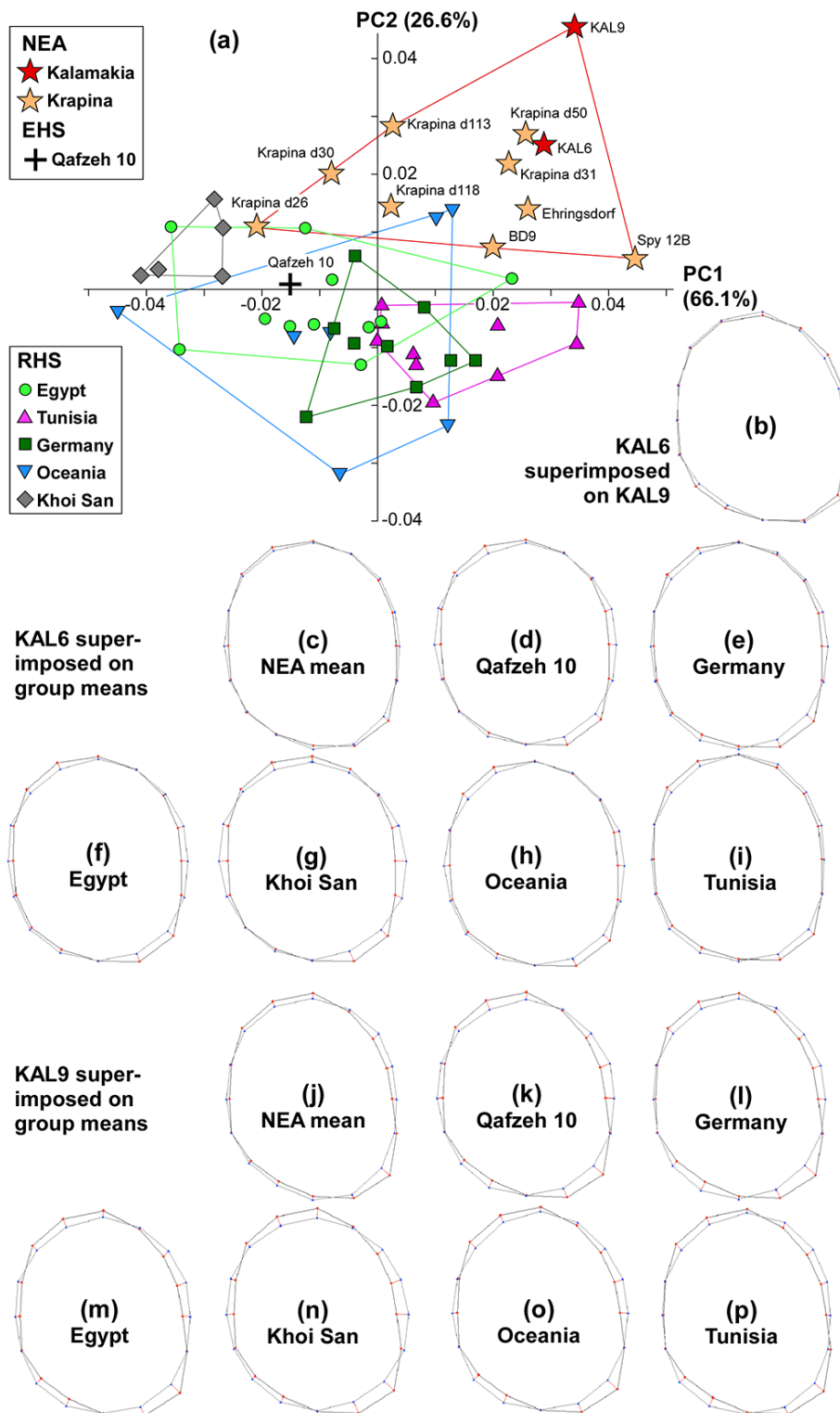


Fig. 4. (a) Scatterplot of the first two principal components. NEA (red stars); EHS (blue triangle); Khoi San (black dots); Neolithic Egyptians (brown dots); recent Oceanian (turquoise dots); medieval Germans (pink dots); Bronze-Age Tunisians (orange dots). Lines indicate convex hulls. Below: Specimen KAL6 (red dots) superimposed on KAL9 (b, blue triangles) and KAL6 (c – i) and KAL9 (j – p) the different group means.

Crown height, lateral dentine surface area and pulp chamber volume measurements

For lateral crown height (LCH, in mm), lateral dentine and pulp chamber volume (LDPV, in mm³) and enamel dentine junction (EDJ) surface (in mm²), we used the best-fit plane (see above) through the cervical line and another plane, the EDJ-plane, which is parallel to the cervical plane and just passes through the last plane showing no enamel in the occlusal basin (see Benazzi et al., 2011b) (Fig. 3). LCH is defined as the distance from the best-fit plane to the EDJ-plane, whereas LDPV is defined as the volume of dentine including the pulp chamber between the best-fit plane and the EDJ-plane (see Toussaint et al., 2010; Benazzi et al., 2011b). . Analysis of variance (ANOVA) was conducted on PC scores and CH, EDJ and LDPV values, using the PAST software (Hammer et al. 2001) to determine whether the difference between our NEA and our RHS sample is statistically significant. Standard- or z-scores were calculated for EDJ- and LDPV-values only, using the JMP 11 software (SAS Institute Inc., © 2013), as CH-values of the different taxa already show a very large overlap.

RESULTS

Outline shape

The first two principal components in the between-group PCA of the outline shape coordinates, accounting for 92,7 % of the total variance, are shown in Figure 4. PC 2 separated NEA and RHS with only little overlap, while PC 1 reflected 66.1 % variation within the Neanderthal, and particularly, within the modern human sample. The Khoi San sample was the most distinctive among the modern human groups: these specimens showed the most negative PC 1 scores (significantly in an ANOVA on the PC scores, $p = 0.0006$) and overlapped only with the Neolithic Egyptian sample. The EHS specimen Qafzeh 10 plotted well within the range of the RHS sample. It showed a lowest Procrustes distance to the Khoi San (0.023) and the Neolithic Egyptian sample (0.024) (Table 2). KAL6 plotted with the other Neanderthal specimens included in the analysis, while KAL9 showed a more extreme positive PC 2 score, and marked the most positive extreme of our Neanderthal sample (Fig. 4). In terms of Procrustes distances, KAL6 shows the smallest PD to an Egyptian Neolithic specimen (0.026) and Krapina D50 (0.027), while KAL9 showed the smallest PD to KAL6

(0.032) and Krapina D50 (0.042). KAL 9 was generally more distinct in its shape from both other fossils and our comparative samples. Both specimens showed the smallest mean Procrustes distance to the NEA sample (Table 2).

TABLE 2. Inter-individual PD.

| Fossil Specimen | KAL 6 | KAL 9 |
|---------------------|-------|-------|
| NEA | | |
| KAL 6 | - | 0.032 |
| KAL 9 | 0.032 | - |
| Spy 12B | 0.052 | 0.075 |
| Krapina d26 | 0.054 | 0.073 |
| Krapina d31 | 0.042 | 0.063 |
| Krapina d32 | 0.045 | 0.064 |
| Krapina d50 | 0.027 | 0.042 |
| Krapina d113 | 0.035 | 0.048 |
| Krapina d118 | 0.032 | 0.051 |
| BD 9 | 0.041 | 0.058 |
| Ehringsdorf G1 1049 | 0.046 | 0.063 |
| EHS | | |
| Qafzeh 10 | 0.054 | 0.075 |
| Mean PD | | |
| NEA | 0.042 | 0.060 |
| EGYPT | 0.054 | 0.076 |
| GERMANY | 0.052 | 0.076 |
| TUNISIA | 0.047 | 0.070 |
| OCEANIA | 0.058 | 0.078 |
| KHOI SAN | 0.067 | 0.084 |

Crown height

Out of the entire dataset, only 49 specimens including 9 Neanderthals (2 from Kalamakia and 7 from Krapina) and the Qafzeh 10 individual could be analyzed for their lateral crown height. Our Neanderthal sample was not different in LCH from the modern humans included in our study (Table 3). There was great overlap between the measurements and the NEA range overlapped completely with that of the RHS ($p = 0.3859$). The Kalamakia specimens plotted well within the range for the rest of the NEA comparative sample. Qafzeh 10 was noteworthy for having a very low value for this parameter, falling outside the range of either RHS of NEA samples. Modern human populations also overlapped greatly with each other in LCH. The Khoi San sample showed the lowest values, while the sample from Oceania showed the highest values for LCH, even exceeding the NEA values.

TABLE 3. Lateral crown height values for KAL 6 and 9 and the groups of our RHS sample.

| KAL Specimen | | Crown height (mm) | | | |
|--------------|----|------------------------|--------------|--------------|-------|
| KAL6 | | 3.069 | | | |
| KAL9 | | 3.685 | | | |
| Taxon/Group | n | Crown Height Mean (mm) | Maximum (mm) | Minimum (mm) | StDev |
| NEA | 7 | 3.209 | 3.810 | 2.676 | 0.398 |
| Qafzeh 10 | 1 | 1.547 (absolute value) | | | |
| RHS | 39 | | | | |
| Oceania | 5 | 3.213 | 3.512 | 2.640 | 0.349 |
| Germany | 8 | 3.246 | 3.975 | 3.045 | 0.321 |
| Egypt | 11 | 3.209 | 3.387 | 2.895 | 0.220 |
| Tunisia | 10 | 2.974 | 3.363 | 2.462 | 0.316 |
| Khoi San | 5 | 2.171 | 2.730 | 1.755 | 0.397 |

TABLE 4. Enamel dentine junction surface area values for KAL 6 and 9 and the groups of our RHS sample.

| KAL Specimen | | EDJ-surface area (mm ²) | | | |
|--------------|----|-------------------------------------|----------------------------|----------------------------|--------|
| KAL6 | | 60.896 | | | |
| KAL9 | | 81.792 | | | |
| Taxon/Group | n | EDJ-surface Mean (mm ²) | Maximum (mm ²) | Minimum (mm ²) | StDev |
| NEA | 5 | 82.170 | 90.474 | 75.446 | 6.397 |
| Qafzeh 10 | 1 | 32.372 (absolute value) | | | |
| RHS | 39 | | | | |
| Oceania | 5 | 71.648 | 110.342 | 54.269 | 20.653 |
| Germany | 8 | 61.373 | 75.235 | 52.409 | 7.464 |
| Egypt | 11 | 59.602 | 68.413 | 49.976 | 6.428 |
| Tunisia | 10 | 57.775 | 93.703 | 40.664 | 14.648 |
| Khoi San | 5 | 35.076 | 42.945 | 30.045 | 5.421 |

Lateral enamel-dentine junction (EDJ) surface

47 specimens, including the 2 Kalamakia individuals, 5 other NEA specimens from Krapina and the EHS specimen Qafzeh 10, could be analyzed. NEA were characterized by a larger lateral EDJ surface than RHS ($p= 0.0017$), and despite two outliers (one specimen from Oceania, one from Tunisia), NEA and RHS overlapped only minimally (Table 4). Qafzeh 10 fell among the lower values for the comparative RHS sample. One of the Kalamakia specimens (KAL9) plotted well within the range of the remaining NEA sample from Krapina (z-score to Krapina specimens is 0.059), while the other (KAL6) fell below the Krapina NEA range (z-score to Krapina specimens is 3.340). In fact KAL6 plotted much closer to the average RHS with a z-score of 0.80. Both overlap with the values for RHS. When separating the data on population level it can be observed that the two specimens from Kalamakia are more variable than the Krapina sample, the latter having larger values for EDJ surface area

than most of the RHS sample (Table 4). Again, Qafzeh 10 and the Khoi San individuals had the lowest values overall, although there is a slight overlap with the lower range of variation of the Tunisian sample. Most of the RHS specimens greatly overlapped in their EDJ surface area values. However, the Oceanian sample showed the greatest range of variation with some values even exceeding the NEA range.

Lateral dentine and pulp chamber volume (LDPV)

For this analysis, 47 specimens, with 7 NEA (2 from Kalamakia and 5 from Krapina) and Qafzeh 10 were included. The NEA Krapina sample showed a distinctly larger LDPV than the RHS and plotted significantly outside the range of our RHS sample (Fig. 7a; $p < 0.0001$). However, KAL6 fell within the range of RHS (z-score to Krapina specimens 6.156, but only 0.140 to RHS), whereas KAL9 plotted well within the Krapina NEA variation (z-score to Krapina specimens is 1.028, versus 2.525 to RHS). The Qafzeh 10 specimen aligned with the lower values of RHS. When separating the samples by population, the Khoi San sample showed low LDPV values (Table 5). There was a large degree of variation in LDPV among the other groups.

TABLE 5. Lateral dentine and pulp chamber volume values for KAL 6 and 9 and the groups of our RHS sample.

| KAL Specimen | | Lateral dentine and pulp chamber volumes (mm ³) | | | |
|--------------|----|---|----------------------------|----------------------------|--------|
| KAL6 | | 89.899 | | | |
| KAL9 | | 145.961 | | | |
| Taxon/Group | n | LDPV mean (mm ³) | Maximum (mm ³) | Minimum (mm ³) | StDev |
| NEA | 5 | 157.205 | 169.223 | 142.602 | 10.934 |
| Qafzeh 10 | 1 | 47.497 (absolute value) | | | |
| RHS | 39 | | | | |
| Oceania | 5 | 95.763 | 125.439 | 63.041 | 24.704 |
| Germany | 8 | 90.050 | 111.856 | 74.700 | 13.762 |
| Egypt | 11 | 90.216 | 109.667 | 69.052 | 12.588 |
| Tunisia | 10 | 81.276 | 98.724 | 54.953 | 15.923 |
| Khoi San | 5 | 44.129 | 52.059 | 38.013 | 5.818 |

DISCUSSION AND CONCLUSIONS

This study aimed to improve our knowledge of P₄ variation among Neanderthals and modern humans, as well as to better document the external and internal morphology of the Kalamakia

P₄ specimens. As is the case with most specimens from Kalamakia, KAL6 and KAL9 exhibit features or combinations of features typical for Neanderthal P₄s such as mesially placed metaconids, transverse crests and crown asymmetry, clearly exhibiting Neanderthal affinities (Harvati et al., 2013). These features were reflected in the crown outline shape analysis. In terms of shape, NEA and especially the KAL specimens, tended to show a mesial displacement of the metaconid and pronounced distal shift of the talonid, which led to the development of a disto-lingual bulge, as reflected by the mean outline configurations of the samples (Fig. 4). Our analysis therefore agrees with Bailey (2002) who found this to be a typical NEA trait, occurring with high frequency (96%). KAL9 exhibited the most extreme NEA shape, characterized by a more elliptic crown and a distinctly distally shifted lingual cusp (Fig. 4). KAL6 was less extreme in these features, but still fell well out of the range of modern humans in the PCA. Both specimens showed the smallest PD to other NEA individuals. Nevertheless, some NEA individuals showed a much more rounded crown outline shape. Krapina d26 in particular, plotted on the border of the convex hull of our Neolithic Egyptian sample in the PCA, increasing the range of variation of our NEA sample. The Spy 12B specimen also plotted away from the other Neanderthals, exhibiting a more elongated outline shape in the bucco-lingual direction, but still showing the distally shifted lingual bulge. The overlap between the Neanderthal and the modern human convex hulls was also driven by the inclusion of modern human samples from Oceania and Africa. This result highlights the great variability of modern human P₄ crown outline shapes (see below) and accentuates the need to include more geographically diverse samples in future analyses of dental crown shape of fossil humans.

The modern human samples showed a large spread in the between-group PCA plot with the exception of the Khoi San sample, which plotted as a relatively homogenous group with negative PC 1 and positive PC 2 scores. In a MANOVA, a significant difference between the Khoi San and the NEA and Tunisian sample could be observed ($p=0.03$ and 0.009 , on PC scores 1 to 6). Although population sample sizes were small, some trends can be tentatively identified. Europeans, Tunisians and Egyptians overlapped greatly with each other, as might be expected. On the other hand, the Oceanic sample showed great variability. The sub-Saharan Khoi San sample represented the most distinct group with round and small teeth, reflecting the gracility of this population.

Our analyses of CH-, EDJ area- and LDPV-data were limited by the restricted fossil sample that could be included. Other than Kalamakia, the Neanderthal sample here was limited to specimens from Krapina, Croatia, and therefore represented a very small portion of Neanderthal variation from a single, early Neanderthal site. Although our Neanderthal sample differed significantly from the combined modern human sample for EDJ area and LDPV, these findings (a) are mainly driven by size, and (b) are likely not representative for Neanderthals in general. In both these analyses KAL9, the larger of the two Kalamakia specimens, fell within the Krapina range, while KAL6 was closer to the modern human values. The difference in size between KAL9 and KAL6 has been noted before, and may be the result of sexual dimorphism (Harvati et al., 2013). Although LDPV and EDJ-surface area were distinctly larger for the Krapina sample when compared to modern humans, crown height did not statistically distinguish among groups. The larger crown cross-sectional area of the Krapina P_{4s}, therefore, was not associated with greater crown height. Among modern human population samples, all groups except the Khoi San largely overlapped in all three parameters. The Khoi San P_{4s}, however, were distinctly smaller, resulting in lower values for all these parameters (Table 3, 4 and 5). It is worth pointing out that the single EHS specimen that could be included, Qafzeh 10, is comparable to the Khoi San in these values.

The use of digital methods in assessing taxonomic affinities has recently been shown to be successful for deciduous and permanent molars (e.g. Olejniczak et al., 2008; Smith et al., 2010; Toussaint et al., 2010; Benazzi 2011a,b; 2012; Harvati et al., 2015). However, digital analyses of premolars have been relatively sparse, although the morphology of these teeth is considered highly diagnostic for Neanderthals (Gómez-Robles et al., 2008; 2011; Martínón-Torres et al., 2006; Bailey and Lynch, 2005). Our results show that analysis of the crown outline using pseudo-landmarks, possibly in combination with LDPV and EDJ surface area measurements, can distinguish Neanderthal from modern human P_{4s}, in accordance with non-metric traits typical for Neanderthals that involve also the shape of the P₄ crown. However, they also show a wide range of variation across modern human populations. Both P₄ shapes and sizes of RHS are highly variable, even within individual population samples. These results highlight the need for better representation of modern human variability in CT-based studies of dental remains.

Acknowledgments

This study was supported by the European Research Council Starting Grant PaGE, No. 283503. The Tübingen Paleoanthropology High-Resolution CT Laboratory is funded through a major-instrumentation grant by the Deutsche Forschungsgemeinschaft (DFG INST 37/706-1 FUGG). We thank Rebecca R. Ackermann for access to the Khoi San sample and Patrick Semal for access to the Spy 12B specimen.

Literature cited

- Bailey, SE. 2002. A closer look at Neanderthal postcanine dental morphology: the mandibular dentition. *Anat Rec (New Anat)* 269:148-156.
- Bailey, SE, Lynch, JM. 2005. Diagnostic differences in Mandibular P4 Shape Between Neandertals and Anatomically Modern Humans. *Am J Phys Anthropol* 126:268 – 277.
- Benazzi, S, Coquerelle, M, Fiorenza, L, Bookstein, F, Katina, S, Kullmer, O. 2011a. Comparison of Dental Measurement Systems for Taxonomic Assignment of First Molars. *Am J Phys Anthropol* 144:342-354.
- Benazzi, S, Fornai, C, Bayle, P, Coquerelle, M, Kullmer, O, Mallegni, F, Weber, GW. 2011b. Comparison of dental measurement systems for taxonomic assignment of Neanderthal and modern human lower second deciduous molars. *J Hum Evol* 61:320–32.
- Benazzi, S, Douka, K, Fornai, C, Bauer, CC, Kullmer, O, Svoboda, J, Pap, I, Mallegni, F, Bayle, P, Coquerelle, M, Condemi, S, Ronchitelli, A, Harvati, K, Weber, GW. 2011c. Early dispersal of modern humans in Europe and implications for Neanderthal behaviour. *Nature* 479:525 – 528.
- Benazzi, S, Fornai, C, Buti, L, Toussaint, M, Mallegni, F, Ricci, S, Gruppioni, G, Weber, GW, Condemi, S, Ronchitelli, A. 2012. Cervical and Crown Outline Analysis of Worn Neanderthal and Modern Human Lower Second Deciduous Molars. *Am J Phys Anthropol* 149:537-546.
- Benazzi, S, Bailey, SE, Mallegni, F. 2013. A morphometric analysis of the Neanderthal upper second molar Leuca I. *Am J Phys Anthropol* 152:300-305.
- Benazzi, S, Peresani, M, Talamo, S, Fu, Q, Mannino, MA, Richards, MP, Hublin, JJ. 2014. A reassessment of the presumed Neanderthal human remains from San Bernardino Cave, Italy. *J Hum Evol* 66:89-94.
- Darlas, A, de Lumley, H. 2004. La grotte de Kalamakia (Aréopolis, Grèce). In: Sa contribution à la connaissance du Paléolithique moyen de Grèce, *BAR* 1293:225–233.
- Gómez-Robles, A, Martínón-Torres, M, Bermúdez de Castro, JM, Prado-Simón, L, Arsuaga, JL. 2011. A geometric morphometric analysis of hominin upper premolars. Shape variation and morphological integration. *J Hum Evo* 61:688–702.

- Gómez-Robles, A, Martínón-Torres, M, Bermúdez de Castro, JM, Prado, L, Sarmiento, S, Arsuaga, JL. 2008. Geometric morphometric analysis of the crown morphology of the lower first premolar of hominins, with special attention to Pleistocene *Homo*. *J Hum Evol* 55:627–638.
- Harvati, K, Panagopoulou E, Karkanas, P. 2003. First Neanderthal remains from Greece: The evidence from Lakonis. *J Hum Evol* 45:465-473.
- Harvati, K, Stringer, C, Karkanas P. 2011. Multivariate analysis and classification of the Apidima 2 cranium from Mani, Southern Greece. *J Hum Evol* 60:246-250.
- Harvati, K, Darlas, A, Bailey, SE, Rein, TR, El Zaatari, S, Fiorenza, L, Kullmer, O, Psathi, E. 2013. New Neanderthal remains from Mani peninsula, Southern Greece: The Kalamakia Middle Paleolithic cave site. *J Hum Evol* 64:486 – 499.
- Harvati, K, Bauer, CC, Grine, FE, Benazzi, S, Ackermann, RR, van Niekerk, KL, Henshilwood, CS. 2015. A human deciduous molar from the Middle Stone Age (Howiesons Poort) of Klipdrift Shelter, South Africa. *J Hum Evol* 82:190-196.,
- Le Cabec, A, Tang, N, Tafforeau, P. 2015. Accessing Developmental Information of Fossil Hominin Teeth Using New Synchrotron Microtomography-Based Visualization Techniques of Dental Surfaces and Interfaces. *PLOS One*, DOI: 10.1371/journal.pone.0123019.
- Le Cabec, A, Gunz, P, Kupczik, K, Braga, J, Hublin, JJ. 2013. Anterior tooth root morphology and size in Neanderthals: Taxonomic and functional implications. *J Hum Evol* 64:169–193.
- De Lumley, H, Darlas, A, Anglada, R, Cataliotti-Valdina, J, Desclaux, E, Dubar, M, Falguères, C, Keraudren, B, Lecervoisier, B, Mestour, B, Renault-Miskovsky, J, Trantalidou, K, Vernet, JL. 1994. Grotte de Kalamakia (Aréopolis, Péloponnèse). *Bull Corresp Hellenique* 118:535 – 559.
- Martinón-Torres, M, Bastir, M, Bermúdez de Castro, JM, Gómez, A, Sarmiento, S, Muela, A, Arsuaga, JL. 2006. Hominin lower second premolar morphology: evolutionary inferences through geometric morphometric analysis. *J Hum Evo* 50:523–533.
- Molnar, S. 1971. Human tooth wear, tooth function and cultural variability. *Am J Phys Anthropol* 34:175 – 190.
- Neubauer, S, Gunz, P, Hublin, JJ. 2009. The pattern of endocranial ontogenetic shape changes in Humans. *J Anat* 215:240–255.
- Hammer, Ø, Harper, DAT., Ryan, PD. 2001. PAST: Paleontological statistics software package for education and data analysis. *Palaeontol Electron* 4 (1):1-9. http://palaeoelectronica.org/2001_1/past/issue1_01.htm
- O’Higgins, P, Jones, N. 2006. Morphologika 2.5. Tools for shape analysis. Hull York Medical School, University of York. <http://www.york.ac.uk/res/fme>.
- Olejniczak, AJ, Smith, TM, Feeney, RNM, Macciarelli, R, Mazurier, A, Bondioli, L, Rosas, A, Fortea, J, de la Rassilla, M, Garcia-Taberner, A, Radovčić, J, Skinner, MM, Toussaint, M, Hublin, JJ. 2008. Dental tissue proportions and enamel thickness in Neanderthal and modern human molars. *J Hum Evo* 55:12 – 23.
- Smith, TM, Tafforeau, P, Reid, DJ, Pouech, J, Lazzari, V, Zermeno, JP, Guatelli-Steinberg, D, Olejniczak, A, Hoffmann, A, Radovčić, J, Makaremi, M, Toussaint, M, Stringer, C, Hublin, JJ. 2010. Dental evidence for ontogenetic differences between modern humans and Neanderthals. *PNAS* 107(49):20923 – 20928.

- Smith, TM, Olejniczak, A, Zermeno, JP, Tafforeau, P, Skinner, MM, Hoffmann, A, Radovčić, J, Toussaint, M, Kruszynski, R, Menter, C, Moggi-Cecchi, J, Glasmacher, UA, Kullmer, O, Schrenk, F, Hublin, JJ. 2012. Variation in enamel thickness within the genus Homo. *J Hum Evol* 62:395-411.
- Spoor, CF, Zonneveld, FW, Macho, GA. 1993. Linear Measurements of Cortical Bone and Dental Enamel by Computed Tomography: Applications and Problems. *Am J Phys Anthropol* 91:469 – 484.
- Toussaint, M, Olejniczak, AJ, El Zaatari, S, Cattelain, P, Flas, D, Letourneux, C, Pirson, S. 2010. The Neandertal lower right deciduous second molar from Trou de l'Abîme at Couvin, Belgium. *J Hum Evo* 58:56 – 67.

CURRICULUM VITAE CATHERINE CLAUDIA BAUER



born on June 22nd 1977 in Hof/Saale, Upper Franconia, Germany.

Education and employment

| | |
|---------------|---|
| 1983 – 1989 | Primary school, Grundschule Fichtelberg |
| 1989 – 1996 | High school, Luisenburg Gymnasium Wunsiedel |
| 1996 | High school Diploma, Luisenburg Gymnasium Wunsiedel |
| 1996 – 1999 | Doctor's Assistant Training, Dr. Dr. Keller, Bayreuth, specialized in Cranio-Facial surgery |
| 1999 – 2006 | Paramedic in the German Air Force, LwSanBschft 1/FlaRakGrp 23 and LeitSanZ 410, Roth, last rank Staff Sergeant |
| 2006 – 2012 | Student at the Eberhard Karls Universität Tübingen Early Prehistory and Quaternary Ecology Paleoanthropology Languages and Cultures of the Christian Near East |
| 2012 | <i>Magister Artium</i> at the Eberhard Karls Universität Tübingen Thesis: A Geometric Morphometric Analysis of Bronze-Age Crania from Qatna, Syria |
| Since 01/2013 | PhD-student at the Eberhard Karls Universität Tübingen within the EU-funded ERC-grant PaGE – Paleoanthropology at the Gates of Europe, awarded to Prof. Katerina Harvati |

LIST OF PUBLICATIONS

Harvati, K., **Bauer, C.C.**, Grine, F.E., Benazzi, S., Ackerman, R.R., van Niekerk, K.L. & Henshilwood, C.S. 2015. A human deciduous molar from the Middle Stone Age (Howiesons Poort) of Klipdrift Shelter, South Africa, *Journal of Human Evolution* 82, 190 - 196, doi:10.1016/j.jhevol.2015.03.001.

Bauer, C.C. & Harvati, K. 2015. A virtual reconstruction and comparative analysis of the KNM-ER 42700 cranium. *Anthropologischer Anzeiger* 72 (2), 129 – 140. doi: 10.1127/anthranz/2015/0387.

Bauer, C.C., Benazzi, S. & Harvati, K. 2015. Geometric morphometric analysis and internal structure measurements of Neanderthal and modern human lower second premolars. Poster presented at the AAPA 2015, St. Louis, USA.

Bauer, C.C., Degenhardt, S., Witzel, C., Flohr, S., Pfälzner, P. & Harvati, K. 2013. A Tale of Two Tombs: Cranial Synostosis Case Reports from Bronze-Age Syria. Poster presented at the AAPA 2013, Knoxville, USA.

Kandel, A.W., **Bauer, C.C.**, Noback, M.L. & Singh, N. 2012. First Annual Meeting of the European Society for the Study of Human Evolution. *Evolutionary Anthropology* 21, 167-168. doi:10.1002/evan.21318.

Bauer, C.C., Pfälzner, P. & Harvati, K. 2012. Craniosynostosis - A Case Report from Ancient Syria. Poster presented at the Quenstedt-Festivities, Department of Geosciences, University of Tuebingen, awarded 2nd best poster.

Fornai, C., Benazzi, S., **Bauer, C.C.**, Kullmer, O., Svoboda, J., Pap, I., Bayle, P., Harvati, K. & Weber, G.W. 2012. Investigation of 2D dental tissue proportions in deciduous first and second upper molars of modern humans and Neanderthals. Poster presented at the ESHE conference, Bordeaux, France.

Benazzi, S., Douka, K., Fornai, C., **Bauer, C.C.**, Kullmer, O., Svoboda, J., Pap, I., Mallegni, F., Bayle, P., Coquerelle, M., Condemi, S., Ronchitelli, A., Harvati, K. & Weber, G.W. 2011. Early dispersal of modern humans in Europe and implications for Neanderthal behavior. *Nature* 479, 525-529. doi:10.1038/nature10617.

Bauer, C.C. & Harvati, K. 2011. Bites and Bytes – Virtual Dental Tissue Segmentation. Poster presented at the StEvE meeting, Tübingen, Germany.

Fornai, C., **Bauer, C.C.**, Benazzi, S., Harvati, K. & Weber, G.W. 2011. Enamel thickness and dental tissue proportions in modern human upper first deciduous molars. Poster presented at the ESHE conference, Leipzig, Germany.

ACKNOWLEDGEMENTS

My last words in this thesis are dedicated to the people who helped me on my way to finish my PhD.

First of all I would like to thank my first supervisor, Prof. Katerina Harvati, who gave me the opportunity to have a PhD-position within the EU-funded Starting Grant PaGE, Paleoanthropology at the Gates of Europe. Thank you so much for all the fruitful discussions and your support in finishing manuscripts by providing useful comments and all the necessary corrections.

My thanks also go to my second supervisor, Prof. Nicholas J. Conard. It was very helpful to feel your support every time we ran into each other.

I am very grateful to have Dr. Stefano Benazzi from the University of Bologna, Italy, as a member of my supervision board. Thank you endlessly for all your incredibly productive ideas and skills you transferred to me. Sorry for pestering you whenever I had software issues or any kinds of problems. I really appreciate your support and I am looking forward to publish even more together with you. Grazie mille!!!

Prof. Joachim Wahl, thank you so much for giving me the opportunity to gain teaching experience. I really enjoy your absolutely interesting lectures and I admire your osteological experience. Already during my time as a student I profited a lot from your expertise.

I also would like to thank all of my co-authors, although I have not met all of you so far, for giving me the opportunity to publish and for all your contributions to the papers that made this thesis.

My colleagues from the department of Paleoanthropology – thanks to all of you. Michael Francken, curator of the osteological collection, here come the professional thanks for letting me sample some of the specimens although I know you were concerned I would brake off several roots when pulling the teeth out of the alveoles. Don't worry, everything went fine. And now the private thanks, for always having an open ear and finding the right words whenever I came and complained. More times on the roof!

My office mates, Dr. Marlijn Noback who already left for Norway, dankjewel voor al je ondersteuning! I now also know what it feels like to finish a thesis and I fully understand you (BB). Alexandra Uhl, the most Irish American in cowboy boots! Thanks for the cheerful times and your creative ideas! Remember fruitful Friday when I learned a lot about EVAN! Judith “der Fuchs” Beier and Hannes "David Beckham" Rathmann, thank you for your Neanderthal site and dental expertise and the fun we always had!

Dr. Heike Scherf, special thanks also to you! Without your help I would know nothing about AVIZO. I know I gave you a hard time when I made my first steps in virtual anthropology. Thank you for your patience and I hope I can pass on all your knowledge to the students. Dr. Sireen El Zaatari, I really appreciate that I had the chance to profit from your knowledge of teeth. Thank you so much for your motivating words whenever I needed them. Dr. Thomas “the incredible” Rein, thank you so much for sharing your knowledge with me. I also will never forget the great times we spent together in Tübingen or in the US – us being behind the scenes of a TV-show. DANKE-CARD! Speaking of the US, I would also like to thank Laura McCarty for being not only an inspiring colleague but also a dear friend. Dr. Hugo Reyes-Centeno (and Miguel Prieto-Valle!), thank you so much for inspiration, help and your support with statistical problems. You always had a solution – and an incredible Guacamole!

I am also very grateful to all the other members of the PaGE-project, Dr. Vangelis Tourloukis, Dr. George Konidaris, Domenico Giusti and Julian Bega. It was great to be a part of the team and having the opportunity to do fieldwork in Greece.

The basement crew, Angelika Wilk, Beatrix Welte and Tina Jahnke – thank you very much for the fun times while having a smoke but also offering me the chance to improve my knowledge about CT-scanned mummies, stone tools and faunal remains from the archaeological record.

Dr. Bernd Trautmann who already left for the Bavarian Capital (beware!), and Dr. Martin and Dr. Iris Trautmann, thank you for sharing your osteological experience with me, especially in the field of Paleopathology.

Wieland Binczik, the IT-wizard and skilled CT-technician, thank you so much for scanning my samples and for the great time we had together in the CT-lab.

Dr. Monika Doll, the most incredible secretary I ever met, thank you so much for your help with all the paperwork and supporting words. Keep up the good work and all the best for your new job. I am sure you will be missed.

Carola “Carhelm” Fuchs, it is always worth spending time with you. The endless fun and awesome times we spent will be unforgettable. Thank you so much for everything we shared, even chewing Birkenpech and the awesome night on THE day.

Susan “Susbert” Böttcher, you are also on your way to your PhD. No one would know better that this way is kind of like a pilgrimage. I am very grateful to have you as my best friend in my life. Your heart is always open and I really appreciate all your help and support. I hope I will also be of so much help when you just need somebody. Egal, ich lass' das jetzt so.

Renate and Rudolf Bauer – my loving parents. Thank you for – everything. Without you, nothing would have been possible. Thank you for endless support and love and always providing a warm and cosy home. You are always with me deep, deep down in my heart. I love you!

Again the solidity of my rock in the waves was heavily tested. Paul Bons, thank you is not enough said. You are the most perfect husband one can imagine. Not only your incredible knowledge but also your endless love – thank you for sharing both with me. Without you this thesis would not have been possible. Ik hou héél erg van jou.

